
Analyse dysregulierter Moleküle des
Nervensystems der Tenascin-R
defizienten Maus (*Mus musculus*
domesticus, Linneaus, 1758; *m.*
musculus TN-R^{-/-}, Weber et al. 1999)

Analysis of dysregulated molecules in
the nervous system of tenascin-R
deficient mice

Dissertation zur Erlangung des Doktorgrades der
Naturwissenschaften
Dr. rer. nat.

vorgelegt von Kai - Oliver Wesche, Hamburg

Hamburg im Juli 2003

Genehmigt vom
Fachbereich Biologie der
Universität Hamburg
auf Antrag von Frau Professor Dr. M. SCHACHNER
Weitere Gutachter der Dissertation:
Herr Professor Dr. L. RENWRANTZ

Tag der Disputation: 11. Juli 2003

Hamburg, den 28. Juni 2003



A handwritten signature in blue ink, consisting of a series of connected, somewhat horizontal strokes.

Professor Dr. A. Frühwald
Dekan

Inhaltsverzeichnis

Index

Einleitung

Introduction 7

The extracellular matrix 7
The tenascin family of ECM molecules 7
Tenascin-R 9

Chondroitin sulfate proteoglycans 10

Integrin cell receptors 11
Integrin associated protein: bodenin/
ICAP 12

Neurite outgrowth 13

Embryonic stem cells 14

Array expression analysis 14

Zielsetzung
Aim of this work 15

Material und Methoden

Materials and Methods 16

Materials 16
Enzymes and reaction kits 16
Reagents, disposables, etc. 16
Other equipment 18
Oligonucleotides 18
Software 18
Vectors 18
Antibodies 18
Bacterial strains 19
Bacterial media 19
Buffers and stock solutions 19

Various molecular biological

methods 20

Photometric quantification of nucleic
acids 20
DNA agarose gel electrophoresis 21
DNA endonuclease restriction 21
Phenol-chloroform DNA extraction 21
DNA sequencing 22
DNA precipitation 22

Cloning in plasmid vectors 22

Insert DNA preparation / enzymatic
manipulation 23
Vector DNA preparation / enzymatic
manipulation prior to cloning 23
Insert DNA and plasmid vector DNA li-
gation 24
DNA transformation into bacteria 24

Nucleic acid purification 25

Plasmid DNA purification from bacterial
cultures 25
DNA / PCR fragment purification 26
DNA fragment extraction from agarose
gels 26
Total RNA isolation from murine brain
tissue 26
Purification of mRNA 26
Genomic DNA isolation 27

Nucleic acid amplification 27

Polymerase chain reaction 27

Nucleic acid labelling 28

RNA in vitro transcription and
labelling 28
Radioactive DNA labelling 29
First strand synthesis and radioactive
labelling 29

Nucleic acid analysis by hybridization 30

Northern blot analysis 30
RNA in situ hybridization on cryosections 30
Expression profile analysis by cDNA array 31
Computer aided evaluation of array data 32

Immunohistochemistry 32

Immunofluorescence on cryosections 32
Immunofluorescence on coverslips 33

ES cell culture 33

Differentiation of ES cells 34
Neurite outgrowth of differentiated ES cells 36

Protein analysis 36

Protein extraction from murine tissue 36
Protein quantification 37
Protein gel electrophoresis 37
Coomassie staining of protein gels 37
Silver staining of protein gels 38
Western blot analysis 38
Immunoprecipitation 39

Proliferation assay 40

MTT test 40
Trypan blue exclusion assay 40
Sphere diameter 40

Ergebnisse Results 41

Detection of dysregulated transcripts in the tenascin-R deficient mouse brain 41

The cDNA array suggests several dysregulated molecules 41
Detailed investigation confirms ICAP dysregulation in total brain 45
Protein levels of ICAP 49
Localization of ICAP dysregulation 49
b1 Integrin mRNA levels detected by in situ hybridization 52
b1 Integrin protein levels 52
CaMKII expression 53

ICAP function in vitro 54

b1 Integrin and tenascin-R binding 54
The proliferation of ICAP deficient ES cells 57
ICAP deficient cells and neurite outgrowth 59

Diskussion Discussion 65

Dysregulation in Tenascin-R deficient mice 65

Dysregulation on the transcript level 65
The cerebellum and ICAP 66
ICAP influence on b1 integrin 67
ICAP on the protein level 69
Further comments 70

Literatur Literature 71

References 71

Bibliography 76

Zusammenfassung Summary 77

English Summary 77

Zusammenfassung 78

Anhang Appendix 80

Abbreviations 80

Curriculum vitae 82

Danksagung Acknowledgements 83

Erklärung 85

Einleitung

Introduction

The extracellular matrix

The generation and maintenance of complex organs like the nervous system requires distinct interactions of cells and their environment. This interaction is mediated by diffusible substances like growth factors, hormones, transmitters and by real contacts like cell-cell interactions or contacts to the extracellular matrix (ECM). This surrounding matrix is a complex network of secreted molecules that defines the areas, types and special properties of the tissue that is intended to be developed or maintained. It consists of collagen, fibronectin, laminin, proteoglycans, polysaccharides and, with special impact on this work, members of the tenascin glycoprotein family. The constitution of the ECM varies in regard to the tissue. For example tenascin-R (TN-R) is a member that almost exclusively appears in the central nervous system's (CNS) ECM (Fuss et al. (1993); see next section). The processes in which the ECM is involved also varies. They range from providing mechanical strength and scaffolding to influencing proliferation, migration, differentiation and apoptosis. In the nervous system the ECM regulates synapse formation, synaptic efficacy and axonal pathfinding.

The tenascin family of ECM molecules

Currently, there are 6 known members of the tenascin (TN) family of multimeric ECM glycoproteins namely TN-C (Chiquet and Fambrough (1984); Erickson and Inglesias (1984); Kruse et al. (1985); Grumet et al. (1985); Erickson and Bourdon (1989)), TN-R (Pesheva et al. (1989); Rathjen et al. (1991); Norenberg et al. Neuron (1992), TN-W (Weber et al. (1998)), TN-X (Bristow et al. (1993)), TN-Y (Hagios et al. (1996)); Tucker et al. (1999)) and TN-**N** (Neidhardt et al. (2003)). They all share a common structural composition: an amino-terminal cysteine-rich domain followed by a succession of epidermal growth factor-like (EGF)

domains and fibronectin type III-like domains (FNIII). A single fibrinogen-like domain (FBG; homologous to fibrinogen beta and gamma chains) is located at the carboxyterminal end. TN-X and TN-Y contain in addition serine and proline rich parts, which are inserted in the succession of FN III domains (Joester and Faissner (2001)).

The best known and extensively studied molecule of this family is **TN-C**. Its expression is generally detected in immature and reactive astrocytes (Bartsch (1996)). Additionally, it is also secreted by subsets of radial glia cells (Kawano et al. (1995)) and by subpopulations of neurons localized in the hippocampus, spinal cord, and retina (Bartsch (1996)). During development of the murine CNS it is expressed in areas of active axonal growth. Retinal ganglion cell axons elongate in a TN-C rich environment (Bartsch (1996)). The fact that in the chick visual system TN-C is associated with the cell surface of glial fibers and growing axons (Bartsch et al. (1995)) proposes that it also possesses guiding properties *in vivo*. In the peripheral nervous system (PNS) TN-C is located to the perineurium and nodes of Ranvier in adult nerves revealed by immunoreactivity (Martini (1994); Bartsch (1996)). In reaction to injury of nervous tissue the expression of TN-C is upregulated. Stab wound induces an upregulation of TN-C by Golgi epithelial cells in the cerebellar cortex (Bartsch (1996)) or the re-expression of the protein by reactive astrocytes in the cerebral cortex. In both paradigms, elevated levels of TN-C mRNA and protein are restricted to the immediate vicinity of the lesion sites. In numerous *in vitro* studies TN-C has been demonstrated to be adhesive or anti-adhesive (Dorries et al. (1996); Faissner and Kruse (1990); Grumet et al. (1985); Kruse et al. (1985)), to support or restrict cell migration (Chuong et al. (1987); Husmann et al. (1992)) and to promote or inhibit neurite outgrowth (Bartsch (1996); Dorries et al. (1996); Faissner and Kruse (1990); Lochter et al. (1991)). There are two independently generated conventional TN-C mouse mutants (Saga et al. (1992); Forsberg et al. (1996)) and one conditional knock out (Evers et al. (2002)). TN-C deficient mice generated by Saga et al. reveals functions for TN-C in the formation, maturation, and stabilization of the neuromuscular junction (Cifuentes-Diaz et al. (2002)). The constitutively TN-C deficient mouse mutant reveals an impairment of hippocampal long-term potentiation (LTP) that is depending on L-type Ca-channels. The theta-burst induced LTP in the CA1 region of the hippocampus is reduced and low-frequency stimulation fails to induce long-term depression (LTD) in comparison to the wild type situation.

The youngest member of the tenascin family is **TN-N**. It is mainly expressed in kidney and spleen and to lower levels in the murine CNS (Neidhardt et al. (2003)). A new tenascin in zebrafish (*Danio rerio*) is called **TN-W** (Weber et al. (1998)). It is absent in the CNS and axial mesoderm but is expressed in neural crest pathways. In several tissues it is colocalized with TN-C during development (Weber et al. (1998)). TN-W is present in the lateral plate mesoderm and in the presumptive sclerotome. Migrating cells of sclerotomal and neural crest origin show high levels of expression in non-neuronal cells of the dorsal root ganglia. The

largest member of the tenascin glycoprotein family is **TN-X**. It is predominantly expressed in connective tissue, muscles (including the heart), skin, in the vicinity of blood vessels and in tumors (Sakai et al. (1996); Hasegawa et al. (1997); Ikuta et al. (2000); Lethias et al. (2001)). The disease „Ehler-Danlos syndrome“ (Burch et al. (1997)) is associated with deletions in the TN-X gene and results in connective tissue disorder, impaired wound healing and vascular fragility. **TN-Y** was identified in the chicken and is expressed by connective tissue that modulates muscle cell growth. It is also expressed in muscles, lung, kidney, skin and in the avian nervous system (Tucker et al. (1999); Hagios et al. (1999 Exp); Fluck et al. (2000)).

Tenascin-R

A major subject of this work is the TN-R molecule described before as J1-160/180, janusin or restrictin (Pesheva et al. (1989); Fuss et al. (1991); Norenberg et al. (1992)). Under native conditions it occurs as an oligomer like TN-C. Its expression is mainly found in the oligodendrocyte lineage. The expression peaks during the period of active myelination (Fuss et al. (1993)). It can be detected in retina, optic nerve, cerebellum, hippocampus and olfactory bulb. On the cellular level it is found at axon-axon contacts of unmyelinated axons, between axons and myelinating oligodendrocyte processes, in myelin sheaths and at the nodes of Ranvier (Bartsch et al. (1993)). Here, TN-R interacts with voltage dependent sodium channels. In the perineuronal nets TN-R plays also an important role. This special ECM structure mainly consisting of chondroitin sulfate proteoglycans (see next section), hyaluronan, lectins and glycoproteins is enwrapping hippocampal inhibitory interneurons (Weber et al. (1999)) that have the following putative functions: synapse stabilization (Hockfield and McKay (1983)), growth factor reservoir for certain neurons (Celio and Blumcke (1994)) and ion-buffering microenvironment (Bruckner et al. (1993)). Within the perineuronal nets TN-R might function as a barrier against the formation of new synapses because it exhibits repellent and non-permissive properties to nerve fibres and growth cones (Xiao et al. (1996)). The investigation of the mouse mutant deficient for this molecule should give insights in TN-R's role *in vivo*. Overall, major brain areas show a normal histoarchitecture, normal formation and structure of myelin (Weber et al. (1999)). The abnormal phenotype of the mutant is depicted by a decreased conduction velocity of action potentials in the optic nerve. Also decreased is the NMDA receptor dependent LTP in the CA1 region of the hippocampus. At the node of Ranvier the amount of a chondroitin sulfate proteoglycan, namely phosphacan, is reduced. The structure composed of such glycans, the perineuronal nets, are affected in their integrity around hippocampal interneurons (Weber et al. (1999)).

Chondroitin sulfate proteoglycans

Another type of molecules that reside in the ECM are chondroitin sulfate proteoglycans (CSPGs). They consist of up to thousand repeating disaccharide units of glycosaminoglycans (GAGs) bound to the core protein. The unbranched GAG-polymers are attached to the protein through a serine residue and certain other characteristic carbohydrate bonds. The GAG units are containing chondroitin sulfate (CS) that is a disaccharide consisting of glucuronate and N-acetylgalactosamine (GalNAc). There are two different GalNAc's present in CS: N-acetyl-D-galactosamine-4-sulfate and N-acetyl-D-galactosamine that is instead sulfated at its C6 position. CSPGs found in the nervous system are aggrecan, brevican, neurocan and versican. Their domain structure consists of N-terminal Ig-like domain, tandem repeats of hyaluronan-binding domain and a C-terminal region containing EGFL repeats, C-type lectin-like and complement regulatory protein-like domains (Yamaguchi (2000)). Many interactions between ECM and cell adhesion molecules (CAM) are described. For example, neurocan and phosphacan bind to L1, NCAM and axonin-1 (Friedlander et al. (1994); Milev et al. (1994); Milev et al. (1996)). CSPGs also bind to tenascins (C and R; Grumet et al. (1994); Milev et al. (1998)). This binding of all CSPGs mentioned above occur at the FNIII domain of TN-R via their lectin-like domain.

Bamacan is a basement membrane CSPG of ~1200 amino acids (Iozzo and Clark (1986); Wu and Couchman (1997); Ghiselli et al. (1999)). It is mapped to 10q25 in human and to the distal region of chromosome 19 of mouse. The high sequence homology with the family of structural maintenance of chromosome proteins (SMC) suggests an influence of bamacan on chromosome dynamics, gene dosage and DNA repair (Koshland and Strunnikov (1996)) but other functions are poorly investigated so far. Bamacan does not share too much homologies with the mentioned CSPG members. One of its unique features is building up two coiled-coil structures that comprise more than 50% of the total protein. Laminin, an essential component of the basal lamina, has been shown to interact with such coiled-coil structures of CSPGs (Engel (1993)). Another feature shared with laminin (β 2 chain) is the LRE sequence that has been shown to be a cell attachment motif. Another cell attachment site of bamacan is the VTXG motif corresponding to that in thrombospondin 1 (Tolsma et al. (1993)).

Due to the fact that distinct changes in the composition and concentration of CSPGs are observable during brain development (Milev et al. (1998)) it can be suggested that these molecules have distinct functions in generation and maintenance of nervous system tissue. Following a CNS lesion, CSPG expression is upregulated forming a barrier to regrowing axons (Bovolenta and Feraud-Espinosa (2000)). This barrier can be overcome by digesting the CS of a lesion site with chondroitinase *in vitro* and *in vivo* (Morgenstern et al. (2002)).

Integrin cell receptors

The mediators between cells and their surrounding, either opposing cells, the ECM or diffusible factors are in many cases heterodimeric transmembrane glycoproteins called integrins. They are expressed in nearly all mammalian cell-types. Their composition can be drawn from a subset of 18 alpha subunits and 8 beta subunits (Hynes (2002)) resulting in 24 distinct integrin receptors that have specific and non-redundant functions. The alpha subunits range in size from 120 to 180 kDa and the non-covalently bound beta subunits range from 90 to 110 kDa. Both contain hydrophobic transmembrane segments and rather short cytoplasmic domains (20 to 70 amino acids; Hynes (1992)) that play an important role in signalling. In contrast, the extracellular domains are larger and complex structures. These parts of the beta subunits are always bigger than 75 kDa and larger than 100 kDa in case of the alpha subunit. Integrins have an active ("ON"-) state. This depends on certain conditions i.e. divalent cations (Mn^{2+} / Mg^{2+}) are required to interact with the extracellular metal ion dependent adhesion site (MIDAS; Emsley et al. (1997)). The activation of the often constitutively inactive integrins may also be triggered from inside of the cell. These cytoplasmic events will be depicted later in this section. Generating and receiving signals makes integrins exceptional. Therefore they are to be considered rather as mediators than "just" receptors.

To fulfil classical receptor properties the recognition of binding motifs on counterreceptors or ligands by the active extracellular domain is necessary. These motifs of the ECM ligand are relatively short peptide sequences. In case of fibronectin and vitronectin it is the Arg-Gly-Asp (RGD; Ruoslahti and Pierschbacher (1987)), in case of collagen type I it is the Asp-Gly-Glu-Ala (DGEA) peptide of the ligand. Further common motifs are Lys-Gln-Ala-Gly-Asp-Val (KQAGDV), Glu-Ile-Leu-Asp-Val (EILDV) and Gly-Pro-Arg-Pro (GPRP; Hynes (2002)). Accepting short peptides as ligands makes integrins vulnerable to so called disintegrins from snake venom toxins (Scarborough et al. (1993)) and artificially generated peptides like Arg-Gly-Asp-Ser (RGDS; Pierschbacher and Ruoslahti (1984)). For interactions with these small ligands the integrins do not have to be in the ON-state (Coller (1986)). Axonal growth cone guidance is also a mechanism in which integrins fulfil classical receptor tasks. Integrins are influencing growth cone advancement by recognizing components of basal lamina ECM. In this case, laminins (i.e. laminin 1, laminin 2, laminin 5 and 11) are axon outgrowth promoting molecules that influence, via integrin ($\alpha1\beta1$ or $\alpha3\beta1$), α -actinin or talin and vinculin, the actin microfilaments that are necessary for the growth cone advancement (Tessier-Lavigne and Goodman (1996)). Integrin mediated cell-ECM adhesion sites are called focal contacts or focal adhesions (Jockusch et al. (1995)).

The cytoplasmic domains give integrins exceptional features. Some of these domains are alternatively spliced in a tissue-type specific and developmentally regulated manner. They can regulate the activation state of the heterodimer, thereby affecting

the structure and function of the extracellular domains. Mediating a signal that is coming from regulatory proteins of the cytoplasm to the external ligand binding domains is called "inside-out" signalling (Ginsberg et al. (1992)), in distinction to the classical outside-in signalling. As an example for cytoplasmic proteins having the ability of triggering a signal to the outside, one has to mention the Ras-related small guanosine triphosphatases (GTPases). The GTPases and their downstream effectors are able to modulate the ligand binding affinity of integrins, either positively or negatively (Laudanna et al. (1996); Zhang et al. (1996)). Transfection of cells with constitutively active R-Ras induces an increase in integrin affinity (Zhang et al. (1996)). Up to now, it was not shown that these proteins interact directly with the cytoplasmic domain of the integrins (in this case $\beta 1$). In contrast, this has been demonstrated for talin, α -actinin and focal adhesion kinase (FAK; Burridge (1996)). The interaction of cytoplasmic proteins with the integrin occurs at the short sequence of Asn-Pro-X-Tyr (NPXY). The NPXY motif was originally found to be necessary for receptor mediated endocytosis (Chen et al. (1990)). Naturally occurring splice variants of the $\beta 1$ subunit lacking the NPXY are no longer localized to focal adhesion sites (Reszka et al. (1992); Balzac et al. (1993)). Most recently it has been shown that a cytoplasmic $\beta 1$ binding Ser/Thr kinase called integrin-linked kinase (ILK) influences nerve growth factor (NGF)-dependent neurite outgrowth (Mills et al. (2003)). Another protein that binds to $\beta 1$ integrin cytoplasmically is described in the next section in view of its importance for my work.

Integrin associated protein: bodenin/ICAP

Integrin Cytoplasmic Domain Associated Protein 1 (in human: ICAP-1 α (Chang et al. (1997); in mouse: bodenin or integrin beta 1 binding protein 1 (Itgb1bp1) (Faisst and Gruss (1998)) is a 200 amino acid phosphoprotein. The distribution of ICAP transcripts suggested by Northern Blot Analysis has a broad tissue spectrum. Bodenin, the mouse ortholog, exhibits a more restricted expression via gene trap LacZ insertion. It reveals transcripts in heart, visual system and regions of the forebrain and cerebellum of newborn and adult mice.

ICAP is binding to the $\beta 1$ integrin cytoplasmic domain. The interaction, which was demonstrated both *in vitro* and *in vivo* (Chang et al. (1997) and Zhang et al. (1999)), is specific for the $\beta 1$ integrins and requires the Asn and Tyr residues of the membrane-distal NPXY motif. The ability of ICAP to interact only with the $\beta 1$ cytoplasmic domain is attributed to an additional requirement of Val residue amino-terminal to the NPXY. In CHO cells, adhesion on fibronectin is regulated by ICAP phosphorylation at threonine 38 through the calcium/calmodulin-dependent protein kinase II (CaMKII; Bouvard and Block (1998)). Recent studies give insights into putative ICAP functions. One of these interactions links ICAP to Krev Interaction Trapped 1 (krit1) (Zhang et al. (2001)). Mutations in KRIT1 account for all cases of Cerebral Cavernous Malformation #1 (CCM1) in the 7q locus (Davenport et al. (2001); Zawistowski et al. (2002)). CCM is an autosomal dominant disorder and is genetically heterogeneous

with loci on 7q (CCM1), 7p (CCM2) and 3q (CCM3). Another interaction partner is the human metastasis suppressor Protein nm23-H2 (also called NDP Kinase B). It belongs to the nm23 family of proteins consisting of currently eight members (nm23-H1 to nm23-H8; Lacombe et al. (2000)). These members play their roles in nucleotide metabolism, cell development and differentiation (Lombardi et al. (2000)). Furthermore, ICAP is linked to the disruption of focal adhesions via competitive inhibition of talin's binding to the β 1 integrin cytoplasmic domain and thereby acting as a key regulator of cell adhesion (Bouvard et al. (2003)).

Neurite outgrowth

In neuronal development, axonal growth and dendritic tree extension are key processes. Axons and dendrites are also referred to as "neurites". By outgrowing such neurites, the neuronal shape is defined and modulated. Neuronal path finding is essential for the establishment of synaptic connections during development. Neuronal plasticity and neuronal regeneration from injuries or neuropathological conditions are further key situations in which neurite outgrowth plays a major role. Extracellular guidance molecules that act as instructive signals give rise to remodelling the neuronal cytoskeleton, promoting or inhibiting axonal outgrowth and inducing axonal turning (Mueller (1999); Nakamura et al. (2000)). These diverse guidance molecules are either soluble or substrate-bound substances. The growth cone is the primary receptor of these signals. Its peripheral and central regions are rich in actin microfilaments and microtubules. Alterations in the levels of actin polymerization and depolymerisation affect the dynamics of the microtubules (Baas (1999)) which is essential for the correct navigation of the axon in response to the submitted signal.

In cell culture, neurite outgrowth is influenced by the binding of a "neurotrophic" ligand to its receptor, resulting in cascades of signal transduction events that induce modulation of cytoskeletal components and membrane trafficking events that execute the process. These ligands are either coated as a substrate or dissolved in the medium. It is also sometimes necessary to modify the way a coated substrate is presented. For example, the way in which TN-R is coated influences growth cone response. If offered as a sharp substrate boundary to dorsal root ganglion (DRG) and retinal ganglion neurites the growth cones avoid growing on this molecule. As a homogenous substrate together with poly-L-lysine (PLL) the DRG growth cones are able to advance faster than on PLL alone. However, outgrowth of retinal ganglion neuron growth cones is completely inhibited under these conditions (Taylor et al. (1993)) showing that not all types of neurons respond in the same manner.

Embryonic stem cells

Embryonic stem (ES) cells are derived from the inner cell mass (ICM) of the blastocyst. The blastocyst is an early (day 3.5 *post coitus* or *post conception*; PC) embryonic stage prior to implantation to the uterine wall. Murine ES cells can be held in long term cultures (Evans and Kaufmann (1981)) staying stable with no changes in karyotype (Evans and Kaufmann (1981)). It was shown that they stay undifferentiated and pluripotent over a period of two years (Smith (2001)). High telomerase activity, no inactivated X-chromosome and continuous DNA replication (mitotic S-phase) are specific for murine ES cells. The pluripotency allows ES cells to differentiate into cells of the three germ layers: endo-, meso- and ectoderm in contrast to omnipotent cells that could additionally give rise to a whole organism. By inserting labelled undifferentiated ES cells into the blastula of a developing embryo the pluripotent ability can be demonstrated. The embryo that develops from this altered blastula has labelled cells in tissues that stem from the three primary germ layers. Such an animal is called a chimera. Transplanting undifferentiated ES cells into animals can give rise to teratomas. These kinds of tumors contain cells from the mentioned germ layers (i.e. epithelial, muscle, cartilage/bone and neural cells). This example indicates that the positive feature of pluripotency makes it necessary to predifferentiate ES cells prior to implantation in order to prevent the generation of tumors. ES cells are inducible to proliferate or differentiate by several *in vitro* techniques. In culture, ES cells are clonogenic. A single ES cell gives rise to a colony of identical cells (clone). To keep them in an undifferentiated state they are cultured on a feeder cell layer of murine fibroblasts (MEF) and under the influence of leukemia inhibitory factor (LIF), an interleukin-6 cytokine. For the presented work it was necessary to generate precursor cells that are limited in their future lineage decision towards the neural direction. For achieving this differentiation, ES cells are induced to form free floating aggregates called embryoid bodies (EBs) by culturing in non-adhesive culture dishes without MEF and LIF. The precursor cells are generated through the adherent growth in medium containing specific factors that trigger differentiation cascades to the desired direction. Like this, ES cells can be directed to differentiate into early neural progenitors and from there into mature neurons and glia (astrocytes and oligodendrocytes; Okabe et al. (1996)).

Array expression analysis

Investigating the question which interplay of molecules or compensatory dysregulation leads to the rather mild phenotype of a knock out animal requires "expression profiling". Additionally, new candidates that are related to the knocked out gene might be found. Classical methods facing these questions are expressed sequence tags (EST) sequencing (Adams et al. (1993);

subtracted suppression hybridization (SSH; also called differential display (DD; Liang and Pardee (1992)) and serial analysis of gene expression (SAGE; Velculescu et al. (1995)). The great advantage of high density arrayed spotted cDNAs (termed microarray) is the enormous number of parallel experiments that can be performed in one step. Achieving high throughput and high sensitivity were the goals that led to the development of microarrays. In this work arrays developed by the Lehrach group at the Max Planck Institute for Molecular Genetics (Berlin, Germany) were used. These consist of a subset of dsDNA polymerase chain reaction (PCR) products that were generated by oligonucleotide fingerprinting (Meier-Ewert et al. (1998)). The oligo fingerprinting provides a good tool to characterize cDNA libraries. In this case the library consisted of 60.000 cDNA clones that evolved from pooling and cloning the mRNAs isolated of embryonic mice (E9 and E12). Through the fingerprinting 5376 unique mRNA species were shown to be each represented by a single cDNA clone. PCR products of these clones are then spotted in duplicates on nylon membranes having the size of a microtiter plate. After processing these membranes they were hybridized with poly A+ mRNA probes that were random primed radioactively labelled. A computer analysis of the phosphoimager pictures gave rise to the expression profile. This profile has to be seen as a snapshot of the very dynamic transcript situation and for a better understanding of its regulatory processes mice of different ages would have to be studied. However, in this case a huge amount of data must be handled and elaborately evaluated. Thus, it is reasonable to pose a precise question that makes it necessary to look at a crucial time point like the period of active myelination when TN-R is most highly expressed.

Zielsetzung

Aim of this work

In the past decade, six members of the tenascin family have been identified and characterized. TN-R is expressed in the central nervous system and shows diverse functions on outgrowing neurites and migrating neural cells. In contrast to these striking *in vitro* findings, a rather mild phenotype is observed in the CNS of mice deficient for the TN-R molecule. Unravelling whether there are compensatory effects by other molecules that lead to this situation was the reason for utilizing the microarray technique. Detecting a dysregulation with impact on the phenotype could give new insights into the interplay of diverse processes and molecules. This can also include previously undescribed or unrelated molecules and give new hints to interesting candidate genes. In this study I will describe what alterations were detected at the mRNA level in the TN-R deficient mouse. The evaluation of these findings is another part of this work and finally, it will be shown which functional impact these alterations have.

KAPITEL 2

Material und Methoden *Materials and Methods*

Materials

Enzymes and reaction kits

DNA polymerases

HotStar Taq Qiagen Hilden, D

PfuTurbo Stratagene Amsterdam, NL

PfuTurbo Hotstart

Taq DNA Polymerase Invitrogen Karlsruhe, D

Restriction endonucleases

Various AGS Hybaid Heidelberg, D

Various MBI Fermentas St. Leon-Rot, D

Various NEB Frankfurt a. M., D

(DNA-dependent) RNA polymerases

T3/T7/SP6 pol. Roche Mannheim, D

Megascript kit Ambion Cambridge, UK

Megaprime system APB Freiburg, D

Reagents, disposables, etc.

If not itemized in this paragraph, origin of enzymes and reaction kits is referenced in the corresponding sections. All chemicals are purchased in *pro analysis* quality from the following manufacturers/vendors: Amersham Pharmacia Biotech (APB, Freiburg, D), Bio-Rad (München, D), GIBCO Invitrogen Life

Technologies (Karlsruhe, D), Macherey-Nagel (Düren, D), Merck (Darmstadt, D), Roche (Mannheim, D), Carl Roth (Karlsruhe, D), Serva (Heidelberg, D), and Sigma-Aldrich (Deisenhofen, D). Cell culture material is supplied from Greiner Bio-One (Frickenhausen, D), Nunc (Roskilde, DK) and TPP (Trasadingen, Ch); solutions and media designated for ES cell culture are obtained from Chemicon international (Temecula, CA, USA), GIBCO Invitrogen, Sigma-Aldrich, PAA (Linz, A) and tebu-bio (Offenbach, D). Plasmids and molecular cloning reagents are obtained from Ambion, Ltd. (Cambridge, UK), APB, BD Biosciences Clontech (Heidelberg, D), Invitrogen (Karlsruhe, D), Promega (Mannheim, D), Qiagen (Hilden, D), and Stratagene (Amsterdam, NL). DNA and RNA purification systems are purchased from APB, Life Technologies, Macherey-Nagel, and Qiagen. Nucleic acid molecular weight markers are purchased from Roche and NEB (Frankfurt a.M., D).

α [³² P]dCTP,	APB Freiburg, D
α [³³ P]dCTP,	APB Freiburg, D
Aqua/PolyMount	Polysciences, Inc. Warrington, PA, USA
BENCHMARK protein marker	Life Technologies Karlsruhe, D
BIOMAX ML, MS	Eastman Kodak Rochester, NY, USA
Complete EDTA-free	Roche Mannheim, D
dNTPs	Roche Mannheim, D; Life-technologies Karlsruhe, D; Carl- Roth Karlsruhe, D
GSTrap GST-sepharose columns	APB Freiburg, D
Whatman 3MM paper	Whatman Kent, UK

Centrifuges

Sorvall Kendro, Hanau, D RC50*plus* with SLA3000, SLA 1500, SA600 and HB-6 rotors
 Eppendorf Hamburg, D Microcentrifuge 5415D, Bench-top centrifuges 5417R and 5403
 Jouan, Inc Winchester, VA, USA Bench-top centrifuge CR422
 Liquid scintillation counting, Wallac Freiburg, D Liquid scintillation counter 1409

Power supplies

Bio-Rad Munich, D Power Pac series

Spectrophotometer

APB Freiburg, D Ultrospec 3000/DPV-411 printer

Thermal cyclers

Eppendorf Hamburg, D Mastercycler *gradient*
MJ Research Waltham, MA, USA PTC-200 DNA EngineTM *classic*

Other equipment

APB Freiburg, D UV crosslinker
Fujifilm Raytest, Straubenhardt, D Phosphorimager BAS-1000 and BAS-5500
Herolab Wiesloh, D E.A.S.Y. UV-light documentation
Leica Bensheim, D Cryostat CM3050
Wallac Freiburg, D Liquid scintillation counter 1409
Zeiss Göttingen, D Axiophot & Kontron

Oligonucleotides

Oligonucleotides (primers) are synthesized by MWG biotech AG Ebersberg, D

Software

Adobe San Jose, CA, USA Photoshop 6.0
DNASTAR, Inc. Madison, WI, USA Lasergene suite 4.05
GPC biotech AG Martinsried, D VisualGrid 2.1 Array Software
Sci&Ed Software Durham, NC, USA Clonemanager 5
raytest Straubenhardt, D Tina 2.09

Vectors

pBluescript. II SK/KS, Stratagene, Cloning vector
pcDNA3.1/myc-His A-C, Invitrogen Karlsruhe, D, Eukaryotic expression vector
pEGFP-C1, BD Bioscience Clontech, enhanced green fluorescent protein marker vector

Antibodies

Following previously described antibodies are used: monoclonal anti TN-R 596 & 597 (Pesheva et al. (1989)) and monoclonal anti TN-R 619 (Morganti et al. (1990)). Furthermore, the following commercially available antibodies are utilized: monoclonal anti β 1 integrin M-106 (Santa Cruz Biotechnology Inc. Santa Cruz, USA); monoclonal β III tubulin (Sigma-Aldrich Deisenhofen, D); anti-CaMKII 22B1 (monoclonal, ALEXIS Biochemicals Grünberg, D); anti GST-HRP conjugate (APB) and polyclonal anti-nestin (Chemicon).

For indirect immunofluorescence, Cy2-, 3- and 5- conjugated antibodies (diluted 1:400) and horseradish peroxidase-conjugated antibodies (diluted 1:400) to rabbit, rat or mouse are used, respectively (all from Dianova, Hamburg, D).

Bacterial strains

E. coli XL1-Blue Stratagene

E. coli DH5 α Life Technologies

E. coli JM 109 Inst. Prof. Schachner Lab.

Bacterial media

Luria broth (LB, per liter)

10g NaCl

10g tryptone or peptone

5g yeast extract

pH 7.0 with 5N NaOH (optional) and 5N NaOH (optional)
and autoclave

LB agar (per liter)

10g NaCl

10g tryptone or peptone

5g yeast extract

20g agar

pH 7.0 with 5N NaOH (optional) and 5N NaOH (optional)
and autoclave

The following antibiotics are added when needed (1000-fold stock solutions): 100 mg/l ampicillin (LB-amp), 25 mg/l tetracycline (LB-tet) and 25 mg/l kanamycin (LB-kan).

Buffers and stock solutions

Buffers and stock solutions are listed below. All more method-specific solutions are specified in the accompanying sections.

Boston lysis buffer 50mM Tris-HCl (pH 8.0), 50mM KCl, 2.5mM EDTA, 4.5g/l Nonidet P-40, 4.5g/l Tween 20
[before use: add 15 μ l proteinase K (15.3mg/ml, Roche) per ml lysis buffer]

DEPC-H₂O 0.1% (v/v) diethylpyrocarbonate autoclave
after stirring overnight.

DIG blocking stock 10 g Blocking reagent (Roche) 100 ml DIG
buffer 1 dissolve blocking reagent by micro-
wave pulses and autoclave.

DIG buffer one (2x) 0.2 M maleic acid 0.3 M NaCl pH 7.5 (solid
NaOH).

DIG buffer two 10% (v/v) DIG blocking stock in DIG buffer
one

DIG detection buffer 0.5 M Tris-HCl (pH 9.5) 0.5 M NaCl
(5x)

DIG washing buffer 3 g/l Tween 20 in DIG buffer one

DNA elution buffer	1mM Tris-HCl (pH 8.0)
DNA loading buffer (20x)	20% (w/v) Ficoll. type 400, 0.5 g/l xylene cyanol, 0.5 g/l bromophenol blue, 0.5 g/l orange G
dNTP-stock solution	5mM dATP 5mM dTTP 5mM dGTP 5mM dCTP or stock solution with 25 mM of each dNTP.
EDTA stock solution	0.5 M EDTA pH 8.0
Formaldehyde RNA-gel running buffer (5x)	0.1M MOPS pH 7.0 40mM sodium acetate 5mM EDTA
Formaldehyde RNA-gel loading buffer (5x)	50% (v/v) glycerol 1mM EDTA 0.25% (w/v) bromophenol blue 0.25% (w/v) xylene cyanol
Paraformaldehyde fixation solution 4%	4% (w/v) paraformaldehyde dissolved at 60°C under stirring in 1x PBS
Phosphate buffered saline (PBS 10x, for Morphology)	1.36M NaCl 0.1 Na ₂ HPO ₄ 27mM KCl 18mM KH ₂ PO ₄ pH 7.4
PBST	0.1% (v/v) Tween 20 in PBS (1x)
Saline Sodium Citrate Buffer (SSC, 20x)	3M NaCl 0.3M tri-sodium citrate
TAE (50x; for DNA-gel electrophoresis)	2M Tris-Acetate pH 8.0 100mM EDTA
TE (10x)	0.1M Tris-HCl pH7.5 10mM EDTA

Various molecular biological methods

If not otherwise indicated, standard biological techniques are carried out as described (Sambrook et al., (1989)). Methods for probe generation for *in situ* hybridization, northern blotting and array analysis, as well as ES cell culture are described in more detail.

Photometric quantification of nucleic acids

DNA, RNA and oligonucleotides are measured directly in aqueous solutions. The concentration is determined by measuring adsorption at 260nm against blank and then evaluated via factor. The absorption of 1 OD (A) is equivalent to approximately 50g/ml dsDNA, 40 g/ml RNA and 30 g/ml for oligonucleotides. Interference by contaminants was recognized by the calculation of ratio. The ratio A₂₆₀ / A₂₈₀ is used to estimate the purity of

nucleic acid, since proteins absorb at 280 nm. Pure DNA should have a ratio of 1.8, whereas pure RNA should give a value of approximately 2.0. Absorption at 230 nm reflects contamination of the sample by substances such as carbohydrates, peptides, phenols or aromatic compounds. In the case of pure samples, the ratio A₂₆₀ / A₂₃₀ should be approximately 2.2.

DNA agarose gel electrophoresis

To analyze restriction digests, quality of nucleic acid preparations, etc. horizontal agarose gel electrophoresis is performed. Gels are prepared by heating 0.8-2.5% (w/v) agarose (Invitrogen Karlsruhe, D, electrophoresis grade) in Tris-acetate buffer (TAE), depending on the size of fragments to be separated. DNA samples are adjusted to 1 x DNA sample buffer and are subjected to electrophoresis at 10 V/cm in BIO-Rad gel chambers in 1 x TAE running buffer. Afterwards, gels are stained in 0.5 µg/ml ethidium bromide in 1 x TAE solution for approximately 20 min. Thermo-photographs of transilluminated gels are taken, or bands are made visible on an UV-screen (at 360 nm) and desired fragments are cut out with a scalpel. Extraction of DNA fragments from agarose plugs is described in a consecutive section.

DNA endonuclease restriction

Restriction enzyme digestions are performed by incubating dsDNA molecules with an appropriate amount of restriction enzyme(s), the respective buffer as recommended by the supplier, and at the optimal temperature for the specific enzyme, usually at 37°C. In general, 20 µl digests are planned. For preparative restriction digests the reaction volume is scaled up to 100 µl. Digests are composed of DNA, 10 x restriction buffer, the appropriate number of units of the respective enzyme (due to glycerol content the volume of the enzyme added should not exceed 1/10 of the digest volume), and the sufficient nuclease-free H₂O to bring the mix to the calculated volume. After incubation at the optimal temperature for a reasonable time period (mostly 2 to 3h or overnight), digests are stopped by incubation for 20min at 65°C. If reaction conditions of enzymes were incompatible to each other, DNA is digested successively with the individual enzymes. Between individual reactions, DNA is purified (described in a consecutive section).

Phenol-chloroform DNA extraction

An equal volume of a neutralized phenol/chloroform solution (1:1) is added to the aqueous, DNA-containing sample and vortexed for 1 to 2min (longer for larger volumes) creating an emulsion. To avoid shearing, samples containing genomic DNA are only gently mixed. After centrifugation at 16,000x g (RT) for 2 to 5 min, the aqueous (upper) layer is carefully transferred to a new tube, avoiding any flocculent material at the interface. For purification of RNase-free DNA templates for in vitro transcriptions, the above described extraction is repeated. The

lower, organic phase is extracted with an equal volume of TE buffer for optimal recovery. In order to remove residual phenol, the combined aqueous phases are extracted with an equal volume of chloroform. After centrifugation at 16,000x g (RT) for 5 min, the aqueous (upper) layer is carefully transferred to a new tube, designated for further DNA purification by precipitation (see a consecutive section).

DNA sequencing

Sequence determination of dsDNA is performed by the sequencing facility of the ZMNH (Dr. W. Kullmann, M. Daeumigen). Fluorescent dye labelled chain-termination products (ABI Prism Dye Terminator Cycle Sequencing Ready Reaction Kit, Perkin Elmer, Wellesly, MA, USA) are analyzed with an ABI Prism 377 DNA Sequencer (Perkin Elmer). For preparation, 0.8 to 1 µg of DNA is diluted in 7 µl ddH₂O and 1 µl of the appropriate sequencing primer (10pM) is added.

DNA precipitation

The salt concentration of an aqueous DNA solution is adjusted by adding 1/10 volume of sodium acetate, pH 5.2. 2.5 volumes of cold ethanol, -20°C are added and the samples mixed well. Following incubation on ice for 30 min, samples are centrifuged for 15 min (16,000 x g, RT). For optimal purity, the pellet is loosened from the tube during inverting and is broken up in ethanol. After removal of the supernatant, a quick 1 to 2s centrifugation step is performed and residual ethanol is aspirated. Supernatants are removed and DNA pellets air dried (approximately 5 min at RT). DNA is resuspended in an appropriate volume of prewarmed water or in TE at 50°C.

Cloning in plasmid vectors

Efficient insert/vector DNA ligation can be observed if the vector and insert DNA contain complementary, protruding ends; cloning is less efficient when both DNA fragments possess blunt ends. The highest efficiency is generally achieved with DNA cleaved by two different restriction enzymes that produce non-complementary overhangs (directional cloning). If insert and vector DNA ends do not coincide, blunt ends suitable for ligation were created by filling-in 5'-protruding DNA ends with Klenow fragment. Blunted DNA fragments are then ligated with the precleaved and at the 5'-ends dephosphorylated vector. Another application is the cloning of PCR products amplified (or treated) with Taq DNA polymerase. This enzyme selectively adds an additional adenosine (A) at the 3'-end of amplified DNA, which facilitates TA cloning, the cloning of PCR products into specially constructed vectors containing an additional thymidine (T) at their respective 5'-ends. Recombinant plasmids obtained after ligation reactions are introduced into

competent *E. coli* cells by transformation. Transformants are analyzed by restriction analysis after minipreps and/or Colony PCR.

Insert DNA preparation / enzymatic manipulation

If the insert DNA does not contain ends compatible with the precleaved vector, several strategies can be followed to overcome this problem; methods are briefly described:

Phage, cosmid or plasmid DNA fragments

For cloning of distinct regions of phage, cosmid or plasmid DNA, donor molecules are digested with appropriate restriction enzyme(s) (see above). Even though direct ligation using DNA from inactivated restriction digests is possible, mostly complete digests are applied to agarose gel electrophoresis, appropriate DNA bands are cut out and DNA is eluted from agarose plugs (see below), thus avoiding unwanted by-products during subsequent ligation reactions. Non-complementary overhanging ends are converted to blunt ends prior to ligation using Klenow enzyme.

Pfu DNA polymerase-derived products

Due to the 3' to 5' exonuclease activity, a major fraction of DNA species amplified with PfuTurbo, or PfuTurbo Hotstart DNA polymerases does not contain an additional adenosine at the 3'-end. These PCR products are directly cloned with vector DNA that is cut with enzymes generating blunt ends after adding an additional thymidine (T) with Taq DNA polymerase. Before ligating DNA from PCR reactions, DNA is cleaned up (see below) or DNA fragments are gel-purified (see below).

PCR products with introduced restriction enzyme sites

Frequently, the ends of insert DNA does not contain suitable restriction enzyme sites, i.e., when a donor cDNA was designated for cloning into a certain reading frame of an expression vector. Restriction enzyme sites are generated by PCR at the desired location. For this technique, restriction sites are designed into the 5'-end of the PCR primers. Because certain restriction enzymes inefficiently cleave recognition sequences located at the end of a DNA fragment, usually four additional bases are included 5' to the restriction enzyme sites. PCR products are gel-purified (see below) and digested with the appropriate restriction enzymes.

Vector DNA preparation / enzymatic manipulation prior to cloning

When used as vectors, plasmids are digested at one locus either by a single restriction enzyme or by two at a multiple-cloning site to achieve insertion of target DNA in a defined orientation. Digestion reactions are carried out as described above using 2 - 5 µg of plasmid DNA as starting material. When digestions are verified as complete and correct by agarose gel electrophoresis, complete restriction digests are subjected to preparative agarose gel electrophoresis and appropriate bands representing digested vectors are cut out and vector DNA is extracted from agarose

gels.

x µl purified vector DNA

1x SAP reaction buffer

y µl SAP (1 U/µl); 1-2 U/pmol 5'ends

ad 60 µl H₂O

Following restriction experiments generating blunt-ends or using a single restriction enzyme, the digested vector DNA is dephosphorylated at the 5'-end with shrimps alkaline phosphatase (SAP). By removing 5'-phosphates from the plasmids, this enzymatic manipulation inhibits self-circularization by DNA ligase. After restriction, Plasmid DNA is purified with the Concert PCR purification kit (GIBCO Invitrogen Karlsruhe, D) and the dephosphorylation reaction mixtures (as shown above) are incubated at 37°C for 30 - 45 min. Reactions are terminated by incubation at 65°C for 20 min. Vector DNA is (a) used directly for ligation reactions, (b) purified with the Concert PCR purification kit or (c) purified by phenol extraction and alcohol precipitation prior to ligation reactions.

Insert DNA and plasmid vector DNA ligation

DNA ligations are performed by incubating DNA fragments with appropriately prepared cloning vectors in the presence of buffer, dATP, and T4 DNA ligase:

Ligation of sticky ends

The following reactions are set up and incubated at RT for 2 h or at 37°C for 2 h:

15 fmol vector DNA (i.e., 50ng of a 5.5kb plasmid)

2x - 5x molar excess of insert DNA

1x ligation buffer

1 U T4 DNA ligase (1 Unit/µl)

ad 20 µl H₂O, nuclease-free

Ligation of blunt ends

The following reactions are set up and incubated at 16°C between 2 h to overnight:

15 fmol vector DNA (i.e., 50 ng of a 5.5 kb plasmid)

5x - 10x molar excess insert DNA

50 g/l polyethylene glycol (PEG 8000; Sigma-Aldrich)

1x ligation buffer (Roche)

2 U T4 DNA ligase (1 Unit/µl; Roche)

ad 20 µl H₂O, nuclease-free

DNA transformation into bacteria

10 ng of plasmid DNA or 20 µl of a ligation mixture are added to 100 µl of competent DH5α and incubated for 30 min on ice. After a heat shock (2 min, 42°C) and successive incubation on ice (3 min), 800 µl of LB-medium are added to the bacteria and incubated at 37°C for 30 min. Cells are then centrifuged (10,000 x g, 1 min, RT) and the supernatant is removed. Cells are resuspended 100 µl LB medium and plated on LB plates containing the appropriate antibiotics. Colonies are developing after incubation at 37°C for 12-16 h.

Nucleic acid purification

Plasmid DNA purification from bacterial cultures

Mini-scale plasmid isolation

3 ml LB/Amp-Medium (100 µg/ml ampicillin) are inoculated with a single colony and incubated over night at 37°C with constant agitation. Cultures are transferred into 2 ml Eppendorf tubes and cells are pelleted by centrifugation (12,000 rpm, 1min, RT). Plasmids are isolated from the bacteria using the GFX *micro* plasmid prep system (APB), according to the manufacturer's protocol. The DNA is eluted from the columns by addition of 50 µl Tris-HCl (10 mM, pH 8.0) with subsequent centrifugation (12,000 rpm, 2 min, RT). Plasmid DNA is stored at 20°C.

Plasmid DNA isolation from 15-ml cultures

To rapidly obtain higher amounts of DNA, the Macherey-Nagel Nucleospin kit is used. 15 ml LB/Amp-Medium (100 µg/ml ampicillin) are inoculated with a single colony and incubated over night at 37°C with constant agitation. Cultures are transferred into 15 ml Falcon tubes and cells are pelleted by centrifugation (12,000 rpm, 1min, RT) in an Eppendorf centrifuge. Plasmids are isolated from the bacteria according to the manufacturer's protocol with the exception that twice the suggested amount of buffers are used. DNA is eluted from the columns by adding 50 µl of prewarmed (70°C) Tris/Cl (10 mM, pH 8.0) with subsequent centrifugation (12,000 rpm, 2 min, RT) twice. Finally, the DNA concentration is determined as described above.

Plasmid DNA isolation from 500 ml-cultures (Maxipreps)

For preparation of large quantities of DNA, the Qiagen Maxiprep kit is utilized. A single colony is inoculated in 2 ml LB/amp (100 µg/ml ampicillin) medium and grown at 37°C for 8 h with constant agitation. Afterwards, this culture is added to 500ml LB/amp medium (100 µg/ml ampicillin) and the culture is incubated at 37°C with constant agitation overnight. Cells are pelleted in a Beckmann centrifuge (6,000g, 15 min, 4°C) and DNA is isolated as described in the manufacture's protocol. Finally, the DNA pellet is resuspended in 600 µl of prewarmed (70°C) Tris-HCl (10 mM, pH 8.0) and the DNA concentration is determined.

Colony-PCR

Alternatively, Colony-PCR is performed to screen bacterial colonies for the presence of the desired recombinants. Single colonies are isolated with a toothpick and, after streaking on a reference plate, dipped into 50 µl boston lysis buffer (without proteinase K). After vortexing, 1 µl is used in hotstart PCR analysis (25 µl reaction) using appropriate primer pairs. Indicative PCR products are analyzed by agarose gel electrophoresis and ethidium bromide staining. In case of a positively identified recombinant, the colony is picked from the reference agar plate and used to inoculate cultures in order to purify larger amount of this particular plasmid DNA.

DNA / PCR fragment purification

For purification of DNA fragments the silica matrix-based High Pure PCR-Purification kit (Roche) is used according to the manufacturer's protocol. The DNA is eluted from the column by addition of 50 µl prewarmed (70°C) Tris-HCl (10 mM, pH 8.0). The DNA concentration is determined using the undiluted eluate.

DNA fragment extraction from agarose gels

For isolation and purification of DNA fragments from agarose gels, ethidium bromide-stained gels are illuminated with UV-light and the appropriate DNA band is excised from the gel with a clean scalpel and transferred into an Eppendorf tube. The fragment is isolated utilizing the silica matrix-based QIAquick Gel Extraction kit (Qiagen) following the manufacturer's protocol. The fragment is eluted from the column by addition of 50 µl prewarmed (70°C) Tris-HCl (10 mM, pH 8.0). The DNA-concentration is determined using the undiluted eluate.

Total RNA isolation from murine brain tissue

Total RNA is purified using the silica-gel-membrane technology as adopted in Qiagen's RNeasy system. All buffers used were provided by the manufacturer. Post natal day 14 (P14) mouse brains are quickly isolated and frozen in liquid nitrogen. 250 mg brain tissue is homogenized in 15ml buffer RLT with a rotor-stator homogenizer for 45 s at maximum speed. The total RNA is isolated following the manufacturer's protocol. Finally, total RNA is eluted in an appropriate amount DEPC-treated water. Integrity of the purified total RNA is assessed by spectrophotometry (scan from 200 - 350nm) and agarose electrophoresis (even under non denaturing conditions, identical to the procedure described above for DNA). Total RNA samples are stored at -80°C.

Purification of mRNA

The isolation of poly A+ mRNA from total RNA samples is performed by the mRNA DIRECT Dynabeads Kit (DynaL Biotech Oslo, N) according to the manufacturers protocol. The oligo (dT)₂₅ magnetic beads are directly incubated in a 1:1 ratio of beads in supplied binding buffer to the sample. All steps accord to

the protocol except that for elution of the mRNA from the beads 12µl elution solution is incubated for 5 min at 65°C. Of the eluted material 1µl is diluted in 99µl DEPC-water and subject to photometric measurement of concentration. The mRNA samples are stored at -80°C.

Genomic DNA isolation

Extraction of genomic DNA from ES cells

ES cells are washed once with PBS and lysed by addition of Boston lysis buffer and incubated overnight in a moist chamber at 55°C. DNA is precipitated overnight at RT by addition of 1/10 volume 8M LiCl and 1 volume isopropanol. Samples are centrifuged for 30 min at 1,300x g and the supernatant is discarded. After washing with 70% ethanol (4°C) and drying of the DNA pellet for 15 min at 37°C, the DNA is solubilized in TE buffer overnight at 37°C.

Extraction of genomic DNA from biopsies

Small biopsies like mice tail cuts for routine mice genotyping (~0.2 cm) are lysed by addition of 0.3 ml Boston lysis buffer and incubated overnight at 55°C. After mixing, the digests are centrifuged for 5 min (16,000x g, RT) and 2µl of the supernatant are subjected to standard 25µl PCR reactions.

Nucleic acid amplification

Polymerase chain reaction

The *in vitro* amplification of DNA fragments using the polymerase chain reaction (PCR) is usually performed in a MJ PTC-200 DNA ENGINE *classic* thermal cycler. Alternatively, the Eppendorf Mastercycler *gradient* is utilized when the PCR does not yield a specific product due to an inadequate annealing temperature. In this case a temperature gradient of +/-5°C of the annealing step is used. Routinely, PCR reactions are set up by adding the following ingredients to a 0.2 ml thin-walled tube (Biozym Diagnostik GmbH, Hessisch-Oldendorf, D): the template DNA (typically plasmid or first strand cDNA), the primers flanking the region(s) to be amplified, dNTPs, buffer and DNA polymerase. Primer sequences are selected manually. Selected primer sequences are evaluated with the web-based Oligo Calculator (<http://www.basic.nwu.edu/biotools/oligocalc.html>) which employs the nearest neighbour algorithm to determine annealing temperatures. Usually, 20-50 µl reactions were performed. The enzymes, that were used during these experiments are as follows (in brackets typical PCR reactions):

- (a) Taq DNA polymerase ("general" PCR reactions)
- (b) PfuTurbo DNA polymerase (PCR to amplify DNA for further cloning steps)
- (c) HotStarTaq DNA polymerase (RT-PCR, general amplification from first strand cDNA, cloning of difficult amplicons)

The table below shows cycling parameters for the DNA polymerases (a), (b) and (c). Number of cycles (25-35 up to 40) required for optimum amplification varied depending on the amount of starting material and the efficiency of each amplification step. A final incubation step at the extension temperature ensured fully double stranded molecules from all nascent products. Following cycling, typically 5-10 μ l aliquots up to complete reactions were analyzed by agarose gel electrophoresis to detect amplified products. In instances where the yield from a single PCR was insufficient, the reaction was purified and an aliquot was used as template for a second PCR with the same or a nested primer set (nested PCR).

step \ pcr type	(a) Taq	(b) Pfu	(c) HotStar
1	1' @ 94°C to 5' @ 95°C	1' @ 94°C to 1' @ 98°C	15' @ 95°C
2	30'' @ 94°C to 1' @ 96°C	1' @ 94°C to 1' @ 98°C	30'' @ 94°C to 1' @ 94°C
3	30'' to 1' T _{NB}	1' T _{NB}	30'' to 1' T _{NB}
4	72°C 1' per kb	72°C 1' per kb	72°C 1' per kb
5	go to step 2; 25-40 cycles	go to step 2; 25-40 cycles	go to step 2; 25-40 cycles
6	> 5' @ 72°C	> 5' @ 72°C	> 5' @ 72°C
7	4°C for ever	4°C for ever	4°C for ever
8	end	end	end

Table 1 PCR thermocycling parameters

Depicted here are typical PCR programs using the indicated polymerase. T_{NB} is indicating the individual annealing temperature of the primer calculated by the method of the nearest neighbour algorithm.

Nucleic acid labelling

RNA *in vitro* transcription and labelling

To generate *in vitro* transcribed RNAs, 5-10 μ g of DNA (cDNA from PCR reaction) containing the desired cDNA and a T3 or T7 polymerase promotor at positions that are located 3' of the DNA strand that is subject to transcription. In order to obtain digoxigenin-11-uridine-5'-triphosphate (DIG) labelled RNA probes for *in situ* hybridization (described in a consecutive

section), transcription of the desired templates is performed with Ambion's MEGAscript system according to their manual. For the generation of DIG-labelled RNAs, the DIG-UTP mix shown below was used instead of NTPs provided by the manufacturer.

DIG-UTP mix (10x)

10 mM ATP

10 mM CTP

10 mM GTP

6.5 mM UTP

3.5 mM DIG-11-dUTP (Roche)

According to the manufacturers protocol, the reaction is performed in 20µl total volume. The generated mRNAs are purified by LiCl precipitation, analyzed by denaturing agarose gel electrophoresis and stored at -80°C.

Radioactive DNA labelling

For generating a radioactively labelled Probe (i.e. Northern Blot probe, see next section) a PCR fragment (or insert fragment) representing a short sequence (300 to 650 bp) of the gene of interest is labelled with ^{32}P ($1 \times 10^8 \text{ cpm}/\mu\text{g}$) by random priming according to the manufacturers protocol (random decamer primer, Ambion; Megaprime-Kit, APB). Therefore, 25ng of cDNA in TE (from PCR or insert digestion) are mixed with sterile water to a total volume of 31µl. After adding 5µl of the decamer primer the probe is boiled for three minutes and cooled down at RT for 15 minutes. 10µl of the dNTP containing labelling buffer is added prior to the addition of the 2µl Klenow DNA polymerase. Afterwards, the probe is mixed with 2µl $\alpha\text{-}^{32}\text{P}$ dCTP (APB) and shortly centrifuged and transferred to 37°C for 30 minutes of labelling reaction. For removing the superfluous dNTPs the sample is loaded to a G-50 sephadex column (ProbeQuant, APB) and centrifuged for two minutes at 2,500rpm. Incorporation of radioactive nucleotides is monitored by scintillation counting. The probe is denatured by incubating five minutes at 100°C and immediate cooling on ice. The probe can now be used in hybridization analysis (i.e. Northern Blot).

First strand synthesis and radioactive labelling

For reverse transcription *in vitro*, an RNA-dependent DNA polymerase activity and a hybrid-dependent exoribonuclease (RNase H) activity of the reverse transcriptase enzyme (RT) were utilized to produce single-stranded labelled cDNA from RNA. The SuperScript reverse transcription system (Invitrogen) was used to produce random primed first strand cDNA from 2µg of mRNA as starting material. This amount of RNA was diluted to a volume of 10µl and 1µl of random hexamer primer ((dN)₆) is added. After denaturing the RNA samples for 10 min at 70°C under soft shaking and immediate chilling on ice for 2 min the SuperScript mix is added to each reaction:

6.0µl 5x RT buffer (Invitrogen)
3.0µl 0.1M 1,4-dithiothreitol (DTT)
1.5µl dNTP mix (20mM dATP, 20mM dGTP, 20mM dTTP,
0.1mM dCTP)
1.0µl RNase Block (Ambion)
7.0µl $\alpha^{32}\text{P}$ dCTP (10µCi/µl, Amersham)

A two minute incubation period under soft shaking is prior to the addition of the 1.5µl SuperScript reverse transcriptase (200U/µl). First strand synthesis is performed during 60 min at 37°C. Hydrolyzation of the probe is done by adding 3.5µl 3M NaOH, 10µl 1M Tris-HCl (pH 7.4), 10.5µl 1M HCl and incubation for 20 min at 68°C. The purification of the probe is done by applying it to a G-50 sephadex column and centrifugation. The whole amount of this reaction is object to hybridization on a microarray describe in the consecutive section.

Nucleic acid analysis by hybridization

Northern blot analysis

For the detection of transcript levels of immobilized and separated RNAs radioactive labelled probes ($\alpha^{32}\text{P}$ dCTP, procedure described above) against TN-R, ICAP, $\beta 1$ integrin and GAPDH were produced by PCR against plasmid DNA containing the respective insert. The protocol* described here resembles the classical capillary blot (Sambrook et al. (1989)) to transfer size separated RNA onto a membrane. Therefore, 2 µg of different RNA samples are resolved in formaldehyde and formamide containing sample buffer and are separated in a formaldehyde agarose gel at 80 V for 3 - 4 h at room temperature. The capillary blot is assembled to transfer the ribonucleotides overnight by 10x SSC at room temperature to Hybond XL nylon membrane (APB). Ribonucleotides were crosslinked to the membrane by UV light exposure.

*[The set-up of the Northern Blot was performed in cooperation with Dr. John Neidhardt (Inst. Mol. Genetik, Uni Zürich, CH)]

RNA *in situ* hybridization on cryosections

The used sense and anti-sense RNA probes are generated by transcribing cDNA from a PCR reaction. This PCR introduces T7 (sense) or T3 (anti-sense) RNA polymerase promotor sequences at the 3'-position to the respective cDNA fragment that is amplified from plasmid DNA. The transcription reaction in which the RNA is labelled with DIG is performed using the MEGAscript-kit (Ambion) according to the manufacturer's protocol (see section "RNA in vitro Transcription and Labelling" above). Performing non-radioactive detection of mRNAs, 14µm sections are cut from fresh-frozen (or embedded in Tissue-Tek, Sakura Finetek Zoeterwoud, NL) tissue on a cryostat and mounted on

SuperFrost Plus (Menzel-Gläser Braunschweig, D) microscope glass slides. The sections are fixed in 4% paraformaldehyde in phosphate-buffered saline (pH 7.3) overnight. The next day, sections are washed three times in 1x PBS, treated with 0.1M HCl for 20 min, acetylated in 0.1M triethanolamine containing 0.25% acetic anhydride and dehydrated in an ascending ethanol series. Finally, sections are air dried and prehybridized for 3 hours at 37°C with hybridization mix. Hybridization with the DIG-labelled probes occurred at 55°C overnight in humid chambers. DIG-labelled probes are diluted 1:250 to 1:1,000 in hybridization buffer. After hybridization, sections are washed twice in 0.2x SSC at 55°C, followed by three washing steps in 0.2x SSC containing 50% formamide (for each 90 minutes at 55°C). To prevent unspecific binding, sections are incubated in blocking buffer for 30 min before anti-DIG AP-conjugated antibodies (Roche Diagnostics, Mannheim, Germany), diluted 1:2,000 in blocking buffer, are applied overnight at 4°C. To remove unbound antibody, sections are washed twice in DIG-buffer 1 for 15 min. The washing solution was poured off and the sections are equilibrated for 5 min with DIG-buffer 3. The signal is developed in the dark with DIG-buffer 3 containing 0.35g/l 4-nitroblue tetrazolium chloride (NBT, Roche Diagnostics), 0.175g/l 5-bromo-4-chloro-3-indolyl phosphate (BCIP, Roche Diagnostics) and 0.25g/l levamisole (Sigma-Aldrich) until signals become visible under a stereo microscope. Sense probes, developed in parallel under the same conditions as the anti-sense probes, do not show any labelling. Finally, sections are washed in 1 x PBS and coverslipped.

Expression profile analysis by cDNA array

In order to detect transcript levels of a high number of genes in one experiment the hybridization of labelled probes to immobilized, arrayed cDNAs is utilized. These so called microarrays were set up by Dr. Holger Eickhoff and colleagues at the Lehrach group of the Max-Planck-Institute for Molecular Genetics (Berlin, D). Therefore, a library of 60,000 mouse mRNAs was used as a template for oligo-fingerprinting (see also introduction). RNAs of embryonic mice of day nine and twelve were pooled for that purpose. By cloning the resulting DNA fragments into the pSPORT-vector 6,000 clones emerged, each representing one mRNA species. Performing colony PCR with pSPORT-primers amplifies the desired insert. This PCR product is spotted directly on the Amersham Hybond-N+ nylon membrane. The spotting is done by a self-made arraying robot that uses 384 needles at a time (five times in a row). These pins have a spotting diameter of 250µm. 384 well microtiter plates contain the PCR-products that are subject to being spotted in two destinations on one array (duplicate spotting). 14 of these 384 well plates were spotted on one array so that there are about 11,000 single spots of dsDNA PCR-products immobilized. To generate ssDNA on the membrane they are processed after spotting by incubation with NaOH, washing with SSC (detergent), drying at 80°C and exposure to UV-light. For hybridization, sets of poly A+ mRNAs (total RNA also possible) are (dN)₆-random

primed to undergo first strand synthesis (described in a previous section). 10 μ Ci/ μ l α^{33} P dCTP is used for radioactive labelling during reverse transcription. In comparison to α^{32} P dCTP, that is taken for labelling Northern Blot probes, α^{33} P dCTP labelled array probes have the advantage that no unsharp signals by "signal bleeding" occurs. In regard to the small diameter of the spots on the array and their low distance between each other this effect is undesirable. That is why the four fold lower sensitivity of α^{33} P dCTP is accepted. The α^{33} P dCTP-cDNAs are hybridized to the arrays at 65°C for approx. 60 hours in modified Church Buffer. Prior to the hybridization procedure and afterwards the membranes are washed twice for 20 min with 2x SSC, 0.1% SDS, 50mM Na₂HPO₄ at RT. Additionally, two washing steps in 0,1x SSC, 0,1% SDS, 4mM Na₂HPO₄ for 20 min at 65°C are following. The radioactive labelled membranes are exposed to Fuji phosphoimager detection plates for several hours and measured at highest resolution in a BAS 5500 series phosphoimager. The resulting pictures are processed by software of GPC AG VisualGrid and Adobe Photoshop for analysis.

modified Church buffer
500ml 1M Na₂HPO₄
500ml 10%SDS
2ml 0.5M EDTA

20x SSC
880g NaCl
440g trisodiumcitrate
ad 1l H₂O dest.

Computer aided evaluation of array data

The read-out of the data from the 11,000 array spot intensities is performed by an automated software program (VisualGrid, GPC). It takes the autoradiograph from the phosphoimager and automatically positions a read-out-grid. This grid has to be adjusted manually for higher accuracy. VisualGrid software calculates the spot intensities in comparison to background (blank space) and duplicate spots on one array. Additionally, the software correlates the signal intensities of corresponding spots on the second array, indicating divergent positions. The divergences are putatively dysregulated transcripts but can also be false positive artifacts (due to fall-out in the respective position). Therefore a manual inspection of the designated areas has to be done. Only signals are taken into account that are not affected by hybridization artifacts and are above the threshold of a minimal 1.5 fold intensity change between the correlated samples. The accuracy of the hybridization experiment is evaluated by correlating two arrays hybridized to the same sample. In this case the correlation coefficient should be almost $r=1$ and the correlation plot a slim median cloud (see figure 1).

Immunohistochemistry

Immunofluorescence on cryosections

For indirect Immunofluorescence 14 µm sections are cut from the designated tissue embedded in Tissue-Tek (Sakura Finetek Zoeterwoude, NL) on a cryostat and mounted on SuperFrost Plus (Menzel-Gläser Braunschweig, D) glass slides. Sections are air-dried and surrounded with a Pap-Pen (Kisker Steinfurt, D) to minimize the amount of the used antibodies. Sections are fixed in methanol for 10 min at -20°C and rehydrated in 1 x PBS for 10 min. To prevent unspecific binding of the primary antibodies, sections are incubated in the appropriate preimmune-serum for 30 min at RT. Sections are incubated with the primary antibodies in a humid chamber at 4°C overnight. Sections are washed four times with 1 x PBS to remove unbound antibodies. To visualize the primary antibodies, fluorescence labelled secondary antibodies (Cy3/FITC/ Cy5, Dianova, Hamburg, D) are diluted 1:200 in 1 x TBST and applied to the sections for 45 min at RT in the dark. Sections are washed four times with 1 x PBS to remove unbound secondary antibodies and coverslipped with Aqua/PolyMount. The analysis is performed with an Axiophot fluorescence microscope equipped with digital camera.

Immunofluorescence on coverslips

Cells from cell culture experiments are generally seeded and grown on cover slips in twelve well dishes when they are object to fluorescence labelling. Prior to fixation through 4% PFA they are washed with 1x PBS. The fixation period is 30 min. Afterwards the fixans is removed by washing three times with 1x PBS. Preimmune incubation is performed with 0.1% BSA for 40 min. The application of diluted primary antibody is performed 1h at RT. After washing with 1x PBS the secondary antibody is applied for 30 - 40 min. Exceeding this time reveals higher background fluorescence. Before mounting the cover slips on a glass slide and sealing it in Aqua/PolyMount a last washing step with 1x PBS is performed. For neurite outgrowth analysis the slides are examined with an Kontron microscope equipped with digital camera and measurement software for qualitative analysis the more sensitive Axiophot microscope is used.

ES cell culture

The cells that were used in these experiments are ICAP deficient ES cells and their respective wildtype cell line. The homozygous knock out cell lines are termed "15" and "21". The cell line from which they are derived is termed "LW1", the respective wild type. These cells were generated in the laboratory of Dr. D. D. Chang (UCLA Los Angeles, USA) and are kindly provided for our experiments. The feeder cells (murine embryonal fibroblasts,

MEF) on which ES cells have to be seeded initially, are prepared and provided by the ZMNH service group for transgenic animals. Expansion and treatment of the MEF cells with cytostatic mitomycin C (MMC, Sigma) is self-performed. In cell culture experiments dishes from Greiner Bio-One (Frickenhausen, D) and TPP (Trasadingen, Ch) are used. The components for media are purchased at CHEMICON international (Temecula CA, USA), GIBCO Invitrogen (Karlsruhe, D), PAA (Linz, A), Roth (Karlsruhe, D), Sigma-Aldrich (Deisenhofen, D) and tebu-bio (Offenbach, D) respectively.

Differentiation of ES cells

The differentiation of ES cells towards neural precursors is performed according to the previously describe procedure (Lee et al. (2000)). This protocol directs the undifferentiated ES cells towards the neural lineage by a multi-step procedure. Each step contains media in a different composition and different growth conditions (free floating/adherent). Briefly, it starts with seeding MMC treated MEF cells on gelatin (0.1% sterile gelatin in H₂O) coated culture dishes at a density of 5×10^4 cells per cm² containing MEF-medium. After at least twelve hours the ES cells can be thawed and seeded in ES-medium containing LIF to give rise to 2.5×10^4 ES cells per cm². The medium has to be exchanged every day and passage is performed through trypsinization. For getting rid of MEF cells at least one passage of ES cells has to be grown on gelatin coated culture dishes. The next step makes use of uncoated and untreated bacterial dishes for non-adherent growth of ES cells. In this step 2 - 2.5×10^4 ES cells per cm² are grown in ES-medium lacking LIF for aggregation and formation of free floating embryoid bodies (EB). This period takes four to five days and requires three times of daily soft shaking of the dishes for prevention of adherence. The color of the medium should be monitored and exchange should take place on day three. Differentiation is happening by transferring the EB's to cell culture dishes containing ITSFn-medium in 1:1 or 1:2 ratio of EB-dish to ITSFn-dish. EB's attach to the dish and cells migrate out of the cluster. A large portion of cells die and medium should be exchanged at least every second day. This stage takes five to twelve days and the majority of cells are nestin positive precursor cells. There are already many young β III tubulin positive neurons at the time point of 5 days in ITSFn-medium in case of the ES cells derived from the Chang lab. This is why this stage was taken for neurite outgrowth experiments (see figure 16). The expansion of the resulting neural precursor cells are performed by passaging the cells in mN3F(L) at a seeding density of $0.5 - 2.0 \times 10^5$ cells per cm² in poly-L-ornithin (15 μ g/ml in H₂O) coated culture dishes. The medium has to be exchanged every second day and this step takes five days prior to freezing the cells in liquid nitrogen.

MEF-medium

500ml

Dulbecco's MEM with GlutaMAX (DMEM)

50ml	fetal bovine serum (FBS research grade, EU approved, Perbio)
6.2ml	MEM non-essential amino acids 100x
6.2ml	Penicillin/Streptomycin (Pen/Strep, 5,000 U Pen. and 5,000µg/ml Strep. 100x)

Trypsin for MEF

trypsin/EDTA (0.05% trypsin; 0.5g/l trypsin and 0.2g/l EDTA)

Trypsin for ES

trypsin/EDTA (0.25% trypsin and 1mM EDTA)

ES-medium

500ml	DMEM with 25mM Hepes, 4,500mg/l glucose and with pyridoxine
92ml	FBS
6.2ml	L-glutamine (200mM, 100x)
6.2ml	MEM non-essential amino acids 100x
6.2ml	Na-Pyruvate MEM (100mM)
6.2ml	Pen/Strep
6.2ml	nucleoside-mix*
1.24ml	2-mercaptoethanol (50mM, 1,000x)
62µl	LIF (10 ⁷ U/ml, recombinant, Cemicor)
[4-10µl/ml]	G418 (Geneticin 50mg/ml) in case of selection]

*Nucleoside-mix

80mg	adenosine
85mg	guanosine
73mg	cytidine
73mg	uridine
24mg	thymidine
ad 100ml in PBS at 37°C and 0.1µm filtration, store at -20°C	

ITSFn-medium

100ml	DMEM/F-12 nutrient mixture (1:1)
50µl	insulin (10mg/ml in 10mM HCl)
100µl	transferrin (50mg/ml)
300µl	selenium chloride (10µM)
500µl	fibronectin (1mg/ml)
1240µl	L-glutamine (200mM)

mN3F(L)-medium

100ml	DMEM/F12
250µl	insulin
100µl	transferrin
1µl	progesterone (2.0mM)
167µl	putrescine (60mM)
300µl	selenium chloride
100µl	FGF2 (20µg/ml)
(100µl	laminin (1mg/ml))

1240µl

L-glutamine

Two milligrams of the cytostatic compound MMC is diluted in 2ml 1x PBS and 150µl aliquots (suitable for treatment of a 15cm diameter culture dish with 15ml medium) are stored in the dark at -80°C. Medium for cell storage in liquid nitrogen is set up from 50% FBS, 10% dimethylsulfoxide (DMSO, Sigma) and 40% DMEM.

Neurite outgrowth of differentiated ES cells

For measuring the performance of the different cell lines in neurite outgrowth experiments they are grown on 15mm diameter cover slips in twelve well plates. For a comparison of the reaction to different growth substrates, pre-coated (poly-L-ornithin, PLO) cover slips are covered with the specific substrate (i.e. TN-R fragments) on top. Therefore, acetone washed and autoclaved cover slips are exposed to ultra violet light for a minimum of 15 min. Then they are put in a dish with PLO solution (15µg/ml) for at least 1.5 hours. The PLO is discarded and the cover slips are washed with H₂O dest. and air dried under a clean bench. The coating with the specific substrate on top is performed in a moisture chamber at 4°C over night. Therefore, the chamber is equipped with parafilm on which 25µl (i.e. 100µg/ml EGF-S fragment of TN-R) of the substrate is placed as a drop. On the substrate drop the cover slip is placed and the chamber is sealed. These cover slips are then placed in twelve well cell culture dishes where the cells are seeded in. In my experiments, the cells are grown on the coated coverslips for five days in the ITSFn medium and are fixed afterwards for immunofluorescence like described in the previous section "Immunofluorescence on Coverslips". Fluorescent detection is performed with a Kontron microscope equipped with a Hamamatsu CCD digital camera. The βIII tubulin labeled neurites are measured making use of a length measurement makro of the KS 400 software (version 2.0, Zeiss). Therefore, the cover slip is scanned for neurites that are not interfering with others. With the 20x objective a picture is acquired at typically +13db and 1.6 seconds exposure (for Cy3 filter). This picture is processed by the KS 400 software and each neurite is outlined manually for length measurement. The data evolving from at least three independent experiments are evaluated by SigmaPlot software (SigmaPlot 5.0 SPSS Inc. Richmond, USA) and subject to an unpaired t-test.

Protein analysis

Protein extraction from murine tissue

Murine tissue samples, freshly prepared or frozen, are Dounce homogenized in lysis buffer on ice. Homogenates are centrifuged at 20,000x g at 4°C for 30 min to remove insoluble material, and

the supernatants are collected. After freezing supernatants at -80°C , the centrifugation step is repeated, and the supernatants are collected and stored at -80°C .

Lysis buffer
20mM Tris-HCl (pH 7.4)
150mM NaCl
0.5% (w/v) Nonidet P-40
1x Complete proteases inhibitors mix (Roche)

Protein quantification

Protein concentrations are determined with the Micro BCA protein assay (Pierce Chemical Co., Rockford, IL). Solutions A and B are mixed in a ratio of 50:1 to give the BCA solution. 10 μl of lysates or dilutions thereof were mixed with 200 μl BCA solution in 96-well microtiter plates and incubated for 30 min at 37°C . A BSA standard curve was co-incubated ranging from 0.1g/l to 2g/l. The extinction of the samples was determined at a wavelength 560nm in a microtiter plate reader (MICRONAUT Skan, Merlin, Bornheim-Hesel, D).

Protein gel electrophoresis

The separation of proteins respective of their size is performed like described by Lämmli (Lämmli (1970)). Therefore, 10% (or 12%; volumina in brackets) SDS-polyacrylamide (PA) gel electrophoresis (SDS-PAGE) under reducing conditions using the Mini-Protean II system (Bio-Rad) is carried out. The used PA gels have following properties:

stock solution	resolving gel	stacking gel
0.5M Tris HCl pH 6.8	-	1.25ml
1.5M Tris HCl pH 8.6	2.0ml	-
30/0.8% acrylamide/ bisacrylamide	2.66ml (3.2ml)	0.75ml
H ₂ O dest.	3.24ml (2.7ml)	2.96ml
20% SDS	40 μl	25 μl
10% amonumpersulfate	64 μl	25 μl
tetraethylenediamine (TMED)	5 μl	5 μl

The volumina described are for standard 0.75mm width gels. For thicker gels (1.5mm) the respective volumina have to be doubled. After polymerization of the PA gel, the chamber is assembled as described by the manufacturer's protocol. Samples with a volume up to 25 μl (exceeding volumina are loaded on thicker gels) are loaded and the gel is run at constant 100V for approx. 15 min and then at 200V for the remainder. The run is stopped when the Pyronin Y running front reaches the end of the gel. In the following, gels are either stained (coomassie/silver staining) or subjected to Western blotting (see below).

Coomassie staining of protein gels

After SDS-PAGE, PA gels are stained in staining solution (1 h, RT) with constant agitation. The gels are then incubated in destaining solution until the background of the gel appears nearly transparent. To fix staining patterns, destaining solution is exchanged against 10% (v/v) acetic acid.

Staining solution	Destaining solution
45% (v/v) ethanol	45% (v/v) ethanol
10% (v/v) acetic acid	10% (v/v) acetic acid
2.5 g/l Coomassie brilliant blue R250	

Silver staining of protein gels

Silver staining of PA gels is performed as described (Morrissey 1981 Anal Biochem 117 (2)). Briefly, gels are incubated for 30 min in Fixing solution 1, 30 min in Fixing solution 2, followed by another fixing step for 30 min in 10% (v/v) glutaraldehyde solution. After rinsing the gel for 2h with H₂O, an incubation in a 5µg/ml DTT solution for 30 min follows. Afterwards, the gel is soaked for 30 min in a 0.1% (w/v) AgNO₃ solution. Rinsing once with H₂O is followed by developing the staining pattern by soaking in developer. Progressing staining is stopped by addition of 2.4 g citric acid per 100 ml developer. Several washes with H₂O follow this staining protocol.

Fixing solution 1	Fixing solution 2
50% (v/v) methanol	5% (v/v) methanol
10% (v/v) glacial acetic acid	7% (v/v) glacial acetic acid
Developer	
30g/l Na ₂ CO ₃	
0.06% formaldehyde solution (37%)	

Western blot analysis

Proteins are transferred from PA gels after SDS-PAGE (see above) onto a nitrocellulose membrane (Protean Nitrocellulose BA 85, 0.45µm, Schleicher & Schuell, Dassel, D) using a MINI TRANSBLOT apparatus (Bio-Rad). After equilibration of the PA gel in blot buffer for approximately 5 min, a blotting sandwich is assembled as described in the manufacturer's protocol. Proteins are transferred at 4°C in blot buffer at constant voltage (80V for 2 h or 35V overnight). The prestained marker BENCHMARK (Invitrogen) is used as a molecular weight marker and to monitor successful protein transfer after blotting.

Blot buffer
192mM glycine
25mM Tris
10% (v/v) methanol
0.1g/l SDS

After electrophoretic transfer, nitrocellulose membranes are

removed from the sandwiches and placed protein-bound site up in glass vessels. Membranes are washed once in TBST for 5 min and were subsequently blocked for 1 h in TBST complement with 2% skimmed milk powder under gentle shaking at RT. Incubation with an appropriate antibody dilution, in TBST, is performed either for 2 h at RT or overnight at 4°C. The primary antibody solution is removed and membranes are washed 3x 10 min with TBST under shaking. The appropriate horseradish peroxidase (HRP)-conjugated secondary antibody is applied in a dilution of 1:10,000 in TBST for 1h at RT. The membrane is washed again 6x 5 min with TBST. Immunoreactive bands are visualized using the enhanced chemiluminescence detection system (APB or Pierce). The membrane is soaked for 5 min in detection solution (1:1 mixture of kit-supplied solutions I and II). The detection solution is drained off and the blot is placed between plastic foils. The membrane is then exposed to BIOMAX ML for several time intervals, starting with a 1min exposure.

TBST
10mM Tris-HCl (pH 7.6)
150mM NaCl
0.05% (v/v) Tween 20

Immunoprecipitation

To show interactions of proteins antibodies can be crosslinked to protein G magnetic beads (rat, Dynal). The bound antibody binds specifically the protein against which it is directed. If this protein is also bound to others the whole complex can be pulled down with the magnetic beads and analyzed in Western analysis.

The crosslinking of protein G magnetic beads to an antibody is performed through taking 300µl of beads and washing them twice in PBS at pH 7.4. Prior to the addition of 15 to 50µg antibody that is diluted in a total volume of 100µl, the beads are eluted in 300µl PBS. The mixture is rotated for 30 min. Thereafter it is washed three times with 1000µl PBS. The crosslinking reaction is started by adding 1mg *Bis*[Sulfosuccinimidyl]suberate (BS³, Pierce) that is linking primary amino-groups. The incubation period takes 60 to 120 min. Afterwards the magnetic beads with the now bound antibody are washed six times in TBS at pH 7.4 and finally once with PBS prior to elution in 300µl PBS. The beads can now be used to precipitate protein complexes or can be stored away at 4°C.

Precipitation is performed through incubating protein solutions/homogenates with the beads over night. The supernatant is taken off through short spinning (10 seconds) in a centrifuge and stored away. The beads are washed with 1ml of wash buffer I. After another short centrifugation the supernatant is discarded and the washing step is repeated two times. Then, the beads are washed in wash buffer II three times and the supernatant has to be removed thoroughly after the last washing step. The sample can now be resuspended in "Lämmli" protein loading buffer and analyzed by PAGE and Western blot.

wash buffer I
20mM HEPES pH 7.5
150mM NaCl
0.1% NP-40 detergent

wash buffer II
20mM HEPES pH 7.5
150mM NaCl

Proliferation assay

MTT test

For viability assays 5×10^3 cells in 100 μ l are seeded into 96-well microtiter plates. Cell survival is judged by phase contrast microscopy and assayed using the methylthiazolotetrazolium (MTT) method (Hansen et al. (1989)). The conversion of the tetrazolium salt (MTT) to colored formazan through metabolic active cells serves as an indirect measurement of cell growth and is monitored by this method. Briefly, MTT (Sigma) solubilized in phosphate buffered saline (PBS, 5mg/ml) is added to the cells to a final concentration of 1mg/ml. Two hours later, cells are lysed by addition of 125 μ l of lysis buffer containing 50% dimethyl formamide, 20% sodium dodecyl sulfate, 2% acetic acid, adjusted to pH 4.7 and incubation at 37°C. Absorbance is measured after 24 hours at a wavelength 550 nm using a microplate reader.

Trypan blue exclusion assay

Routinely, when cells are passaged and the number of cells per volume has to be assessed or for measurement of cell death this assay is performed. Trypan blue selectively stains dead cells. For trypan blue exclusion cells are trypsinized and resuspended in a suitable amount of fresh medium. 100 μ l cell suspension and 10 μ l 0.4% trypan blue (Sigma) are mixed. Viable cells per microliter are counted using a Neubauer cell counting chamber to calculate total cell number.

Sphere diameter

For assessing the proliferation of cells that are growing in free floating spheroid structures like the embryoid bodies (EB) the diameter of the spheres are measured. Therefore, the culture dishes were examined under an microscope with inverse optical pathway and equipped with an ocular micrometer. The diameter of 60 random selected clonal, separated and round EB's is measured per group and timepoint. The numbers given on the ocular micrometer serve as arbitrary units. The arbitrary units are not calculated to absolute values because the experiment is comparing identically measured groups.

KAPITEL 3

Ergebnisse *Results*

The results section contains two major parts. The first describes the analysis of gene expression in case of the TN-R deficient mouse. Furthermore, the findings and evaluation of the detected dysregulation is recounted. The second part outlines how the function of the dysregulated ICAP is analyzed and the *in vitro* findings which are made.

Detection of dysregulated transcripts in the tenascin-R deficient mouse brain

The cDNA array suggests several dysregulated molecules

Analyzing knock out mice is a common procedure for gaining new insights in the function of the missing gene. Severe phenotypes indicate the importance of a molecule whereas an unpredictable mild phenotype suggests redundancy and compensatory effects. Detecting these effects is done by expression profiling. In the case of the TN-R deficient mouse the rather mild phenotype suggests compensatory effects. Therefore the microarray analysis is performed with female TN-R deficient mice of P14 from homozygous breeding and the wildtype counterparts of C57BL6. In this work material only from female mice is used. For genotyping the mice a PCR is set up on genomic DNA. In this PCR primers against a part of the Y-chromosome specific Ube1y pseudogene (Chang and Li (1995); yA: 5'CGG CAC ACC CAG TAT TCT CAC 3'; yB: 5'AGG TGA GAG GAT GTG GAC AGC 3'; amplicon: 670bp) are used.

The labelled total brain mRNA probes of the female mice are subject to microarray hybridization. In the experiment three arrays are hybridized to probes derived from the TN-R deficient

mice and three arrays to the wildtype probes. A comparison of two arrays hybridized to the same wildtype probe reveals a very good correlation coefficient of 0.9688 indicating that artifacts and false positive signals are below the 5% margin (see correlation plot below).

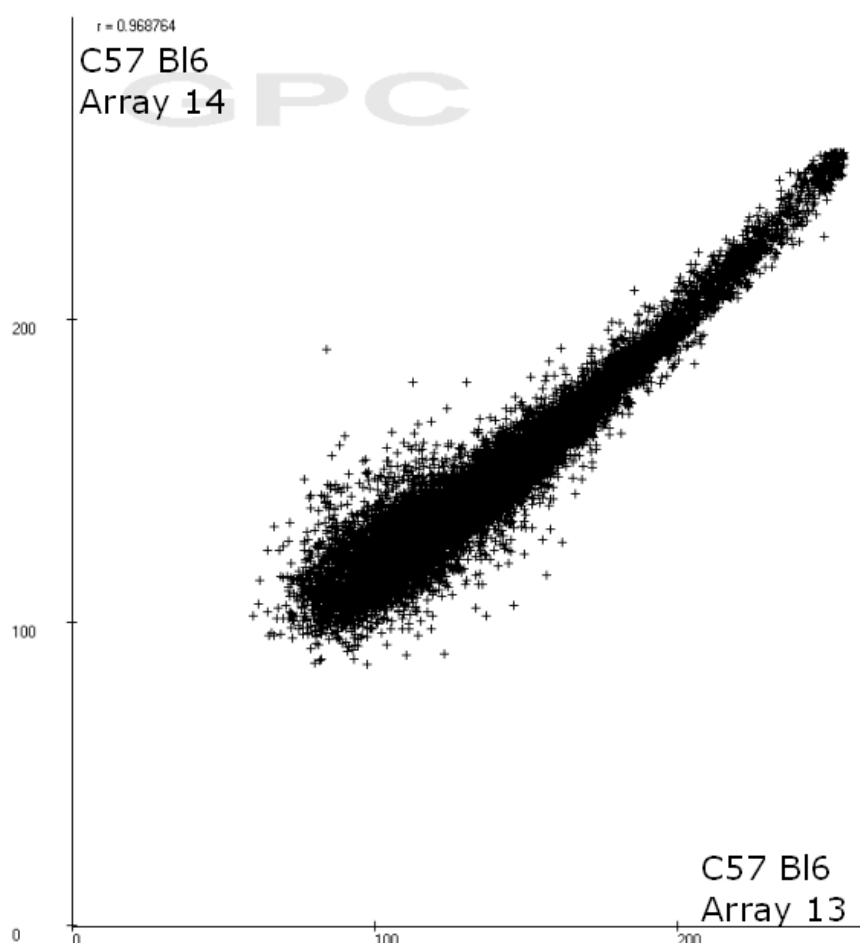


Figure 1 Correlation plot of array signals from the same probe

The plot shows the correlated signal intensities from two arrays (13= x-axis; 14= y-axis) hybridized to the same sample depicting the reliability of the experiments ($r=0.9688$).

In the comparative situation the correlation between the wildtype and the knock out signals is much lower ($r= 0.5523$) than in the control correlation mentioned above ($r= 0.9688$). This difference indicates the dysregulation in the gene deficient animal. The correlation plot below shows a bolder correlation cloud with more values lying outside the cloud. These separated values represent the strongest dysregulated molecules. Especially, in case of the knock out situation there are a number of upregulated molecules.

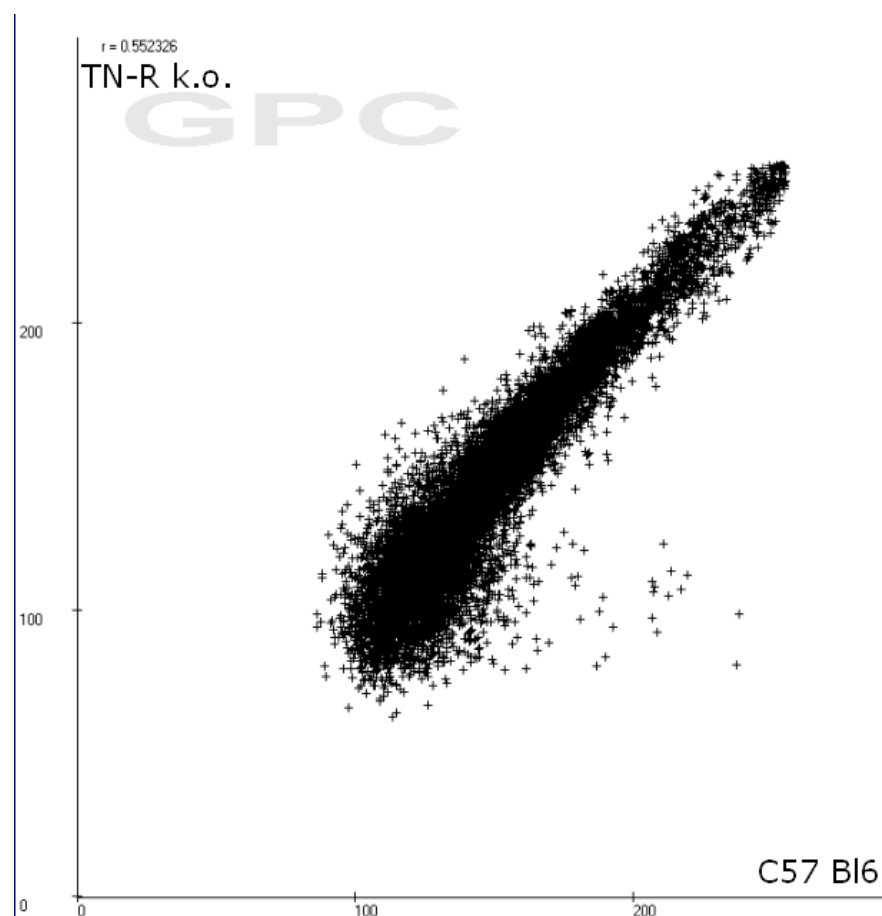


Figure 2 Correlation plot of array signals comparing k.o. and WT situation
 The plot shows the correlated signal intensities from two arrays (WT C57Bl6= x-axis; TN-R k.o.= y-axis) depicting the dysregulation in the comparative situation. The signals that are lying separate from the cloud represent the highest dysregulated molecules.

Entering the data into the analysis software and evaluating the putative dysregulated signals in respect to hybridization artifacts and regulation threshold of 1.5 fold (minimal difference in signal intensity) gives rise to a list of signals (see table 2). The highest upregulation is suggested for the expressed sequence tag vy95h07.r1 (IMAGE consortium, <http://image.llnl.gov>) with a 2.9 fold increase in the knock out. A nucleotide database search (BLAST; <http://www.ncbi.nlm.nih.gov/blast>) results in no noteworthy similarities so that the identity of the corresponding transcript remains unclear. Ue20a10.y1 (IMAGE) is another expressed sequence tag (EST) that is upregulated (1.8 fold). Performing a blast search reveals such a significant similarity to the mouse heterogeneous nuclear ribonucleoprotein A1 (hnRPA1, hnRNP A1 Glisovic et al (2003)) that it can be assumed identical (98% identical nucleotides (nt), 17 nt - 736 nt). This protein has influence the splicing process by stabilizing mRNA's through binding to the hairpin loop. This prevention of mRNA degradation

yields higher mRNA levels. Further analysis is performed on the 1.9 fold upregulated GAPDH, also the 1.9 fold upregulated bodenin (ICAP) and the 1.7 fold higher bamacan signal.

1 TN-R intens	1BG	2WT intens	2BG	factor	Δ intens	Δ BG	signal identity
103.21	126.49	164.09	136.12	1.60	60.88	51.25	human ubiquinol cytochrome-c reductase core I protein
99.02	126.49	168.57	138.48	1.70	69.55	57.56	mus musculus Xist gene 5' region
122.90	127.47	211.20	123.23	1.70	88.30	92.54	rattus norvegicus basement membrane associated 4104 (Bamacan)
104.43	126.49	189.24	136.12	1.80	84.81	75.18	EST ue20a10.y1
109.83	126.03	206.83	135.88	1.90	97.00	87.15	mus musculus bodenin gene
108.01	126.03	207.75	135.88	1.90	99.74	89.89	mus musculus glyceraldehyde 3-phosphate dehydrogenase (GAPDH) mRNA
104.77	127.90	212.93	121.18	2.00	108.16	114.88	mus musculus type II DNA topoisomerase beta mRNA
81.00	126.49	237.22	136.12	2.90	156.22	146.59	EST vy95h07.r1

Table 2 Detected signal intensities of TN-R^{-/-} and WT hybridized arrays

1TN-R: signal intensity for the TN-R^{-/-} probe hybridized array; 1BG: background intensity for the TN-R^{-/-} probe hybridized array; 2WT: signal intensity for the wildtype probe hybridized array; 2BG: background intensity for the wildtype probe

hybridized array; factor: fold increase of signal 1 compared to signal 2; Δ intens: absolute mean difference of signal intensity; Δ BG: absolute difference of background intensity; signal identity: the name of the spotted clone derived from nucleotide database

The array hybridization experiment can be seen as a “reverse” Northern Blot. In the next figure the areas where the ICAP and bamacan signals are observed are displayed.

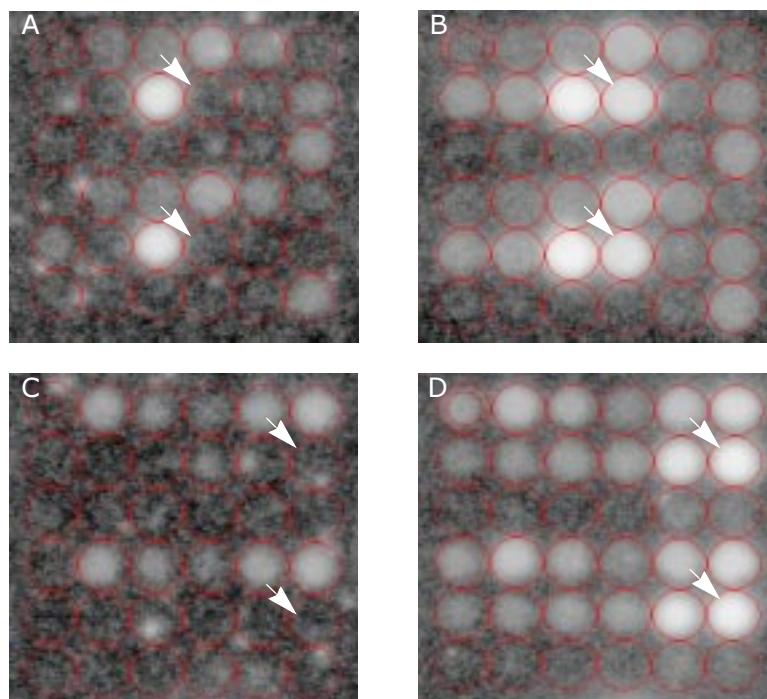


Figure 3 Close up of cDNA array autoradiograph

In A and C magnified areas of arrays hybridized to the ^{33}P -labelled WT probes are displayed. B and D show the same areas hybridized to the ^{33}P -labelled k.o. samples. The arrowheads in A and B point out the bamacan signal position and in C and D the position for the ICAP signal. In comparison (A+B; C+D) the upregulation in the k.o. situation is suggested by the array experiment for both molecules. The red grid is positioned by the evaluation software.

The arrowheads in A and B indicate the position of the bamacan signal. In A the ^{33}P -labelled WT sample is hybridized producing no signal in the bamacan area. The k.o. sample gives rise to a clear signal in the bamacan region as seen in B. In C and D the arrowheads are marking the areas where the ICAP cDNA is spotted. The respective areas are without a signal in case of the ^{33}P -labelled WT probe (C) and give rise to a strong signal in case of the ^{33}P -labelled k.o. probe (D). In both cases (bamacan and ICAP) the array suggests an upregulation of transcripts in the TN-R deficient mouse brain. Further evaluation of this matter is describe in the consecutive section.

Detailed investigation confirms ICAP dysregulation in total

brain

Proofreading of the cDNA sequences spotted on the array is a first step in confirmation of the array experiment results. Therefore, clones from the spotting masterplates undergo sequencing. All cDNA inserts are cloned equally into the pSPORT vector and are amplified in the sequencing reaction from the 5' end with primer ForwMPI (5' ACT CCG CCC AGT TCC GCC CAT TCT 3') and with RevMPI (5' AAG CAG CAA GCA TAT GCT AGT TTA ACA CAT TA 3') from the 3' position. The sequencing results are confirming the bamacan and ICAP sequence on the array (data not shown). To investigate the quantitative amount of transcripts and the distribution in certain brain areas the Northern Blot analysis is performed. On the first Northern membrane 3 µg of total brain RNA's are blotted. The RNA is derived from different age stages and genotypes. The lanes are loaded in an alternating order with RNA derived from TN-R deficient brains and their respective wildtype littermates (emerging from heterozygous breeding). For densitometric quantification (Tina 2.09 software) the signals of the investigated probes are calculated against the respective GAPDH signal intensities that are set as 100%.

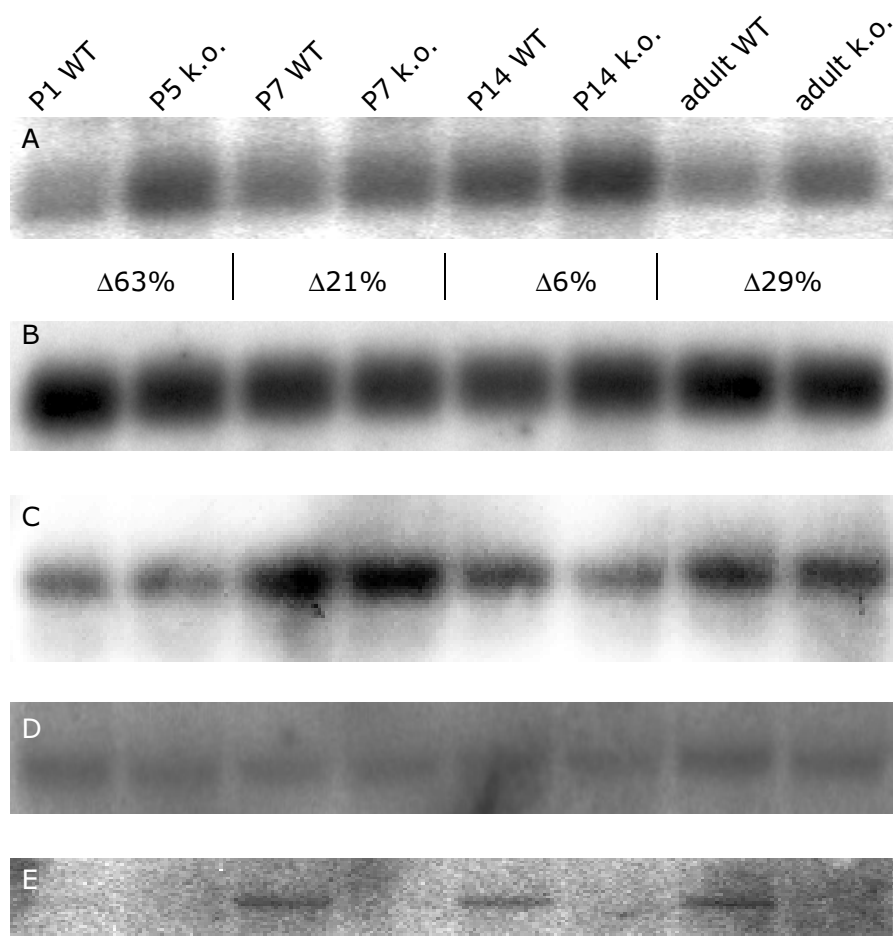


Figure 4 Northern blot autoradiographs for ICAP (A), GAPDH (B), $\beta 1$ integrin (C), bamacan (D) and TN-R (E)

The lanes represent different age stages (as marked on top from left to right:

postnatal day (P) 1, P5, 2x P7, 2x P14, 2x adult). In A the Northern Blot is hybridized to a ³²P-labelled cDNA probe specific for ICAP depicting the dysregulated transcript levels in WT compared to k.o. The densitometric signal difference is given in percentage (normalized signal intensities to GAPDH signal set as 100%). In B the levels of GAPDH signals indicate that equal amounts of RNA are loaded. The ³²P-labelled cDNA probe for β 1 integrin (C) reveals no difference between the corresponding WT and k.o. lanes of each age stage. In D the levels of ³²P-labelled bamacan probe signal does not confirm the dysregulation between WT and k.o. suggested by the array (equal levels in all lanes). The loading of the correct genotype is depicted by hybridization to a ³²P-labelled TN-R probe (E).

The presence of equal amounts of RNA loaded to the blot and the correct loading in respect of the genotype is monitored by hybridizing the membrane with ³²P-labelled cDNA probes for GAPDH and TN-R. The GAPDH probe gives rise to signals of indistinguishable levels (see B in figure 4) and the TN-R probe only produces signals in lanes where RNA from WT brains is loaded (see E in figure 4). The ³²P-labelled cDNA probe against the ICAP transcript is produced from a PCR generated template. The PCR is performed taking the pAF III-39 plasmid (pBluescript SK, mouse ICAP insert 5' BamHI - 3' XhoI, kindly provided by Prof. Dr. P. Gruss, Department of Molecular Cell Biology, Max-Planck-Institute for Biophysical Chemistry, Göttingen, D) as a template and primers bodenin2Forw (5' GGC CGT GTC TGA GGG GAA G 3') and bodenin2Rev (5' TAA GTG GAG AGT GGG CCA GA 3') amplifying a 500bp product. Such prepared probe is hybridized to the Northern membrane confirming the dysregulation in all ages stages (see A in figure 4). The levels of ICAP signals are in all cases higher in the k.o. situation. The difference between WT and k.o. are 63% in case of the comparison of postnatal day (P) 1 against P5, 21% at P7, 6% at P14 and 29% in the adult stage, respectively. The higher ICAP signal could be a secondary effect due to an upregulation of its binding partner the β 1 integrin. Signal intensities raised by the hybridization with the ³²P-labelled β 1 integrin probe (C) do not confirm such an effect and support the distinct ICAP upregulation. The levels of bamacan signals (D) do not confirm the results from the array experiment. In this case indistinguishable signal intensities are detected in the Northern hybridization. Although the Northern Blot is a more robust experimental procedure than the error-prone array it remains unclear whether bamacan is dysregulated until further methods give additional indications.

The ICAP upregulation in the k.o. situation is also investigated by reverse transcription PCR (RT-PCR). Therefore, total RNA from total brain preparations is subject to a reverse transcription (RT) followed by a PCR performed on a dilution series of the reversly transcribed cDNA (RT-cDNA). The dilution series contains photometrically determined amounts of RT-cDNA used as the PCR template. In addition to the PCR performed detecting the ICAP amplicon (approx. 500bp) the GAPDH fragment is detected by amplification with primers mGAPDHForw383 (5' GGA GCC AAA CGG GTC ATC ATC TCC 3') and mGAPDHRev837 (5' GAT GCC TGC TTC ACC ACC TTC T 3'). The levels of GAPDH signals (450bp

amplicon) serve as reference values for the ICAP signals from the corresponding lane (see figure 5).

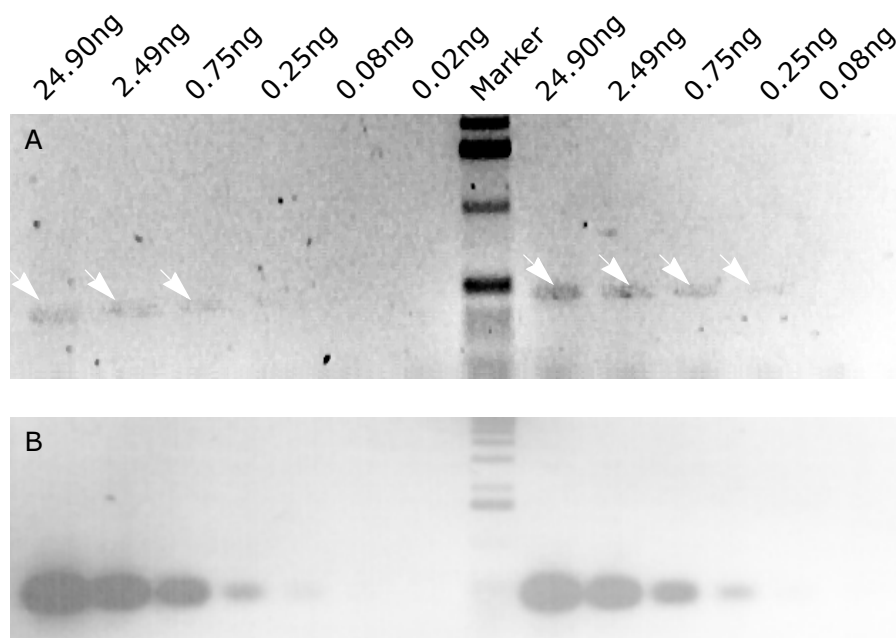


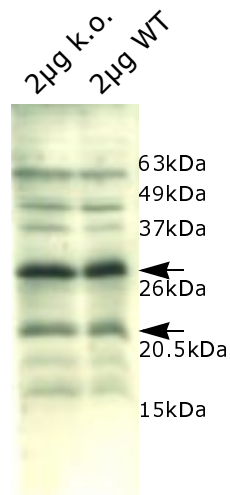
Figure 5 RT-PCR of ICAP in WT/k.o. comparison relative to GAPDH detected by agarose gel electrophoresis and ethidium bromide staining

Both gels (A and B) are loaded on the left hand with PCR products from WT sample and on the right hand with k.o. derived material. The amount of RT-cDNA used as a template is indicated on top of each lane and decreases from left to right. In A the RT-PCR reactions for the ICAP amplicon are loaded to the agarose gel. The arrowheads point out the signal position. The signals in the WT derived RT-PCR (left hand side) are weaker and only detectable in reactions down to 0.75ng of template. Whereas, the signals in the experiment depicting the k.o. situation (right hand side) are stronger and go further down to 0.25ng of template RT-cDNA. The GAPDH PCR products are visualized in B and serve as reference values and control.

The RT-PCR depicted in figure 5 is performed in both cases (A= ICAP, B= GAPDH) on the same template of RT-cDNA. The GAPDH intensities are slightly higher in the WT situation (B, left of marker) suggesting a higher presence of GAPDH transcripts in the WT template RT-cDNA. The template amount subject to GAPDH RT-PCR is equal in the WT and k.o. reaction because the signals are occurring in both at the same template concentrations up to a detection limit of 0.25ng (B, both sides of marker lane). Comparing the ICAP signal intensities in WT (A, left of marker lane) to the k.o. (A, right of marker lane) it can be found that in the WT all signals are lower than the respective k.o. ones. Additionally, in the k.o. situation there is a faint band detectable in the lane loaded with PCR reaction with 0.25ng of RT-cDNA template where none is detectable in the WT. This corroborates the ICAP upregulation in TN-R deficient mice brains indicated by array and Northern experiments.

Protein levels of ICAP

The expression level of ICAP protein is assessed with a polyclonal antibody against human ICAP-1 α (ICAP α 1035; not published; kindly provided by Dr. D. D. Chang UCLA Los Angeles, USA). 2 μ g



of Crude brain homogenates are subject to PAGE.

Figure 6 Western blot analysis of crude brain homogenate from TN-R deficient and WT mice detecting ICAP and phosphorylated ICAP

The two lanes are loaded with 2 μ g crude brain homogenate of k.o. and WT animals. The ICAP α 1035 polyclonal antibody detects several distinct bands with equal intensities in both lanes. The arrowheads indicate the ICAP-specific bands at 30 kDa (phosphorylated) and 22kDa (non-phosphorylated). Their intensities are also indistinguishable between the genotypes but indicating the ratio between the two isoforms. In both genotypes the amount of phosphorylated ICAP is much higher than the amount of the inactive, unphosphorylated isoform.

After PAGE the proteins are transferred to a nitrocellulose membrane where they are detected with the mentioned antibody. The genotypes of the protein samples are indicated on top of the lanes of figure 6. The two arrowheads indicate the bands representative for the two ICAP variants detected by the antibody. The upper band (~30kDa) is the phosphorylated form of ICAP-1 α and the lower (~22kDa) the non-phosphorylated, respectively. This blot indicates that the amount of the active and β 1 integrin binding phospho-ICAP is much higher than the inactive isoform. Alterations between the two genotypes are not detectable. The measured dysregulation on the transcript level can not be transferred to the protein level by this experiment. Unfortunately, the antibody does not work in immunofluorescence experiments, so that the protein levels can not be examined in further details. The analysis at the protein level remains a major experiment to be performed as soon as a suitable antibody is available.

Localization of ICAP dysregulation

The upregulation of ICAP is shown in the previous section for total brain. The experiments in this section are set up to localize the brain region in which this upregulation occurs or whether this effect is rather broadly distributed in the CNS. In a Northern Blot comparing adult TN-R deficient mice and their respective

littermates 3µg RNA of following brain areas is immobilized for each lane: cerebellum, cortex, hippocampus and olfactory bulb. The WT and k.o. RNA is loaded in an alternating order. The investigation of the mentioned brain areas in respect to ICAP and bamacan is performed by hybridizing ³²P-labeled cDNA probes to the blot. The probe design is mentioned in the previous section where the functionality was demonstrated.

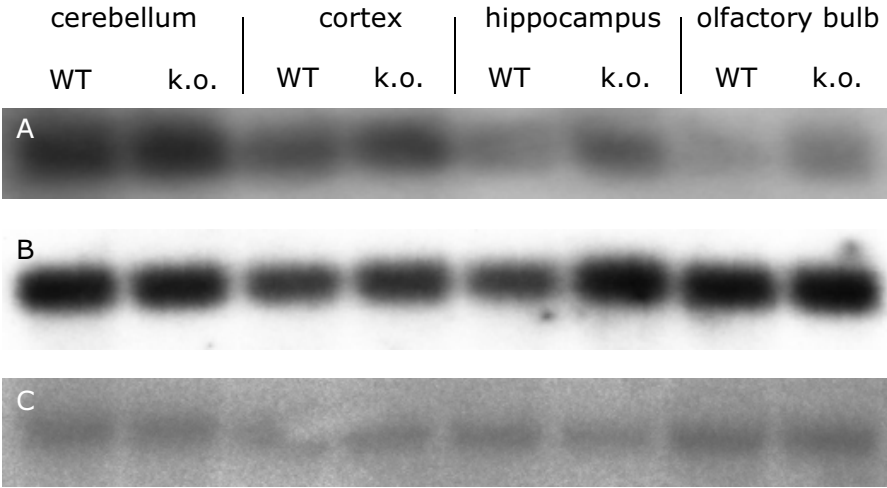


Figure 7 Autoradiograph of Northern Blot experiments assessing transcript levels of certain brain regions

The expression levels of transcripts from certain brain areas (indicated on top) is investigated. The lanes are loaded in alternating order with WT and k.o. derived RNA (indicated on top of each lane). In A the Northern membrane is hybridized to the ICAP probe indicating the highest level of expression in the cerebellum (left two lanes). The reference probe is the GAPDH cDNA (B). Bamacan is tested in C for its expression levels and shows rather ubiquitous levels.

In figure 7A the ICAP distribution in the respective brain regions (indicated on top) is seen. The highest amount is detected for the lanes where cerebellum RNA is loaded. The cortex holds similar amounts of ICAP transcripts. In hippocampus and olfactory bulb these levels are not reached. In cerebellum and olfactory bulb the GAPDH-normalized signal values supporte the upregulation in the k.o. situation (+2.99% and +12.14%). However, in the cortex and hippocampus the opposite (-5.69% and -23.48%) is true. In case of the bamacan (C) distribution the signal appears ubiquitous with no evidence of dysregulation. It has to be kept in mind that these findings only represent the adult situation and not the one of P14. The results from the array experiment and RT-PCR were drawn from this younger stage.

A method that is more qualified to elucidate the localization of certain transcripts in respect to their distribution in tissues is the *in situ* hybridization. This method is performed on 14µm sagittal cryo-sections of brains from P14 of mice deficient for TN-R and their respective WT. The construction of ribo-probes was performed by PCR. Therefore, primers described in the previous sections are modified to introduce promotor sites for T7 (sense probe) and T3 (anti-sense probe) RNA polymerase promotor at the 3' position to the respective cDNA fragment that is amplified from plasmid DNA. Figure 8 shows close up views of these *in situ*

hybridizations.

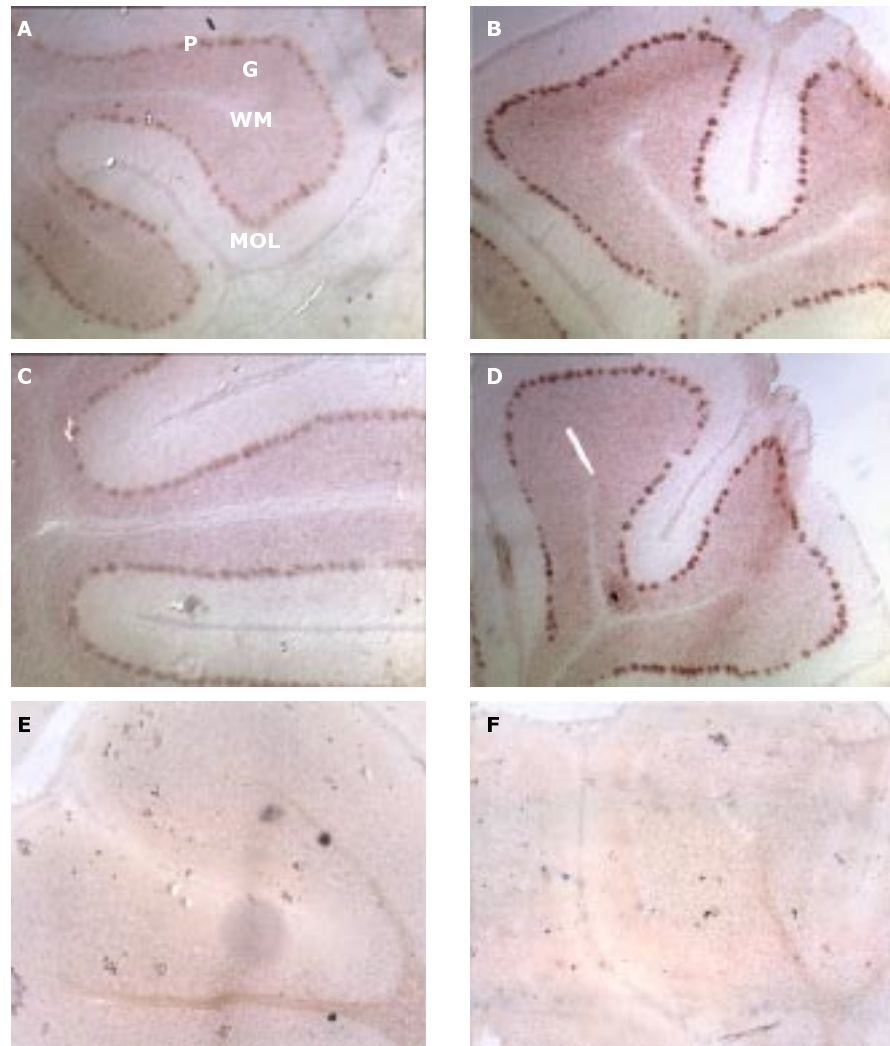


Figure 8 *in situ* hybridizations of sagittal brain sections reveal ICAP expression in the cerebellar cortex and locate the dysregulation to the Purkinje cell layer

This figure displays close up views from sagittal cerebellum sections. Through comparison between WT (left panels A, C, E) and k.o. (right panels B, D, F) it is shown that the Purkinje cells (P) display a stronger intensity of ICAP mRNA in the k.o. situation. Another positive area is the granule cell layer but the intensity between the two genotypes is indistinguishable. The white matter is free of ICAP staining. The ICAP mRNA is detected in A - D through the anti-sense ribo-probe. The control is shown in E and F hybridized to the sense probe. P: Purkinje cell layer; G: granule cell layer; WM: white matter; MOL: molecular layer.

Hybridizing the sections with the anti-sense ribo-probe (T3) against ICAP reveals rather ubiquitous levels of expression in the P14 brain. The strong exception to that is the cerebellar cortex. As shown in the figure above the ICAP mRNA is staining this brain region, especially in its Purkinje cell layer (P) and granule cell layer (G). In cells of the Purkinje cell layer the ICAP expression is higher in TN-R deficient (right panels) cerebella. Though, the expression in the WT (left panels) is obvious too. The granule cell layer shows a clear positivity for ICAP mRNA that is not

distinguishable between the two genotypes. The white matter (WM) is free of ICAP staining. In the panels E and F the sections are probed against the sense (T7) control. These findings confirm the high expression in the cerebellar cortex that was suggested through the Northern blot experiment (figure 7) and locate it to certain substructures, Purkinje cells and granule cell layer.

Further *in situ* hybridizations are performed for the investigation of ICAP expression levels at different age stages. Mice brain sagittal sections of four days (post natal), five weeks and three months old animals are probed with the ICAP ribo-probe. The overall distribution and levels of the ICAP expression is not altered at these stages in comparison to the described situation at P14 (data not shown).

β 1 Integrin mRNA levels detected by *in situ* hybridization

Although there are no indications from the Northern blot experiments that the β 1 integrin message distribution and level could be affected in the TN-R deficient mouse, it is worthwhile checking it in parallel with the ICAP probe in *in situ* hybridizations. Thereby, dilution or extinction effects that could occur in Northern experiments are circumvented. Probing the brain sections against β 1 integrin mRNA shows that it is co-expressed in regions of ICAP presence. The expression levels are equal in both genotypes investigated (data not shown).

β 1 Integrin protein levels

For the same reason that lead to the investigation of β 1 integrin transcript levels a Western blot analysis is performed on crude brain homogenates. Hereby, it can be detected whether an altered β 1 integrin protein level leads to the secondary upregulation of ICAP.

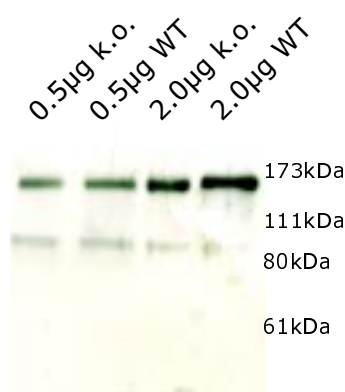


Figure 9 Western blot analysis of crude brain homogenates with M-106 monoclonal anti- β 1 integrin antibody detecting equal protein levels within k.o. and WT samples

The monoclonal antibody M-106 against β 1 integrin is used in this Western blot to detect the amount of the protein in total brain homogenate. The blot compares TN-R deficient and its respective wildtype mice. The amount of protein loaded per lane as well as the genotype of the sample is indicated on top. Two bands are visible in each lane after detecting the primary antibody with the horse radish

peroxidase conjugated secondary antibody. The upper band (150kDa) represents the $\beta 1$ integrin subunit and the lower band (92 kDa) a degradation product of the $\beta 1$ subunit.

The comparison of $\beta 1$ integrin in brain homogenate of mice lacking the TN-R molecule and their respective wildtype littermates is performed with the monoclonal antibody M-106 (Santa Cruz Biotechnology Inc. Santa Cruz, USA). This Western blot analysis (see figure 9) reveals equal $\beta 1$ integrin protein amounts in k.o. and WT situation. The band at approx. 150kDa represents the $\beta 1$ integrin subunit signal. It is indistinguishable in both genotypes and at both loading amounts (0.5 μ g and 2.0 μ g crude brain homogenate) confirming the results at the transcript level and the assumption that the ICAP dysregulation is not due to an altered amount of the binding partner $\beta 1$ integrin.

CaMKII expression

The phosphorylation of ICAP by CaMKII is responsible for its activation. Thus CaMKII is a target for further investigation. The expression level of CaMKII is checked on the transcript level through Northern Blot and on the protein level through Western blot.

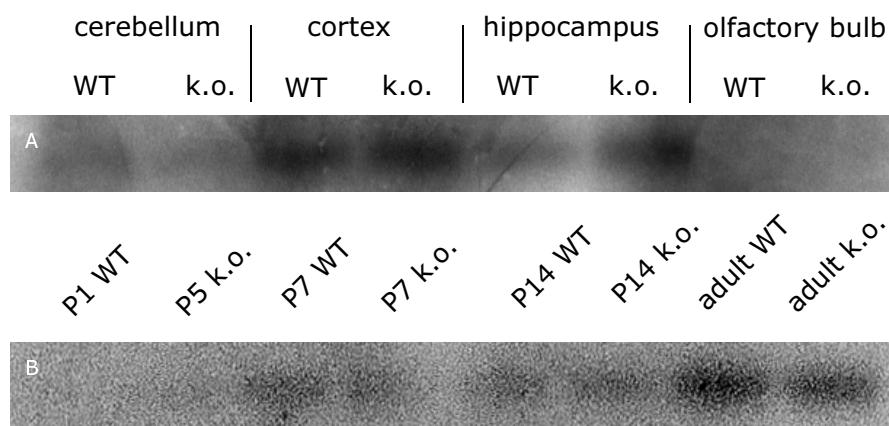


Figure 10 Autoradiograph of Northern blots for brain regions and age stages detecting CaMKII transcript levels

In the upper panel (A) the CaMKII distribution in certain brain regions and their respective genotype (as indicated on top; all adult samples) is investigated. Cortex and hippocampus are strongly positive for CaMKII transcripts. The cerebellum exhibits positivity, though weaker than in the other areas. Due to strong background activity it stays unclear whether the olfactory bulb is CaMKII positive. In the lower panel (B) a time lapse of CaMKII expression is investigated (ages and respective genotypes indicated on top). The CaMKII message comes up at the age of P7 and peaks in the adult stage at equal levels in both genotypes.

The distribution of CaMKII transcripts in certain areas of the brain is investigated by the Northern blot displayed figure 10A. It should be co-expressed in the areas of ICAP expression because it is necessary for the activation of ICAP. This holds true for cortex, hippocampus and cerebellum, though in the latter the intensity is not as strong as it was for the ICAP signal. The expression in olfactory bulb remains unresolved due to high background staining. The overall diminished quality of this northern blot is

result of many parallel experiments and stripping procedures. This is also why the quantification of signal intensities between the two genotypes is not evaluated but the qualitative statement remains reliable.

The lower panel (B) in figure 10 depicts the height of CaMKII expression levels at certain timepoints and their respective genotypes (as indicated on top of the panel). The expression is detectable from P7 onwards and peaks in the adult stage. The level of CaMKII message in respect to the k.o./WT comparison is not altered.

On the protein level, crude brain homogenates of total mouse brain are subject to Western blot analysis. 30µg and 10µg of the respective protein samples are loaded per lane to a polyacrylamide gel and transferred to nitrocellulose membrane. On this membrane the signals specific for the α -subunit of the phosphorylated CaMKII is detected by antibody 22B1 (monoclonal, ALEXIS Biochemicals Grünberg, D). The blot reveals no dysregulation of the CaMKII protein (data not shown).

ICAP function *in vitro*

β 1 Integrin and tenascin-R binding

As demonstrated the lack of extracellular TN-R leads to an upregulation of ICAP. The ICAP molecule binds to the cytoplasmic domain of transmembrane β 1 integrin. Whether an interaction of the transmembrane β 1 integrin and TN-R exists is not published to date. The interaction of another tenascin family member, namely TN-C, with several integrins is extensively studied (i.e. Chiquet-Ehrismann (1995); Yokosaki et al. (1998); Hauzenberger et al. (1999); Yokoyama et al. (2000)). The interactions are either via α -subunits or mapped to the third fibronectin type III domain (FNIII) in case of interaction with the β 1 integrin containing heterodimers.

A				B				
Tenascin-R				Tenascin-C				
name	begin	end	E-value		name	begin	end	E-value
signal peptide	1	32	-		signal peptide	1	11	-
coiled coil	127	157	-		low complexity	121	138	-
Pfam:EGF	204	230	4.10e-02	EGF-S	EGF	184	217	2.00e+01
Pfam:toxin_5	221	252	2.00e+01		EGF_like	220	248	3.50e+01
Pfam:EGF	235	261	5.20e-02		EGF	251	280	5.00e+00
Pfam:toxin_5	283	314	7.80e+00		EGF	283	311	3.30e+00
Pfam:EGF	292	323	8.10e-01		EGF	340	373	1.60e+01
FN3	326	404	8.00e-08		EGF	402	435	1.30e+01
FN3	415	493	5.20e-07		EGF	464	497	7.50e+00
FN3	504	583	3.60e-06		EGF	526	559	5.00e-01
FN3	594	675	3.40e-05		EGF	562	590	1.80e+01
FN3	686	763	5.60e-11		EGF	593	621	3.70e-02
FN3	774	851	5.40e-07		FN3	623	701	8.90e-08
FN3	864	942	6.30e-10	FNIII 6-8	FN3	712	794	1.50e-06
FN3	953	1031	4.00e-05		FN3	803	884	7.50e-08
FN3	1041	1118	1.50e-09		FN3	893	974	1.70e-09
FBG	1133	1343	4.80e-133		FN3	985	1062	2.60e-08
					FN3	1074	1152	8.80e-01
					FN3	1165	1245	2.70e-03
					FN3	1256	1334	4.60e-02
					FN3	1347	1427	5.00e+00
					FN3	1438	1517	3.50e-04
					FN3	1528	1606	1.50e-07
					FN3	1617	1694	1.50e-06
					FN3	1705	1782	7.80e-08
					FBG	1797	2007	4.20e-124

Figure 11 Tenascin's domain structure, RGD-like binding motif localization and recombinant TN-R fragments

The multi-domain structure of murine tenascin-R and tenascin-C are displayed in a consecutive order beginning with the amino-terminal end. In blue the type of domain is indicated (EGF: EGF-like domain, FN3: fibronectin type III -like domain, FBG: fibrinogen-like domain). The first and last amino acid number of each domain is indicated in the next two columns. The arrowheads indicate the location of the unique RGD-like binding motif (in TN-R the FNIII number 8 and in TN-C the FNIII A4). Displayed values are calculated with the web-based simple modular architecture research tool (SMART 3.5 <http://smart.embl-heidelberg.de/> Schultz et al. (1998)). The red boxes display the range of the recombinant TN-R fragments (EGF-S and FNIII 6-8, Xiao et al. (1996)) used in consecutive experiments. In case of alternative motifs the program indicates this possibility by naming it "Pfam:" followed by domain's description.

β 1 integrin binding to ECM molecules occurs most likely through RGD-like motifs (i.e. RGD, RAD and RAA). The murine TN-C molecule lacks this motif in the third FNIII domain (see figure 11B) where binding was shown for tenascins from other species (Yokosaki et al. (1994) and Schnapp et al. (1995)). Therefore, an RGD-like motif is existing in the alternatively spliced FNIII repeat A4 (arrowhead in figure 11B). For the molecule investigated in this work, the murine TN-R, the RGD-like Tenascin-R motif is found on a

FNIII repeat near the carboxy terminal end (eighth FNIII, arrowhead in figure 11A). This is why binding assays are performed with the TN-R fragments EGF-S (lacking the binding motif) and FNIII 6-8 (containing the putative RAA binding site) both produced as described in Xiao et al. (1996).

The analysis of crude brain homogenate with $\beta 1$ integrin antibody M-106 crosslinked to protein G magnetic beads for precipitation of proteins that bind to $\beta 1$ integrin revealed no TN-R detectable with monoclonal 619 antibody. As this might be due to the poor performance of the 619 antibody the GST pull-down experiment is performed. In the pull-down, 100 μ g GST-fusion TN-R fragment is loaded to the GSTrap FF column (APB) for binding. Then, 3000 μ g of crude brain homogenate is run over the column. After washing, the GST-protein associated proteins are eluted. In the eluted material there is a band at approx. 75kDa coming up when detected with M-106 $\beta 1$ integrin antibody (see figure 12). This band corresponds to the one observed in the brain homogenate control lane. Whether the native (120kDa) integrin is eluted from the columns remains unresolved. In elution fraction 4 there might be a band at that specific molecular weight but due to high background it remains unclear. In previous blots this question also was left unanswered. Thus, the binding of the $\beta 1$ integrin degradation product (75kDa) to the FNIII 6-8 TN-R fragment is confirmed through this pull down experiment (lower arrowhead in figure 12).

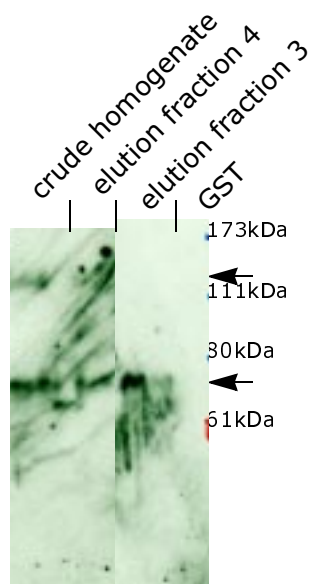


Figure 12 Western blot of GST-pull down experiment

The eluted fractions from the GST columns are evaluated in a 10% SDS-PAGE blotted on membrane. The detection of proteins that bound to the TN-R FNIII 6-8 GST-fragment is performed with M-106 anti $\beta 1$ integrin antibody. The crude brain homogenate (left lane) as a control gives rise to $\beta 1$ integrin band at 120 kDa (native) and the degradation product at 75 kDa both indicated with arrowheads. The elution fractions 3 and 4 exhibit the lower weight integrin band (lower arrowhead). In the negative control, the GST loaded lane, no bands arise.

The proliferation of ICAP deficient ES cells

For characterization of the ES cell clones prior to further investigations proliferation parameters are assessed. This is necessary for demonstrating that their proximity in terms of genetic background is not affected. Due to the time of parallel passaging since their common ancestry (between passage 9 to 18), they might exhibit differences in the proliferation behavior. The ES cells are monitored in two stages of the differentiation protocol with the MTT test where the conversion of the tetrazolium salt (MTT) to colored formazan correlates to the proliferation rate. The first situation in which the cells are measured is equivalent to attached growth of 3×10^6 cells on a 10cm diameter culture dish.

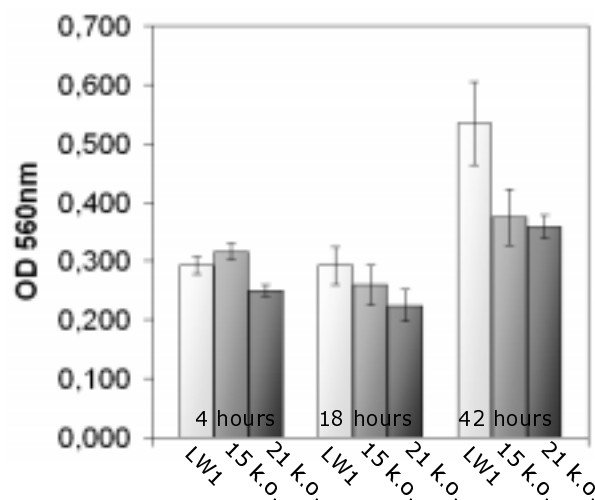


Figure 13 MTT proliferation assay of ES cells growing attached

The increase of formazan as a measurement of proliferation is determined at a wavelength of 560nm. The timepoints are 4 hours, 18 hours and 42 hours after seeding the cells (indicated at the base of the bars). LW1 is the wildtype cell line from which the two ICAP knock out variants (15 and 21) are derived (all indicated below the bars). The three cell lines do not show significant differences in proliferation.

The expansion of ES cells is performed in the attached situation. In this state three timepoints after seeding of the cells are measured (4, 18 and 42h; see figure 13). No significant differences in proliferation rate are found between the three cell lines (LW1 wildtype, 15 and 21 knock out for ICAP). Another critical stage of the differentiation protocol is the formation of ES cell derived embryoid bodies (EB). These free floating sphere-like aggregates are measured at two different seeding densities for their formazan production.

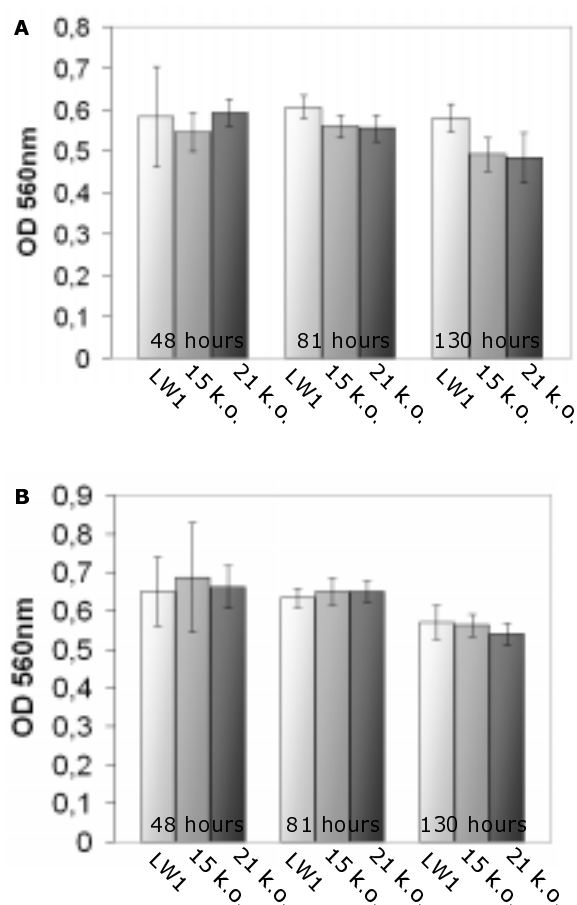


Figure 14 MTT assay for ES cells in the situation of EB formation

Trypsinized ES cells are seeded in uncoated and untreated dishes for free floating EB formation at two densities (A: 3500 per well; B: 7000 per well; in 96-well plate). The three timepoints reveal no differences for all three cell types in proliferation/ cell death. The levels stagnate over a period of 130 hours.

Proliferation in this situation stagnates over the measured period of 130 hours with no detectable differences between the three cell lines (figure 14).

For investigation of the mentioned genetic proximity of the three cell lines it has also to be measured if they still display equal behaviour in embryoid body formation. The formation of embryoid body aggregates is not connected to an initial increase in proliferation. Early generation of EBs is rather an aggregation phase in which the cells do not tend to expand. This aggregation is measured in respect of the diameter of developing EBs.

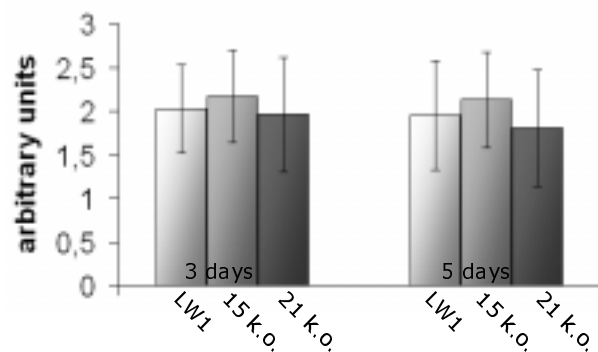


Figure 15 Diameter of ES derived embryoid bodies after 3 and 5 days of growth

The diameter of free floating round EB's is measured with an ocular micrometer in arbitrary units at 3 and 5 days of growth. EB's from all three cell lines (LW1 wildtype, 15 and 21 knock out) remain stable at a certain size that does not differ significantly in all three cases.

The stagnation of proliferation in the observed period is supported by the finding that the size (diameter) of EB's also remains stable in comparison of the 3 day and 5 day situation (see figure 15). Measuring the diameter reveals equal behavior of all three cell lines as it is shown in the previous experiments. This is a good basis for further comparative experiments like neurite outgrowth measurements.

ICAP deficient cells and neurite outgrowth

The dysregulation of ICAP in neural cells in reaction to the lack of the ECM molecule TN-R suggests a functional relevance. The neurite outgrowth assay is performed to test the role of TN-R on the behavior of young neurons that are starting to project their neurites. In this assay the impact of the previously mentioned TN-R fragments on the outgrowth behavior shall be studied. Assuming that the FNIII 6-8 fragment exhibits its special properties in regard to $\beta 1$ integrin binding because of its RGD-like domain, it is offered in the assay as a coated substrate. As a control the EGF-S fragment with no apparent binding motifs is another studied substrate. The non-related control group is growing on a gelatin coated surface. Prior to measurement the cells are characterized by staining with certain antibodies. This is necessary to monitor the differentiation of ES derived cells. An important marker protein is nestin. It is a large intermediate filament protein (type VI) expressed during development in myotendinous and neuromuscular junctions, typically disappearing by E18. It is used as a marker protein for undifferentiated young neurons. Further antibodies used as neuronal markers are β III tubulin and heavy neurofilament.

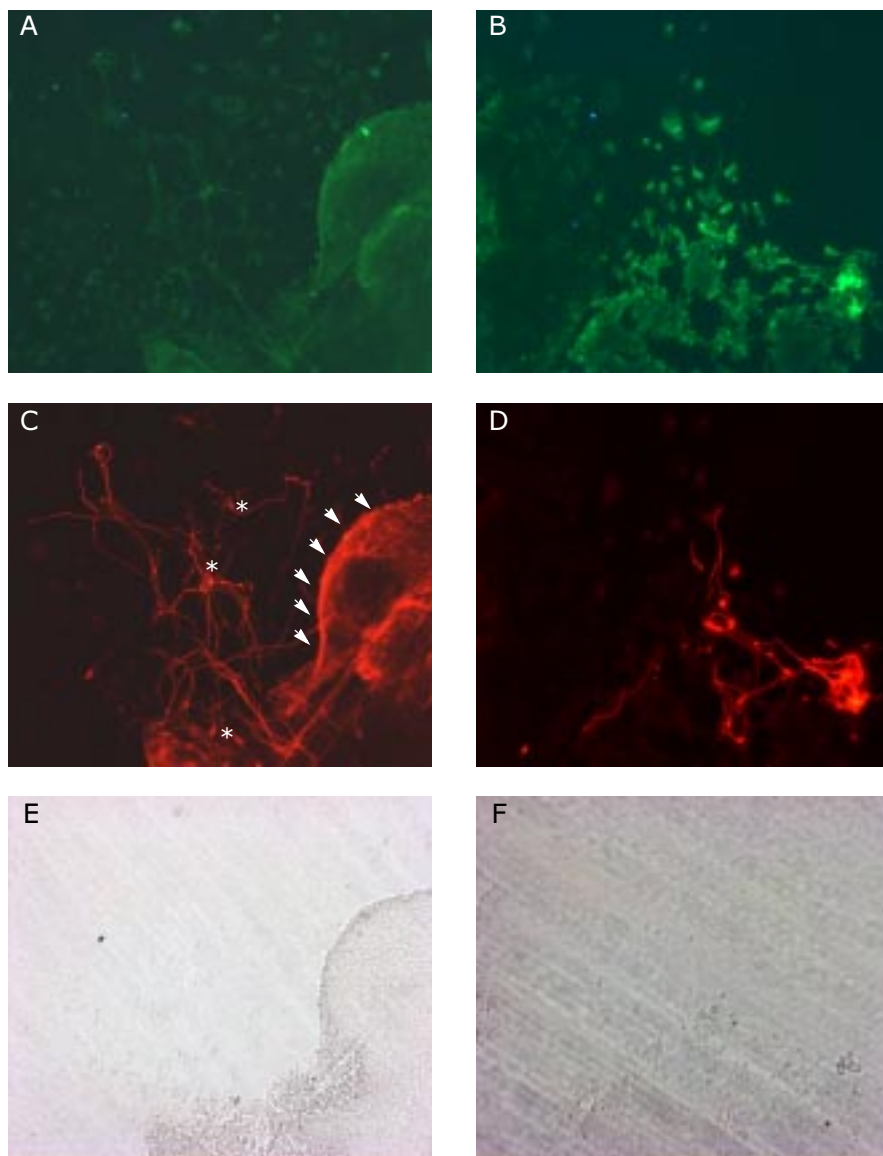


Figure 16 Immunofluorescence of ES derived cells after 5 day in ITSFn medium (stage 3 of differentiation protocol). Nestin (FITC) staining for assessment of immature neurons and β III tubulin (Cy3) for maturing neurons and their neurites.

For monitoring the differentiation towards the neuronal lineage the ES derived cells are stained for marker proteins nestin and β III tubulin. The cells of both genotypes (A,C and E are ICAP deficient "21" cells whereas B, D and F are wildtype "LW1" cells) differentiate equally into immature neurons as seen in A and B by nestin (FITC) staining and mature, neurite projecting neurons as seen by β III tubulin (Cy3) staining in C and D. In C the border of an attached EB sphere is outlined (arrowheads). Some neurons that migrated out of this structure are indicated with asterisks. Brightfield pictures are shown in E and F. Cells are grown on PLO precoated gelatin coverslips and fixed with 4% paraformaldehyde prior to staining. All pictures have the dimension of 870 μ m width and 690 μ m height.

In figure 16 the immunofluorescence is depicted monitoring the differentiation of the ES derived cells at the end of stage three of the differentiation protocol. At this timepoint they are grown five days in ITSFn medium attaching to cover slips coated with gelatin

or the tenascin fragments that are object to evaluation. Prior to the depicted situation, the cells are growing free floating in sphere-like structures (EBs). Transferring the EBs to coated cover slips leads to the attached growth and migration of cells out of the formerly sphere cell aggregate. This situation is indicated in figure 16C. The arrowheads line out the former EB-border and the asterixes indicate neurons that migrated out of the aggregate. The amount of undifferentiated neurons is visualized in figure 16A&B by immunostaining against nestin (FITC). Both genotypes (ICAP deficient "21": A; wildtype "LW1": B) have a high amount of nestin positive cells. In contrast to it, in C and D the postmitotic differentiated neurons with their projecting neurites are stained with β III tubulin (Cy3). The amount of β III tubulin positive cells is much lower than the number of nestin positive ones. This picture is showing the correct situation of the differentiation process at the end of stage three. The majority of cells follow the protocol towards the neuronal lineage via nestin positive neural progenitor cells. A small amount of cells differentiates directly into β III tubulin positive neurons by a so called "default mechanism" (Tropepe et al. (2001)). These differentiated neurons are object to the neurite outgrowth measurement. The pictures in figure 16 are only representative of the differentiation stage figure 17 shows the analyzable neurite outgrowth assay situation.

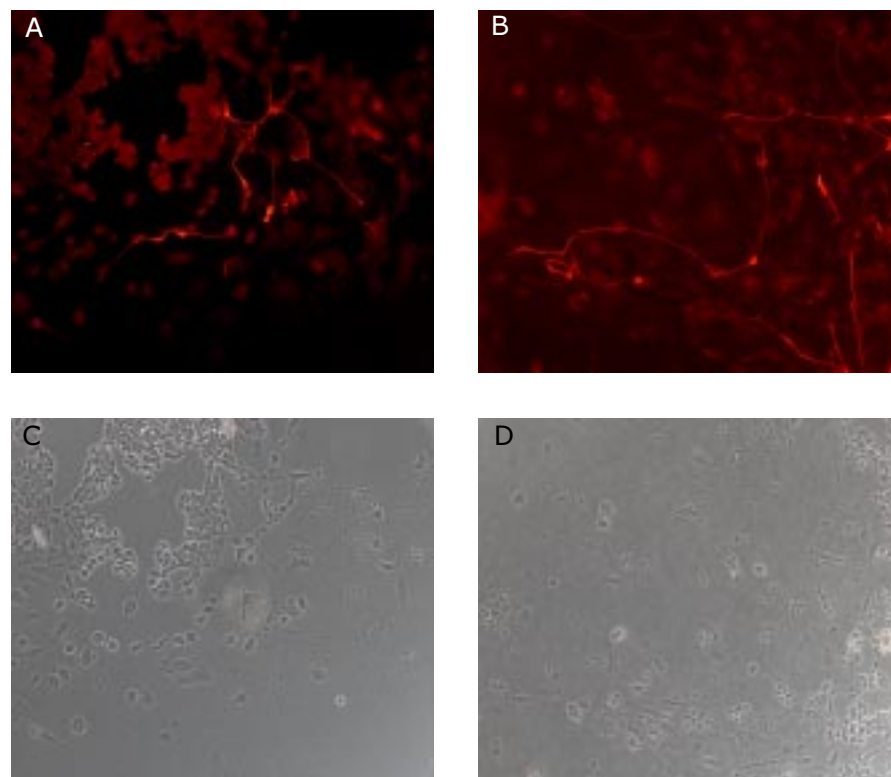


Figure 17 Representative pictures of ES derived β III tubulin positive young neurons after 5 days in culture of ITSFn medium

This figure depicts the situation in which the neurite outgrowth measurement is performed. In this case, the cells are growing attached on a gelatin (in the other cases EGF-S or FNIII 6-8 TN-R fragments) coated cover slip for 5 days in ITSFn medium (end of stage 3). Prior to β III tubulin staining they are fixed with 4% PFA. In A and C ICAP deficient "21" cells are shown. B and D show wildtype "LW1" cells.

A and B are Cy3 fluorescent β III tubulin stained cells outlining the neurites and cellbodies of young neurons. In C and D the respective brightfield pictures are shown [visible area: 870 μ m width, 690 μ m height].

Due to the β III tubulin labelling the neurites of neurons are nicely stained and thus easily distinguishable from other cell extensions (see figure 17 A and B). The measurement is performed by copying the fluorescent picture of the microscope's CCD camera to an evaluation software program (Kontron, Zeiss). In this program the neurites are outlined manually and the measured distance is copied to another software program for statistical calculations (SigmaPlot, SPSS). The results of the measurements are depicted in the consecutive figures.

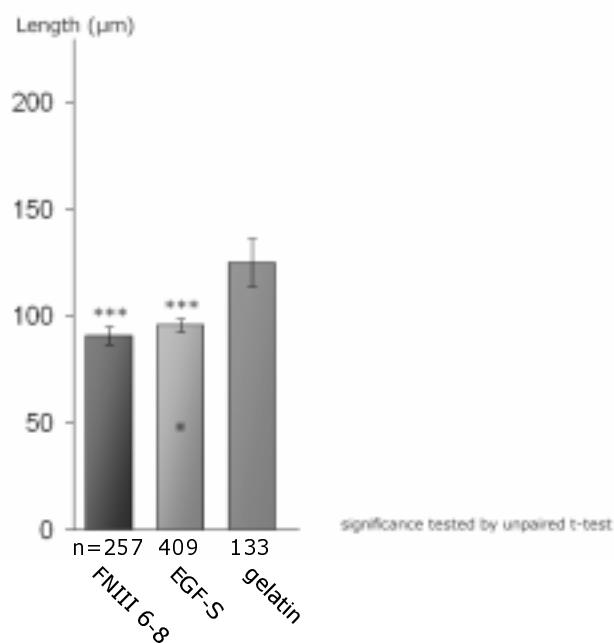


Figure 18 Neurite outgrowth of wildtype ES derived young neurons on different substrates

Wildtype ES cell derived young neurons after 5 days in ITSFn medium (end of stage 3) are cultured on the indicated substrates. β III tubulin positive neurites are measured with Kontron software (Zeiss) and mean values of neurite length in μ m are plotted. The wildtype cells show a highly significant reduced neurite outgrowth on both TN-R fragments (FNIII 6-8 and EGF-S) in comparison to the control (gelatin).

Figure 18 displays the normal (wildtype) reaction of ES derived β III tubulin positive neurons to the presented substrates. In comparison to the situation on gelatin the two tenascin fragments exhibit properties that decrease the neurite outgrowth. This effect was expected for the FNIII 6-8 fragment in regard to its β 1 integrin binding domain. But also for the EGF-S fragment a highly significant decrease of neurite outgrowth is observed. The inhibiting effect of TN-R to neurite outgrowth is in accordance with previous findings (Xiao et al. (1996)). The effect observed in the EGF-S group might be due to another type of β 1 integrin

binding to a binding motif other than the RGD-like.

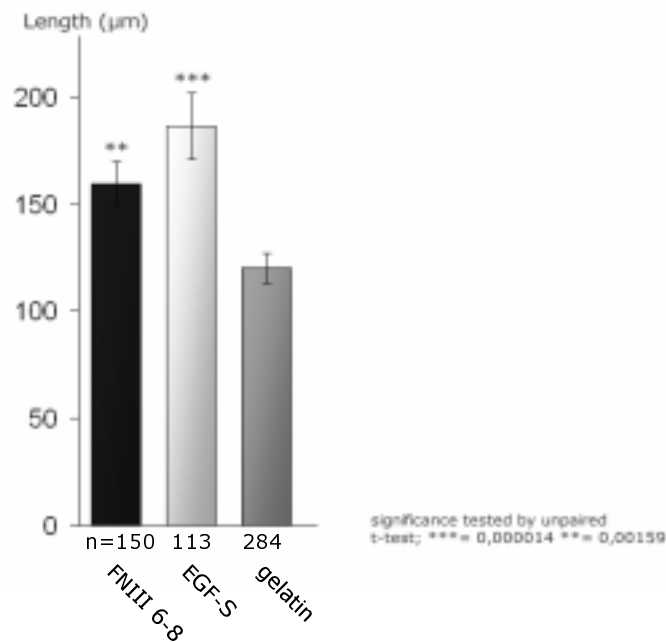


Figure 19 Neurite outgrowth performance of ICAP deficient young neurons derived from ES cells

ICAP deficient ES cells are held in ITSFn medium on the indicated substrates (FNIII 6-8, EGF-S or gelatin) for differentiation towards the neural lineage. After 5 days (end of stage 3) β III tubulin positive neurites are measured with the Kontron software (Zeiss) for length in μ m (mean values depicted). For ICAP deficient cells the TN-R fragments are significantly enhancing neurite outgrowth in comparison to the control situation on gelatin.

The influence of ICAP on β 1 integrin mediated neurite outgrowth is examined by culturing ICAP deficient ES cell derived young neurons on tenascin fragments including the RGD-like binding domain for β 1 integrin (FNIII 6-8) or lacking it (EGF-S). A further control group are cells that are plated on gelatin substrate. Figure 19 demonstrates that cells lacking the ICAP molecule display an altered behavior on the TN-R fragments, though their behavior to gelatin substrate does not differ from the wildtype situation (figure 18: WT mean on gelatin = 120 μ m; figure 19: k.o. mean on gelatin = 124 μ m). With high significance ($t = 0,00159$) the β III tubulin positive neurites on the FNIII 6-8 fragment substrate exhibit an enhanced neurite outgrowth in comparison to the situation on gelatin. The outgrowth promoting effect of the EGF-S fragment for neurons lacking the ICAP molecule is highly significant ($t = 1.4 \times 10^{-5}$). As shown before for the wildtype situation the EGF-S fragment exhibits an unpredicted influence on the neurite outgrowth properties. In the ICAP deficient cells the EGF-S fragment is an outgrowth enhancing substrate although it lacks the RGD-like motif. This experiment supports the postulated influence of ICAP via β 1 integrin although the manner of interaction between the EGF-part of tenascin and the integrin remains to be resolved. The exciting finding of the conversion from an inhibiting substance to an neurite outgrowth promoting through the knock out of the ICAP molecule becomes even clearer when the values for outgrowth on TN-R fragments are compared

directly to each other (figure 20).

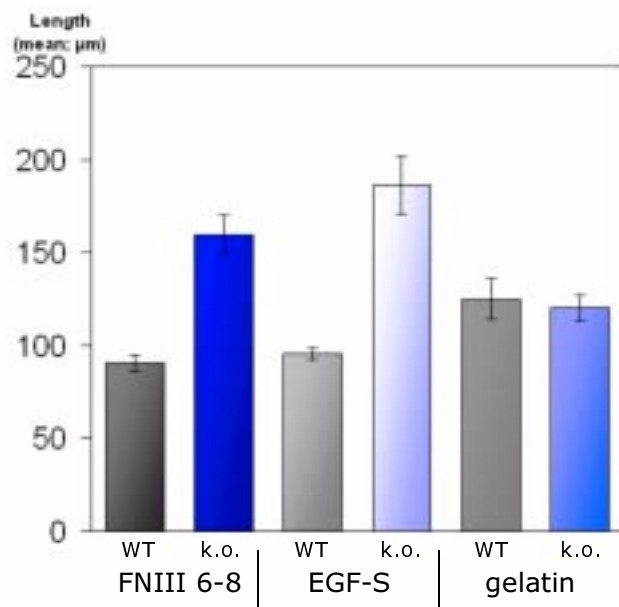


Figure 20 The conversion of inhibiting to promoting properties of TN-R fragments in neurite outgrowth through the ICAP knock out

In this figure the mean values of neurite length in μm are given for all three substrates and the two genotypes compared in the neurite outgrowth experiments. The difference between the wildtype (gray bars) and the ICAP deficient (blue bars) neurite length observed on the two tenascin substrates indicates the conversion of its inhibitory properties to outgrowth promoting ones when ICAP is lacking.

KAPITEL 4

Diskussion

Discussion

Dysregulation in Tenascin-R deficient mice

Dysregulation on the transcript level

Upregulation of hnRNP A1 indicated by the array signal for the corresponding EST (Ue20a10.y1; table 2; Glisovic et al. (2003)) could be representative of alterations in the expression machinery upon reaction to the TN-R deficient situation. When hnRNP A1 levels are elevated the half life of mRNA transcripts is longer. This decreased mRNA degradation is not specific for one transcript but elevates the total mRNA levels. It can be one reason why the array is detecting mainly upregulated signals that meet the selection criteria of the evaluation process. This does not mean that an exclusive upregulation is observed but the downregulated signals did not meet the high thresholds to become selected as candidates for further investigation. The indication of GAPDH as regulated through the array data can also be due to the mainly elevated mRNA levels. In retrospect, the selection of GAPDH as a reference for Northern blot and RT-PCR experiments is not the optimal choice. But as all transcript levels are calculated in percentage of the GAPDH signal and the other signals still remain upregulated on this background, it emphasizes the strength of their upregulation. If the GAPDH expression is really elevated in the knock out (figure 4B), the dysregulation of the ICAP transcript has to be seen as even stronger than indicated. Nevertheless, the reliability of the ICAP dysregulation is not questioned by this matter. It is confirmed by four types of experiments (array, Northern, RT-PCR and *in situ* hybridization) as reliably dysregulated at P14. Going into more detail, the regulation of ICAP transcripts are monitored in regard to certain brain structures through Northern (figure 7A) and *in situ* experiments

(figure 8). For the region respective Northern blot it is important to mention that the age stage differs in regard to the other experiments (adult instead of P14). Though, the highest expression and upregulation is found for the cerebellum which coincides with the *in situ* data. The dysregulation in other brain areas like olfactory bulb, cortex and hippocampus is not detectable by the *in situ* experiments. For certain ages (4 days, 5 weeks and 3 months) the *in situ* hybridization indicates that the distribution of ICAP transcripts remain unaltered with age. The cerebellum has exceptionally high amounts of ICAP transcripts at all stages. With the Purkinje cells and the granule cell layer being especially strong. The white matter is free of ICAP signal which was not quite clear from the literature (Faisst and Gruss (1998)). The remaining brain areas exhibit a rather ubiquitous expression of ICAP with no further eye-catching hot spots. Why is the cerebellum and within it the Purkinje cells and the granule cell layer exceptional?

The cerebellum and ICAP

The cerebellum is a brain area that has only 10% of the total brain's volume but harbors about 50% of all neurons. It is the main center of motor control in terms of correcting movements and monitoring the accuracy and coordination of them. Furthermore, it plays a major role in motor learning. To fulfill these tasks it is connected to motor centers in the cortex and brain stem. The Purkinje cells are the "output neurons" in this context. Their axons project out of the cerebellar cortex into deep nuclei. The GABAergic inhibitory Purkinje cells are rather large (50 to 80µm diameter) cells that make up a cell layer of their own. Their dendritic tree develops between P8 and P15 and is located in the molecular layer above. The orientation of the arborization is in a right angle to the parallel fibers. These fibers are granule cell axons which give the Purkinje dendritic tree the planar orientation. Without granule cells and their parallel fibers aberrant arborization is observed, with the dendrite even growing backwards into the Purkinje cell layer. At the time of this process the dysregulation of the ICAP molecule is detected in mice that lack the ECM TN-R. All cells of the molecular layer (basket and stellate cells) contribute to the TN-R positive ECM that is involved in the process of Purkinje arborization and parallel fiber defasciculation. It was shown by Xiao et al. (1998) that TN-R is involved in generation of the correct cytoarchitecture in the molecular layer by defasciculating the dense formation of parallel fibers giving room for stellate cells, basket cells and Purkinje cell dendrites. When the parallel fibers of the granule cells and the developing dendritic tree of the Purkinje cells encounter an altered ECM (TN-R deficient) in the molecular layer they have to react, generating the observed unaltered histoarchitecture. To balance this situation the ICAP molecule is upregulated and thereby the neurite outgrowth behavior is altered as described in the results section. The influence of ICAP on the $\beta 1$ integrin mediated neurite outgrowth is discussed in the next section.

ICAP influence on $\beta 1$ integrin

The influence of ICAP on the examined situation is part of the $\beta 1$ integrin mediated properties. Through its cytoplasmic binding it modulates the adhesive properties of the integrin heterodimer. In the observed situation the lack of an extracellular binding partner induces an upregulation of ICAP or the cells compensate for the missing ECM component by increasing the level of ICAP. It is shown in this work that its increase is not a secondary effect due to the upregulation of other involved components like the CaMKII or the $\beta 1$ integrin subunit (figure 9). In the *in situ* experiment it is demonstrated that ICAP is co-expressed in areas of $\beta 1$ integrin presence. The phosphorylation of ICAP is necessary for its binding to the integrin subunit and it is shown that the amount of phospho-CaMKII, responsible for this process, remains equal in TN-R deficient mice brains. The three situations examined in this work are depicted in figure 21. What was found through the neurite outgrowth experiments are the two situations in figure 21A&B. The initial finding that lead to this work is depicted in C of the same figure.

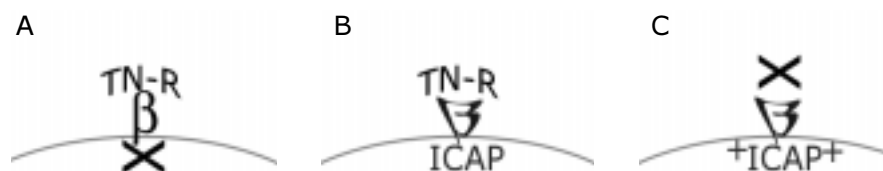


Figure 21 The three examined situations of ICAP, $\beta 1$ integrin and TN-R interplay

In A the figure depicts the situation encountered when ICAP deficient neurons grow on the tenascin substrates. The conformation of the integrin heterodimer allows binding and outgrowth on TN-R. The wildtype situation is depicted in B. It is the same situation that is observed when the WT neurons grow on the TN-R substrate and the ICAP decreases the binding and outgrowth through cytoplasmic binding and conformational change of the integrins. In C the situation encountered in the TN-R deficient mice is depicted. The lack of the inhibitory ECM component leaves the heterodimer blank and ICAP is upregulated in compensation.

Wildtype neurites display a decreased outgrowth on the tenascin substrates (figure 21B) suggesting either an inhibitory outside-in signaling or an inside-out signalling that tells the integrin to avoid tenascin structures. The latter one would implicate bi-directional signaling over the integrin subunits: recognizing the TN-R, sending the information into the cell and reacting to it by conformational change of the heterodimer. Another possibility is that an independent TN-R receptor (i.e. F3 or L1) transduces the information about the ECM composition and the cells react to it by decreasing the adhesive properties through inside-out signaling, implicating ICAP phosphorylation and binding to $\beta 1$ integrin (figure 22A). The reaction to both TN-R fragments, either containing $\beta 1$ integrin binding motif or not, supports the latter scenario. Support for the bi-directional signaling only over the $\beta 1$ integrin is given by reports showing RGD-independent adhesion and signaling (Chi-Rosso et al. (1997)) allowing the EGF-S fragment to exhibit $\beta 1$ integrin specific properties though lacking the RGD-like motif (figure 22B).

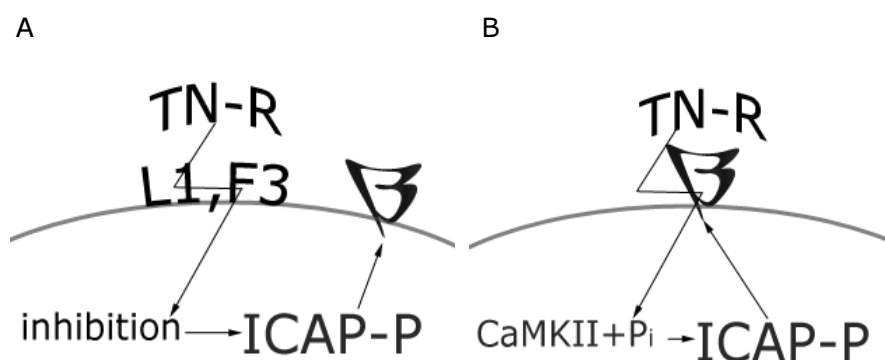


Figure 22 The two possible variants of TN-R signaling in the wildtype situation

The inside-out scenario is depicted in A. Here, $\beta 1$ integrin only reacts with a conformational change after ICAP is bound to the cytoplasmic domain. The inhibitory signal is transduced from outside of the cell via another ECM receptor. The bi-directional function of $\beta 1$ integrin is outlined in B. The integrin receives the inhibitory signal of the TN-R and reacts later through change in conformation to it. Prior to it the phosphorylated ICAP binds the cytoplasmic domain and triggers the alteration of heterodimer structure.

ICAP deficient neurites display enhanced outgrowth on the tenascin substrate (figure 21A) suggesting either a promoting outside-in signaling that is usually blocked by bound ICAP (figure 23B) or the incapability of transducing the outgrowth decreasing inside-out signal because of the gap that the knocked out ICAP leaves in the signal cascade (figure 23E). The latter one is the most reasonable scenario because the evidence from the situation in the TN-R deficient mice points to compensatory upregulation of ICAP (figure 23F). In this situation $\beta 1$ integrin is not only involved in signal perception but also reacting to it through ICAP triggered change in conformation and thus altering the cells outgrowth properties. Thereby, the ICAP upregulation compensates for the lacking inhibitory signal that normally is triggered by the now missing ECM component. Now, the integrin heterodimer is left blank and calls for the inhibition through the thus upregulated ICAP. The other scenario would be that TN-R triggers the outgrowth promotion via $\beta 1$ integrin (outside-in; comparable to figure 23A). When it is lacking in the ECM the cells simply get no stimulating input and then there is no need of compensatory upregulation of ICAP because the heterodimer would be used as receptor only (figure 23C).

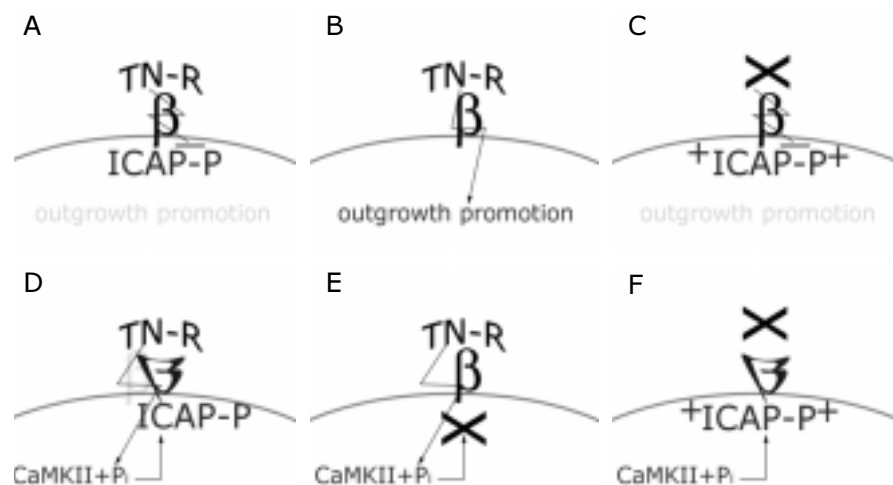


Figure 23 The two possible mechanisms of reaction to TN-R for all three observed situations

The upper panels (A, B and C) depict the mechanism presuming that TN-R triggers an outgrowth promoting signal that is received via $\beta 1$ integrin but not executed through it. In contrast to it in the lower panels (D, E and F) the scenario for the bi-directional behavior of $\beta 1$ integrin is displayed. Here, the integrin serves as a receptor for the tenascin and executes the inhibitory reaction through its conformational change. A and D represent the situation of wildtype neurons on tenascin. The mechanism for ICAP deficient neurons is shown in B and E. Which mechanisms are possible for the situation in TN-R deficient mice is explained in C and F.

The mentioned mechanisms are based on this work's findings from neurite outgrowth experiments on homogeneously coated substrates. It is known and most recently shown *in vivo* that TN-R is a repellent guidance molecule for neurites if they encounter the substrate boundary (Becker et al. (2003)). Becker et al. show that developing optic axons on their way to the optic tectum are growing along borders to TN-R positive regions, avoiding these areas. The impact of ICAP on these pathfinding properties are to be studied in current *in vitro* experiments where the ES derived ICAP deficient neurons are grown on heterogeneously coated coverslips. Another part of these experiments is studying the influence of other tenascin fragments on the neurite outgrowth. In addition to other stretches of the TN-R molecule there are also TN-C fragments to be monitored. These experiments shall also address the question whether the gelatin control fulfils its purpose better than taking GST as a control substrate. Gelatin, as heat-inactivated collagen, is considered an outgrowth permissive, though poor substrate. In the described experiments (figure 18, 19 and 20) it serves very well as a control, exhibiting almost identical values for the two genotypes studied.

ICAP on the protein level

The experiments assessing ICAP properties on the protein level include the detection of its amount in total brain homogenates and immunofluorescence on cryosections and ES derived cells. Unfortunately, the only antibody available is raised against

human ICAP (ICAP α 1035) and does not perform well in these experiments on mouse tissue, cells or homogenates. The best result of the various Western blots with this antibody is depicted in figure 6 of the results section. In most Western analysis the antibody produces high background staining and an unspecific band pattern, also seen mildly in this figure. Nevertheless, the blot includes the two specific ICAP bands. Furthermore, it gives an indication that a much higher amount of phosphorylated, thus activated ICAP is present. The phospho-ICAP is the molecule that binds to the β 1 integrin, thereby exhibiting its signaling properties. When available, Western blots for the brain areas studied in the previous sections have to be performed with a better antibody, ideally only detecting the ICAP isoforms and additionally working in immunofluorescence experiments as well. Immunofluorescent studies of brain cryosection and cultured ES derived cells could corroborate the exciting findings on the transcript levels.

Further comments

Another upregulated transcript is represented by the EST vy95h07.r1 with up to date no significant similarities in the databases. Its regulation factor of 2.9 fold (see table 2) is striking and characterization of the corresponding transcript could reveal exciting insights.

The suggested upregulation of the chondroitin proteoglycan bamacan is not confirmed through experiments other than the array (compare figures 4D and 7C). Although a functional relatedness is not to be excluded there is no evidence for further investigation.

The verification of β 1 integrin and TN-R interaction is performed through immunoprecipitation (IP) and GST pull-down experiments in this work (figure 12). In the IP no interaction can be demonstrated with the polyclonal 619 antibody against TN-R. Now there are other anti-TN-R antibodies available for repetition. A problematic feature of this analysis might be the sizes of the two interacting molecules. TN-R has a molecular weight of 160 and 180kDa respectively. The β 1 subunit of the integrin is about 120 to 150kDa (depending on cell type) in size. This might be the reason why only a 75kDa degradation product of the β 1 subunit is undoubtedly pulled down with the FNIII 6-8 fragment in the GST pull-down (see figure 12). A band at the correct molecular weight of the intact β 1 subunit was observable in elution fraction 4 of all pull-down Western blots but always arguable because of high background intensities. Perhaps the interaction of both molecules could be shown when there are β 1 integrin deletion variants available, exhibiting smaller sizes.

KAPITEL 5

Literatur

Literature

References

- Adams MD, Soares MB, Kerlavage AR, Fields C, Venter JC (1993) Rapid cDNA sequencing (expressed sequence tags) from a directionally cloned human infant brain cDNA library Nat Genet 4:373-80
- Baas PW (1999) Microtubules and neuronal polarity: lessons from mitosis. Neuron. 22(1):23-31
- Balzac F, Belkin AM, Koteliansky VE, Balabanov YV, Altruda F, Silengo L, Tarone G (1993) Expression and functional analysis of a cytoplasmic domain variant of the beta 1 integrin subunit. J Cell Biol. 121:171-8
- Bartsch U (1996) The extracellular matrix molecule tenascin-C: expression in vivo and functional characterization in vitro. Prog Neurobiol. 49:145-68
- Bartsch S, Husmann K, Schachner M, Bartsch U (1995) The extracellular matrix molecule tenascin: expression in the developing chick retinotectal system and substrate properties for retinal ganglion cell neurites in vitro. Eur J Neurosci. 7:907-16
- Becker CG, Schweitzer J, Feldner J, Becker T, Schachner M (2003) Tenascin-R as a repellent guidance molecule for developing optic axons in zebrafish J Neurosci (in press)
- Bouvard D and Block MR (1998) Calcium/calmodulin-dependent protein kinase II controls integrin alpha5beta1-mediated cell adhesion through the integrin cytoplasmic domain associated protein-1alpha. Biochem Biophys Res Commun. 252:46-50
- Bouvard D, Vignoud L, Dupe-Manet S, Abed N, Fournier HN, Vincent-Monegat C, Retta SF, Fassler R, Block MR (2003) Disruption of focal adhesions by integrin cytoplasmic domain-associated protein-1 alpha J Biol Chem. 278:6567-74
- Bovolenta P and Feraud-Espinosa I (2000) Nervous system proteoglycans as modulators of neurite outgrowth Prog Neurobiol 61:113-32
- Bristow J, Tee MK, Gitelman SE, Mellon SH, Miller WL (1993) Tenascin-X: a novel extracellular matrix protein encoded by the human XB gene overlapping P450c21B J Cell Biol 122:265-78
- Bruckner G, Brauer K, Hartig W, Wolff JR, Rickmann MJ, Derouiche A, Delpech B, Girard N, Oertel WH, Reichenbach A (1993) Perineuronal nets provide a polyanionic, glia-associated form of microenvironment around certain neurons in many parts of the rat brain Glia 8:183-200

- Burch GH, Gong Y, Liu W, Dettman RW, Curry CJ, Smith L, Miller WL, Bristow J (1997) Tenascin-X deficiency is associated with Ehlers-Danlos syndrome *Nat Genet* 17:104-8
- Burridge K and Chrzanowska-Wodnicka M (1996) Focal adhesions, contractility, and signaling *Annu Rev Cell Dev Biol* 12:463-518
- Celio MR and Blumcke I (1994) Perineuronal nets - a specialized form of extracellular matrix in the adult nervous system *Brain Res Brain Res Rev* 19:128-45
- Chang DD, Wong C, Smith H, Liu J (1997) ICAP-1, a novel beta1 integrin cytoplasmic domain-associated protein, binds to a conserved and functionally important NPXY sequence motif of beta1 integrin *J Cell Biol* 138:1149-57
- Chen WJ, Goldstein JL, Brown MS (1990) NPXY, a sequence often found in cytoplasmic tails, is required for coated pit-mediated internalization of the low density lipoprotein receptor *J Biol Chem* 265:3116-23
- Chiquet M and Fambrough DM (1984) Chick myotendinous antigen. II. A novel extracellular glycoprotein complex consisting of large disulfide-linked subunits *J Cell Biol* 98:1937-46
- Chiquet-Ehrismann R (1995) Inhibition of cell adhesion by anti-adhesive molecules *Curr Opin Cell Biol* 7:715-9
- Chi-Rosso G, Gotwals PJ, Yang J, Ling L, Jiang K, Chao B, Baker DP, Burkly LC, Fawell SF, Koteliensky VE (1997) Fibronectin type III repeats mediate RGD-independent adhesion and signaling through activated β 1 integrins *J Biol Chem* 272:31447-31452
- Chuong CM, Crossin KL, Edelman GM (1987) Sequential expression and differential function of multiple adhesion molecules during the formation of cerebellar cortical layers *J Cell Biol* 104:331-42
- Cifuentes-Diaz C, Faillle L, Goudou D, Schachner M, Rieger F, Angaut-Petit D (2002) Abnormal reinnervation of skeletal muscle in a tenascin-C-deficient mouse *J Neurosci Res* 67:93-9
- Collier BS (1986) Activation affects access to the platelet receptor for adhesive glycoproteins *J Cell Biol* 103:451-6
- Davenport WJ, Siegel AM, Dichgans J, Drigo P, Mammi I, Pereda P, Wood NW, Rouleau GA (2001) CCM1 gene mutations in families segregating cerebral cavernous malformations *Neurology* 56:540-3
- Dorries U, Taylor J, Xiao Z, Lochter A, Montag D, Schachner M (1996) Distinct effects of recombinant tenascin-C domains on neuronal cell adhesion, growth cone guidance, and neuronal polarity *J Neurosci Res* 43(4):420-38
- Emsley J, King SL, Bergelson JM, Liddington RC (1997) Crystal structure of the I domain from integrin α 2 β 1 *J Biol Chem* 272:28512-7
- Engel J (1993) *Molecular and Cellular Aspects of Basement Membranes*, Academic Press, San Diego
- Erickson HP and Bourdon MA (1989) Tenascin: an extracellular matrix protein prominent in specialized embryonic tissues and tumors *Annu Rev Cell Biol* 5:71-92
- Erickson HP and Inglesias JL (1984) A six-armed oligomer isolated from cell surface fibronectin preparations *Nature* 311:267-9
- Evers MR, Salmen B, Bukalo O, Rollenhagen A, Bosl MR, Morellini F, Bartsch U, Dityatev A, Schachner M (2002) Impairment of L-type Ca^{2+} channel-dependent forms of hippocampal synaptic plasticity in mice deficient in the extracellular matrix glycoprotein tenascin-C *J Neurosci* 22:7177-94
- Faissner A and Kruse J (1990) J1/tenascin is a repulsive substrate for central nervous system neurons *Neuron* 5:627-37
- Faisst AM and Gruss P (1998) Bodenin: a novel murine gene expressed in restricted areas of the brain *Dev Dyn* 212:293-303
- Fluck M, Tunc-Civelek V, Chiquet M (2000) Rapid and reciprocal regulation of tenascin-C and tenascin-Y expression by loading of skeletal muscle *J Cell Sci* 113:3583-91

- Forsberg E, Hirsch E, Fröhlich L, Meyer M, Ekblom P, Aszodi A, Werner S, Fassler R (1996) Skin wounds and severed nerves heal normally in mice lacking tenascin-C *Proc Natl Acad Sci USA* 93:6594-9
- Friedlander DR, Milev P, Karthikeyan L, Margolis RK, Margolis RU, Grumet M (1994) The neuronal chondroitin sulfate proteoglycan neurocan binds to the neural cell adhesion molecules Ng-CAM/L1/NILE and N-CAM, and inhibits neuronal adhesion and neurite outgrowth *J Cell Biol* 125:669-80
- Fuss B, Pott U, Fischer P, Schwab ME, Schachner M (1991) Identification of a cDNA clone specific for the oligodendrocyte-derived repulsive extracellular matrix molecule J1-160/180 *J Neurosci Res* 29:299-307
- Fuss B, Wintergerst ES, Bartsch U, Schachner M (1993) Molecular characterization and in situ mRNA localization of the neural recognition molecule J1-160/180: a modular structure similar to tenascin *J Cell Biol* 120:1237-49
- Ghiselli G, Siracusa LD, Iozzo RV (1999) Complete cDNA cloning, genomic organization, chromosomal assignment, functional characterization of the promoter, and expression of the murine Bamacan gene *J Biol Chem* 274:17384-93
- Ginsberg MH, Du X, Plow EF (1992) Inside-out integrin signalling *Curr Opin Cell Biol* 4:766-71
- Grumet M, Hoffman S, Crossin KL, Edelman GM (1985) Cytotactin, an extracellular matrix protein of neural and non-neural tissues that mediates glia-neuron interaction *Proc Natl Acad Sci U S A* 82:8075-9
- Grumet M, Milev P, Sakurai T, Karthikeyan L, Bourdon M, Margolis RK, Margolis RU (1994) Interactions with tenascin and differential effects on cell adhesion of neurocan and phosphacan, two major chondroitin sulfate proteoglycans of nervous tissue *J Biol Chem* 269:12142-6
- Hagios C, Koch M, Spring J, Chiquet M, Chiquet-Ehrismann R (1996) Tenascin-Y: a protein of novel domain structure is secreted by differentiated fibroblasts of muscle connective tissue *J Cell Biol* 134:1499-512
- Hagios C, Brown-Luedi M, Chiquet-Ehrismann R (1999) Abstract Tenascin-Y, a component of distinctive connective tissues, supports muscle cell growth *Exp Cell Res* 253:607-17
- Hansen MB, Nielsen SE, Berg K (1989) Abstract Re-examination and further development of a precise and rapid dye method for measuring cell growth/cell kill *J Immunol Methods* 119:203-10
- Hasegawa K, Yoshida T, Matsumoto K, Katsuta K, Waga S, Sakakura T (1997) Differential expression of tenascin-C and tenascin-X in human astrocytomas *Acta Neuropatho* 93:431-7
- Hauzenberger D, Olivier P, Gundersen D, Ruegg C (1999) Tenascin-C inhibits beta1 integrin-dependent T lymphocyte adhesion to fibronectin through the binding of its fnIII 1-5 repeats to fibronectin *Eur J Immunol* 29:1435-47
- Hockfield and McKay (1983) A surface antigen expressed by a subset of neurons in the vertebrate central nervous system *Proc Natl Acad Sci USA* 80:5758-6
- Husmann K, Faissner A, Schachner M (1992) Tenascin promotes cerebellar granule cell migration and neurite outgrowth by different domains in the fibronectin type III repeats *J Cell Biol* 116:1475-86
- Hynes RO (1992) Integrins: versatility, modulation, and signaling in cell adhesion *Cell* 69:11-25
- Hynes RO (2002) Integrins: bidirectional, allosteric signaling machines *Cell* 110:673-87
- Ikuta T, Ariga H, Matsumoto K (2000) Extracellular matrix tenascin-X in combination with vascular endothelial growth factor B enhances endothelial cell proliferation *Genes Cells* 5:913-927
- Iozzo RV and Clark CC (1986) Biosynthesis of proteoglycans by rat embryo parietal yolk sacs in organ culture *J Biol Chem* 261:6658-69
- Jockusch BM, Bubeck P, Giehl K, Kroemker M, Moschner J, Rothkegel M, Rudiger M, Schluter K, Stanke G, Winkler J (1995) The molecular architecture of focal adhesions *Annu Rev Cell Dev Biol* 11:379-416

- Joester A and Faissner A (2001) The structure and function of tenascins in the nervous system *Matrix Biol* 20:13-22
- Kawano H, Ohyama K, Kawamura K, Nagatsu I (1995) Migration of dopaminergic neurons in the embryonic mesencephalon of mice *Brain Res Dev Brain Res* 86:101-13
- Koshland D and Strunnikov A (1996) Mitotic chromosome condensation *Annu Rev Cell Dev Biol* 12:305-33
- Kruse J, Keilhauer G, Faissner A, Timpl R, Schachner M (1985) The J1 glycoprotein - a novel nervous system cell adhesion molecule of the L2/HNK-1 family *Nature* 316:146-8
- Lacombe ML, Milon L, Munier A, Mehus JG, Lambeth D (2000) The human Nm23/ nucleoside diphosphate kinases *J Bioenerg Biomembr* 32:247-58
- Laudanna C, Campbell JJ, Butcher EC (1996) Role of Rho in chemoattractant-activated leukocyte adhesion through integrins *Science* 271:981-3
- Lee SH, Lumelsky N, Studer L, Auerbach JM, McKay RD (2000) Efficient generation of midbrain and hindbrain neurons from mouse embryonic stem cells *Nat Biotechnol* 18:675-9
- Lethias C, Elefteriou F, Parsiegla G, Exposito JY, Garrone R (2001) Identification and characterization of a conformational heparin-binding site involving two fibronectin type III modules of bovine tenascin-X *J Biol Chem* 276:16432-8
- Liang P and Pardee AB (1992) Differential display of eukaryotic messenger RNA by means of the polymerase chain reaction *Science* 257:967-71
- Lochter A, Vaughan L, Kaplony A, Prochiantz A, Schachner M, Faissner A (1991) J1/tenascin in substrate-bound and soluble form displays contrary effects on neurite outgrowth *J Cell Biol* 113:1159-71
- Lombardi D, Lacombe ML, Paggi MG (2000) nm23: unraveling its biological function in cell differentiation *J Cell Physiol* 182:144-9
- Martini R (1994) Expression and functional roles of neural cell surface molecules and extracellular matrix components during development and regeneration of peripheral nerves *J Neurocytol* 23:1-28
- Meier-Ewert S, Lange J, Gerst H, Herwig R, Schmitt A, Freund J, Elge T, Mott R, Herrmann B, Lehrach H (1998) Comparative gene expression profiling by oligonucleotide fingerprinting *Nucleic Acids Res* 26:2216-23
- Milev P, Friedlander DR, Sakurai T, Karthikeyan L, Flad M, Margolis RK, Grumet M, Margolis RU (1994) Interactions of the chondroitin sulfate proteoglycan phosphacan, the extracellular domain of a receptor-type protein tyrosine phosphatase, with neurons, glia, and neural cell adhesion molecules *J Cell Biol* 127:1703-15
- Milev P, Maurel P, Haring M, Margolis RK, Margolis RU (1996) TAG-1/axonin-1 is a high-affinity ligand of neurocan, phosphacan/protein-tyrosine phosphatase-zeta/beta, and N-CAM *J Biol Chem* 271:15716-23
- Milev P, Maurel P, Chiba A, Mevissen M, Popp S, Yamaguchi Y, Margolis RK, Margolis RU (1998) Differential regulation of expression of hyaluronan-binding proteoglycans in developing brain: aggrecan, versican, neurocan, and brevican *Biochem Biophys Res Commun* 247:207-12
- Milev P, Chiba A, Haring M, Rauvala H, Schachner M, Ranscht B, Margolis RK, Margolis RU (1998) High affinity binding and overlapping localization of neurocan and phosphacan/protein-tyrosine phosphatase-zeta/beta with tenascin-R, amphoterin, and the heparin-binding growth-associated molecule *J Biol Chem* 273:6998-7005
- Mills J, Digicaylioglu M, Legg AT, Young CE, Young SS, Barr AM, Fletcher L, O'Connor TP, Dedhar S (2003) Role of integrin-linked kinase in nerve growth factor-stimulated neurite outgrowth *J Neurosci* 23:1638-48
- Morganti MC, Taylor J, Pesheva P, Schachner M (1990) Oligodendrocyte-derived J1-160/180 extracellular matrix glycoproteins are adhesive or repulsive depending on the partner cell type and time of interaction *Exp Neurol* 109:98-110
- Morgenstern DA, Asher RA, Fawcett JW (2000) Chondroitin sulphate proteoglycans in the CNS injury response *Prog Brain Res* 137:313-32

- Mueller BK (1999) Growth cone guidance: first steps towards a deeper understanding *Annu Rev Neurosci* 22:351-88
- Nakamura F, Kalb RG, Strittmatter SM (2000) Molecular basis of semaphorin-mediated axon guidance *J Neurobiol* 44:219-29
- Neidhardt et al. 2003 MCN in press
- Norenberg U, Wille H, Wolff JM, Frank R, Rathjen FG (1992) The chicken neural extracellular matrix molecule restrictin: similarity with EGF-, fibronectin type III-, and fibrinogen-like motifs *Neuron* 8:849-63
- Okabe S, Forsberg-Nilsson K, Spiro AC, Segal M, McKay RD (1996) Development of neuronal precursor cells and functional postmitotic neurons from embryonic stem cells in vitro *Mech Dev* 59:89-102
- Pesheva P, Spiess E, Schachner M (1989) J1-160 and J1-180 are oligodendrocyte-secreted nonpermissive substrates for cell adhesion *J Cell Biol* 109:1765-78
- Pierschbacher MD, Ruoslahti E (1984) Cell attachment activity of fibronectin can be duplicated by small synthetic fragments of the molecule *Nature* 309:30-3
- Rathjen FG, Wolff JM, Chiquet-Ehrismann R (1991) Restrictin: a chick neural extracellular matrix protein involved in cell attachment co-purifies with the cell recognition molecule F11 *Development* 113:151-64
- Reszka AA, Hayashi Y, Horwitz AF (1992) Identification of amino acid sequences in the integrin beta 1 cytoplasmic domain implicated in cytoskeletal association *J Cell Biol* 117:1321-30
- Ruoslahti E and Pierschbacher MD (1987) New perspectives in cell adhesion: RGD and integrins *Science* 238:491-7
- Saga Y, Yagi T, Ikawa Y, Sakakura T, Aizawa S (1992) Mice develop normally without tenascin *Genes Dev* 6:1821-31
- Sakai T, Furukawa Y, Chiquet-Ehrismann R, Nakamura M, Kitagawa S, Ikemura T, Matsumoto K (1996) Tenascin-X expression in tumor cells and fibroblasts: glucocorticoids as negative regulators in fibroblasts *J Cell Sci* 109:2069-77
- Sambrook et al. (1989) "Molecular cloning: A Laboratory Manual" Cold Spring Harbor, Cold Spring Harbor Laboratory
- Scarborough RM, Naughton MA, Teng W, Rose JW, Phillips DR, Nannizzi L, Arfsten A, Campbell AM, Charo IF (1993) Design of potent and specific integrin antagonists. Peptide antagonists with high specificity for glycoprotein IIb-IIIa *J Biol Chem* 268:1066-73
- Scarborough RM, Rose JW, Naughton MA, Phillips DR, Nannizzi L, Arfsten A, Campbell AM, Charo IF (1993) Characterization of the integrin specificities of disintegrins isolated from American pit viper venoms *J Biol Chem* 268:1058-65
- Schnapp LM, Hatch N, Ramos DM, Klimanskaya IV, Sheppard D, Pytela R (1995) The human integrin alpha 8 beta 1 functions as a receptor for tenascin, fibronectin, and vitronectin *J Biol Chem* 270:23196-202
- Schultz J, Milpetz F, Bork P, Ponting CP (1998) SMART, a simple modular architecture research tool: identification of signaling domains *Proc Natl Acad Sci USA* 95:5857-64
- Smith AG (2001) Embryo-derived stem cells: of mice and men *Annu Rev Cell Dev Biol* 17:435-62
- Taylor J, Pesheva P, Schachner M (1993) Influence of janusin and tenascin on growth cone behavior in vitro *J Neurosci Res* 35:347-62
- Tessier-Lavigne M, Goodman CS (1996) The molecular biology of axon guidance *Science* 274:1123-33
- Tolsma SS, Volpert OV, Good DJ, Frazier WA, Polverini PJ, Bouck N (1993) Peptides derived from two separate domains of the matrix protein thrombospondin-1 have anti-angiogenic activity *J Cell Biol* 122:497-511
- Tropepe V, Hitoshi S, Sirard C, Mak TW, Rossant J, van der Kooy D (2001) Direct neural fate specification from embryonic stem cells: a primitive mammalian neural stem cell stage acquired through a default mechanism *Neuron* 30:65-78
- Tucker RP, Hagios C, Chiquet-Ehrismann R (1999) Tenascin-Y in the developing and adult avian nervous system *Dev Neurosci* 21:126-33

- Velculescu VE, Zhang L, Vogelstein B, Kinzler KW (1995) Serial analysis of gene expression *Science* 270:484-7
- Weber P, Montag D, Schachner M, Bernhardt RR (1998) Zebrafish tenascin-W, a new member of the tenascin family *J Neurobiol* 35:1-16
- Weber P, Bartsch U, Rasband MN, Czaniera R, Lang Y, Bluethmann H, Margolis RU, Levinson SR, Shrager P, Montag D, Schachner M (1999) Mice deficient for tenascin-R display alterations of the extracellular matrix and decreased axonal conduction velocities in the CNS *J Neurosci* 19:4245-62
- Wu RR and Couchman JR (1997) cDNA cloning of the basement membrane chondroitin sulfate proteoglycan core protein, bamacan: a five domain structure including coiled-coil motifs *J Cell Biol* 136:433-44
- Xiao ZC, Taylor J, Montag D, Rougon G, Schachner M (1996) Distinct effects of recombinant tenascin-R domains in neuronal cell functions and identification of the domain interacting with the neuronal recognition molecule F3/11 *Eur J Neurosci* 8:766-82
- Xiao ZC, Revest JM, Laeng P, Rougon G, Schachner M, Montag D (1998) Defasciculation of neurites is mediated by tenascin-R and its neuronal receptor F3/11 *J Neurosci Res* 52:390-404
- Yamaguchi Y (2000) Lecticans: organizers of the brain extracellular matrix *Cell Mol Life Sci* 57:276-89
- Yokosaki Y, Palmer EL, Prieto AL, Crossin KL, Bourdon MA, Pytela R, Sheppard D (1994) The integrin alpha 9 beta 1 mediates cell attachment to a non-RGD site in the third fibronectin type III repeat of tenascin *J Biol Chem* 269:26691-6
- Yokosaki Y, Matsuura N, Higashiyama S, Murakami I, Obara M, Yamakido M, Shigeto N, Chen J, Sheppard D (1998) Identification of the ligand binding site for the integrin alpha9 beta1 in the third fibronectin type III repeat of tenascin-C *J Biol Chem* 273:11423-8
- Yokoyama K, Erickson HP, Ikeda Y, Takada Y (2000) Identification of amino acid sequences in fibrinogen gamma chain and tenascin C C-terminal domains critical for binding to integrin alpha v beta 3 *J Biol Chem* 275:16891-8
- Zawistowski JS, Serebriiskii IG, Lee MF, Golemis EA, Marchuk DA (2002) KRIT1 association with the integrin-binding protein ICAP-1: a new direction in the elucidation of cerebral cavernous malformations (CCM1) pathogenesis *Hum Mol Genet* 11:389-96
- Zhang Z, Vuori K, Wang H, Reed JC, Ruoslahti E (1996) Integrin activation by R-ras *Cell* 85:61-9
- Zhang XA and Hemler ME (1999) Interaction of the integrin beta1 cytoplasmic domain with ICAP-1 protein *J Biol Chem* 274:11-9
- Zhang J, Clatterbuck RE, Rigamonti D, Chang DD, Dietz HC (2001) Interaction between krit1 and icap1alpha infers perturbation of integrin beta1-mediated angiogenesis in the pathogenesis of cerebral cavernous malformation *Hum Mol Genet* 10:2953-60

Bibliography

- Kandel ER, Schwartz JH, Jessel TM (2000) Principles of neural science, fourth edition, McGraw-Hill Health Profession Division
- Lewin B (2000) Genes VII, Oxford University Press
- Paxinos G (1995) The Rat Nervous System, second edition, Academic Press, Inc.
- Suzuki DT, Griffiths AJF, Miller JH, Lewontin RC (1991) Genetik, VCH Verlagsgesellschaft Weinheim, D
- Voet D and Voet JG (1995) Biochemistry, second edition, John Wiley & Sons, Inc.
-

KAPITEL 6

Zusammenfassung

Summary

English Summary

During development and in plasticity as well as regeneration in the adult central nervous system (CNS), neural cell recognition molecules are expressed in order to mediate cell-cell contacts or the contact between cells and the extracellular matrix (ECM). The tenascins are a substantial family of proteins belonging to the neural recognition molecules. One member with special impact in the CNS is the tenascin-R (TN-R). It contributes to processes of neurite outgrowth and pathfinding. TN-R properties depend on the cell type and the way it is offered as a substrate to the cells. It can be promoting or decreasing neurite outgrowth and in a border-like situation serve as a repellent guiding cue. Furthermore, the interaction with voltage dependent sodium channels at the node of Ranvier, its location around synapses and in perineuronal nets indicate the important role in generation, function and maintenance of the CNS. The unexpected mild phenotype of the mouse deficient for TN-R led to the assumption of compensating effects. Therefore, this work analyzes the altered gene expression in TN-R knock out animals first to detect molecules involved in this balancing process. Dysregulation is detected for several molecules by the microarray technique. The integrin cytoplasmic associated molecule-1 α (ICAP-1 α , bodenin or Itgb1bp1) was investigated more in detail to unravel its role in the compensating mechanism. Its dysregulation is verified by three further methods. A hot spot of ICAP upregulation is the cerebellum as identified through Northern blot analysis and *in situ* hybridization. The cerebellum is a center for controlling, correcting, fine-tuning and learning of movements. Its "output neurons" are the Purkinje cells with dendrites in the molecular layer containing densely packed parallel fibers, the axons of granule cells. Interestingly, these two cell types are strongly positive for ICAP in *in situ* experiments. For Purkinje cells the

upregulation is clearly visible. The ICAP dysregulation is detected at a time point of Purkinje cell arborization, a process where the correct orientation of the dendritic tree is a matter of cell-cell interaction between parallel fibers and the dendrite and an interaction between cells and the altered ECM. The compensation for the missing TN-R is displayed by this ICAP upregulation and its modification of neurite outgrowth, shown in *in vitro* experiments. In these, ICAP deficient embryonic stem (ES) cells are differentiated into neurons. In neurite outgrowth experiments with the ES derived neurons it is shown that TN-R is an outgrowth decreasing molecule for wildtype cells. ICAP deficiency inverses this effect to promoted outgrowth on TN-R. $\beta 1$ integrin is co-expressed in areas of ICAP presence by Northern blot analysis and in situ hybridization. Taken together, the findings indicate that neurite outgrowth is integrin mediated and that the integrin binding protein ICAP participates in it. The detected upregulation of this molecule in reaction to the altered ECM of TN-R deficient animals points to compensation effects that participate in maintaining the observed grossly normal histoarchitecture in the CNS of these animals.

Zusammenfassung

Neurale Zellerkennungsmoleküle spielen in der Entwicklung, der Plastizität und in regenerativen Prozessen des zentralen Nervensystems (ZNS) eine wichtige Rolle. Ihre Expression im ZNS dient der Vermittlung von Kontakten zwischen Zellen und von solchen zwischen Zellen und der extrazellulären Matrix (ECM). Die Familie der Tenascin Glycoproteine ist eine elementare Gruppe dieser Molekülklasse. Dem Tenascin-R (TN-R) kommt eine besondere Rolle im ZNS zu. Es ist dort an Prozessen beteiligt die das Neuritenwachstum und deren Wegfindung beeinflussen. Die Art der Beeinflussung durch TN-R hängt davon ab in welcher Form es von den Neuriten angetroffen wird. Wenn TN-R als Substratgrenze angetroffen wird, wirkt es abstoßend auf den Neuriten und verhindert somit das Einwachsen. Eine solche Grenze von TN-R dient auch als Leitstruktur, an der Neuriten auf ihrem Weg zum Projektionsziel entlang wachsen. Als Substrat kann TN-R in Abhängigkeit vom Zelltypus eine Neuritenwachstum fördernde oder inhibierende Wirkung entfalten. Diese Beobachtungen und die bekannte Wechselwirkung von TN-R mit spannungsabhängigen Natriumkanälen am Ranvier'schen Schnürring, seine Expression in perineuralen Netzen und um Synapsen unterstreicht die elementare Rolle dieses Moleküls. Es ist dadurch in die Prozesse der Entstehung, der Funktionalität und der Aufrechterhaltung des ZNS involviert. Die Charakterisierung der TN-R defizienten Maus ergab einen unerwartet schwachen Phänotyp, der nur durch Redundanz und Kompensationsprozesse zu erklären ist. Zur Aufklärung welche Moleküle an diesem Prozess beteiligt sein könnten, wird in dieser Arbeit das Expressionsmuster der TN-R defizienten Mausmutante untersucht. Die Erstellung des genetischen Profils dieser Mäuse

erfolgt durch einen sogenannten "microarray". Die beobachtete Dysregulation mehrerer Transkripte wird mit anderen Methoden reproduziert und charakterisiert. Das dysregulierte Transkript des $\beta 1$ Integrin cytoplasmatisch assoziierten Proteins (ICAP-1 α , bodenin oder Itgb1bp1) wird zur Aufklärung seiner Rolle im Kompensationsprozess näher untersucht. Die erhöhte Expression des ICAP Transkripts kann durch drei weitere Methoden bestätigt werden. Durch diese weitergehenden Untersuchungen kann das Kleinhirn als eine Region mit besonderer Auffälligkeit identifiziert werden. Das Kleinhirn ist ein Zentrum der motorischen Kontrolle, Korrektur und Feinabstimmung. Es ist auch in das Erlernen von Bewegungen involviert. Der Ausgang der Informationen erfolgt über die Purkinjezellen des Kleinhirns. Diese Zellen bilden ihre Dendriten in der Molekularschicht aus. In dieser Schicht befinden sich die Axone der Körnerzellen, die hier die Parallelfasern bilden. Im rechten Winkel zu diesen Axonbündeln richtet sich der dendritische Baum der Purkinjezellen aus. Die Ausbildung des Dendriten erfolgt zu dem Zeitpunkt wo die Dysregulation des ICAP Moleküls gefunden wird (P14). Die in der *in situ* Hybridisierung zu beobachtende starke Anfärbung der Purkinjezellen und der Körnerzellschicht weist darauf hin, daß diese Zellen in Reaktion auf die TN-R Defizienz ICAP verstärkt exprimieren. Diese Expression verändert die Eigenschaften des Neuritenwachstums zu diesem kritischen Zeitpunkt, in der in den *in vitro* Experimenten gezeigten Art. Für von embryonalen Stammzellen (ES) abgeleitete Neurone des Wildtyps wirkt TN-R inhibierend auf das Auswachsen der Neuriten. Durch das Unterbinden der ICAP Expression (ICAP knock out Zellen) wird diese Eigenschaft des TN-R's in das Gegenteil umgekehrt - es stimuliert das Neuritenwachstum. Die Arbeit zeigt, daß eine Verbindung zwischen Neuritenwachstum und TN-R besteht. Desweiteren ist auch nachgewiesen, daß das Integrin bindende Protein ICAP nicht nur in Reaktion auf die TN-R Defizienz hochreguliert wird sondern auch einen Einfluß auf das Neuritenwachstum hat. Darüber hinaus kann die räumliche Koexistenz von ICAP und $\beta 1$ Integrin, wie in Northern Blot und *in situ* Hybridisierungen gezeigt, in Kombination mit Erkenntnissen aus den zuvor genannten Experimenten darauf hinweisen, daß das Auswachsen von Neuriten ein Integrin vermittelter Prozess ist. Diese Erkenntnisse geben Einsichten in kompensatorische Prozesse, die zu der kaum veränderten Gewebszusammensetzung in der TN-R defizienten Maus beitragen.

KAPITEL 7

Anhang

Appendix

Abbreviations

μ	micro (10 ⁻⁶)
x g	g-force
°C	degree centigrade
aa	amino acid
A	adenine
Acc.	accession number
Amp	ampicillin
ATP	adenosine triphosphate
bp	base pairs
BSA	bovine serum albumine
C	Cytosine
cDNA	complementary deoxyribonucleic acid
CTP	cytosine triphosphate
Da	dalton
dATP	2'-desoxyadenosinetriphosphate
dCTP	2'-desoxycytidinetriphosphate
DEPC	diethylpyrocarbonate
dGTP	2'-desoxyguanosinetriphosphate
DMSO	dimethylsulfoxide
DNA	deoxyribonucleic acid
DNase	desoxyribonuclease
dNTP	2'-desoxyribonucleotide-5'-triphosphate
DTT	dithiothreitol
EB	embryoid body
<i>E. coli</i>	escherichia coli
EDTA	ethylenediaminetetraacetic acid

f.c.	final concentration
g	gramm
G	guanosine
h	human, hour
HEPES	2-(4-(2-Hydroxyethyl)-piperzino)-ethansulfonic acid
IPTG	isopropylthiogalactoside
Kan	kanamycin
kb	kilo base pairs
l	liter
LB	Luria Bertani Broth
m	milli (10^{-3})
min	minute
MOPS	(4-(N-morpholino)-propan)-sulfonic acid
MMC	mitomycin C
mRNA	messenger ribonucleic acid
n	nano (10^{-9})
Nt	nucleotide(s)
OD	optic density
ORF	open reading frame
p	pico (10^{-12})
PAGE	polyacrylamide gel electrophoresis
PBS	phosphate-buffered saline
PCR	polymerase chain reaction
PFA	paraformaldehyde
PLO	poly-L-ornithin
rpm	rounds per minute
psi	pounds per square inch
RNA	ribonucleic acid
RNase	ribonuclease
RT	room temperature
s	second
SDS	sodium dodecyl sulfate
T	thymine
Tab.	table
TE	tris-EDTA
TEMED	N,N,N',N'-tetraethylenamine
Tet	tetracycline
Tm	melting temperature
TM	transmembrane segment
Tris	tris(-hydroxymethyl)-aminomethane
U	unit (enzymatic)
V	volt
v/v	volume per volume
Vol.	volume
w/v	weight per volume

ZMNH Zentrum für Molekulare Neurobiologie Hamburg

Curriculum vitae

- 1971 geboren am 28. Mai in Walsrode, Deutschland
- 1978 Einschulung in Braunschweig Querum-Nord
- 1991 Abitur am Hoffmann von Fallersleben
Gymnasium Braunschweig
- 1991 Immatrikulation im Fach Biologie der TU Braunschweig
- 1994 Vordiplom Biologie, Note: GUT
- 1995 Studienortwechsel an die Uni Hamburg,
Hauptfach: Humanbiologie
- 1997 ERASMUS-Stipendium für Studium an der Uni Zürich,
Schweiz
- 1998 Diplomarbeit bei Prof. Dr. Ernst Heinz, Uni Hamburg
Titel: "Untersuchungen zur Expression und funktionalen
Charakterisierung der UDP-Galaktose:Ceramid
Galaktosyltransferase von Säugern"
- 1999 Diplom im Fach Biologie, Note: SEHR GUT
- 1999 Beginn der Doktorarbeit bei Prof. Dr. Melitta Schachner,
Uni Hamburg als Stipendiat des Graduiertenkollegs 255
der DFG
- 2000 Beginn des Aufbaustudiengangs Molekularbiologie, Uni
Hamburg
- 2002 Abschluß des Aufbaustudiengangs Molekularbiologie,
Note: SEHR GUT

Besondere Tätigkeiten:

Betreuung mehrerer Genetik Praktika und Überarbeitung des
Praktikumsskripts in Zusammenarbeit mit Dr. habil. F. P. Wolter
am Biozentrum Klein Flottbek in den Jahren 1996 bis 1999

Projektstudie am Anthropologischen Institut der Universität
Zürich „Ethologie und genetische Verwandtschaft bei nicht-
menschlichen Primaten“ 1997/ 1998

Projektstudie in der Arbeitsgruppe von Prof. Dr. Ernst Heinz „Umklonierung der UDP-Galaktose:Ceramid Galaktosyltransferase“ in den Semesterferien 1998

Teilnahme und Vortrag im Rahmen des Graduiertentreffens der biowissenschaftlichen Graduiertenkollegs Deutschlands, Februar 2000 in Ulm

Sprecher des Graduiertenkollegs 255 und Organisation des Seminarwochenendes im Rahmen der „BioDigital“, Oktober 2000 in Freiburg

Molekularbiologisches Projekt 2001 mit Schülern der Leistungskurse Biologie der Raabe Schule und der Hoffmann von Fallersleben Schule anlässlich des 125 jährigen Bestehens des Hoffmann von Fallersleben Gymnasiums in Braunschweig

Danksagung Acknowledgements

Ein ganz besonderer Dank gilt Frau Prof. Dr. Melitta Schachner, die mir nicht nur das Arbeiten an einem so spannenden Thema und unter optimalen Bedingungen ermöglicht hat, sondern auch jederzeit mit Rat und Tat mir zur Seite stand.

Für die Begutachtung meiner Arbeit möchte ich mich auch ganz herzlich bei Herrn Prof. Dr. L. Renwrantz bedanken.

I have to thank my two native speaking colleagues Dr. Heather Ostendorff and Martin Hammond for correcting my thesis.

Meinen beiden Kollegen Dr. Christian Bernreuther und Dr. Marcel Dihn e danke ich f r die vielen gemeinsamen Stunden in der ES Zellkultur und den zahllosen Diskussionen in diesem Themenbereich.

Ein weiterer kollegialer Dank gilt Dr. John Neidhardt, der mir im Thema Northern Blot auf die Spr nge half und Dr. Udo Bartsch sowie Dr. Marius Ader die mir beide in morphologischen Themen stets ein offenes Auge und Ohr gaben.

Den Kollegen der "Mittagessensgruppe" geh rt auch Dank f r die Gesellschaft und zahlreiche, u.a. auch nicht-wissenschaftlichen, Gespr che.

Ferner danke ich allen Kollegen des Instituts und Zentrums f r die jahrelange, gute Zusammenarbeit.

Bei meinen Eltern mu  ich mich zu tiefst bedanken, da  sie mir bei diesem langen Weg immer an meiner Seite standen. Ich habe

es nie als selbstverständlich gesehen, so eine aufwendige und langwierige Ausbildung zu unterstützen, obwohl es sich immer so angefühlt hat. Meine beiden Brüder tragen auch maßgeblich zu der allgemeinen Unterstützung bei. Die gesamte Familie, insbesondere auch meine Großmutter, ist eine sehr große Hilfe gewesen, diesen Abschnitt abschließen zu können.

Der letzte Dank gilt meiner Katja, die mir in den letzten Wochen dieser Arbeit besonders viel Verständnis, Unterstützung und Kraft gegeben hat.

Erklärung

Hiermit versichere ich, daß ich die vorliegende Arbeit selbständig angefertigt habe. Fremde Hilfe ist, soweit sie in Anspruch genommen wurde, vermerkt.

Diese Arbeit ist zuvor keiner Prüfungsbehörde in gleicher oder ähnlicher Form vorgelegt worden.

Hamburg, den

(Kai - Oliver Wesche)